CARBONATITE VEINS IN LAMPROPHYRE DYKES, MT TAPUAENUKU, NEW ZEALAND

A THESIS SUBMITTED IN PARTIAL FULFILMENT

OF THE REQUIREMENTS FOR THE DEGREE OF

Master of Science in Geology

AT THE

DEPARTMENT OF GEOLOGICAL SCIENCES,

UNIVERSITY OF CANTERBURY

by Patrick Didier Turner

UNIVERSITY OF CANTERBURY

2015

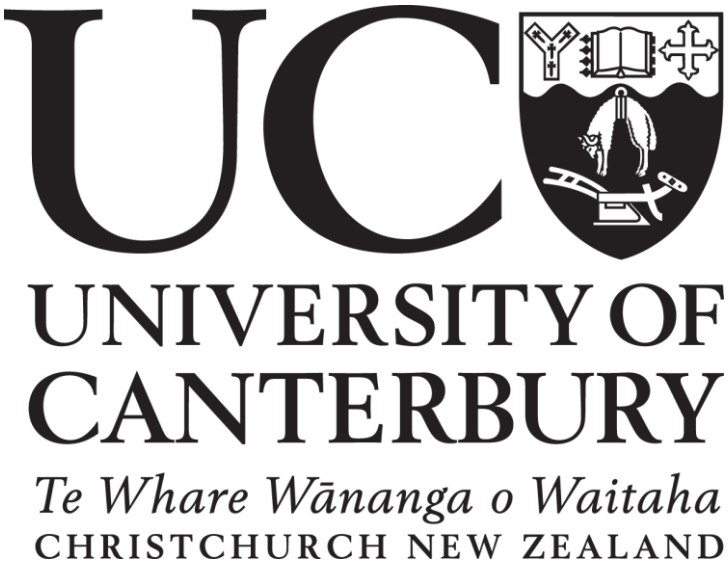

Frontispiece

"Learn from yesterday, live for today, hope for tomorrow. The important thing is not to stop questioning."

- Albert Einstein

ABSTRACT

Carbonatites are rare igneous rocks that are predominantly composed of carbonate minerals. At Mount Tapuaenuku, Inland Kaikoura Ranges, New Zealand, a series of highly alkaline lamprophyre dykes with subordinate calcite and dolomite carbonatite veins intrudes the Tapuaenuku Igneous Complex (TIC). Crystallisation of the Tapuaenuku Igneous Complex produced volatile- and alkali-enriched residual melts present as a series of lamprophyres exposed in the TIC. Cross cutting these dykes are planar laminate carbonatite veins and chaotic non-directional carbonatite veinlets. Previous studies of the TIC field classified these veins as carbonatites; however, in-depth investigation of the petrography, geochemistry and petrogenesis of the carbonatites was not completed prior to this thesis. This thesis presents a detailed mineralogical, chemical and stable isotopic investigation of the TIC carbonatite veins that outcrop in the Gut Stream area. The veins exhibit comb and crustiform textures and are primarily composed of rhombohedral limpid calcite and turbid calcite of igneous origin. X-ray diffraction results indicate that the carbonate present in the veins is a mixture of predominantly calcite and subordinate dolomite. Petrographical investigation further indicates accessory quartz, epidote and aegirine are common in the calcite dominated carbonatite veins. The Tapuaenuku carbonatites have a wide range of $\delta^{13}C_{PDB}$ (-1.88 to -4.32‰) and $\delta^{18}O_{SMOW}$ (+6.09 to +16.75‰) values. Vein type and mineralogy appears to be correlated with oxygen isotope compositions; limpid calcite laminates range from 12.00 to 13.99 ‰, with turbid laminate calcite veins ranging from 7.35 to 8.53 ‰, both limpid and turbid have similar $\delta^{13}C$ values and the chaotic spider veinlets exhibiting a larger variation in $\delta^{18}O$ ca. +11.41 to +15.15‰ and lower $\delta^{13}C$ values of -4.00 to -4.32‰ than laminated veins. Carbon ($\delta^{13}C$) and oxygen ($\delta^{18}O$) isotopic composition of the carbonatite veins and veinlets are compatible with a magmatic carbonate melt/carbohydrothermal fluid origin with $\delta^{18}O$ variation attributed to limpid and turbid carbonate kinetic fractionation and isotopic exchange with $\delta^{18}O$ magmatic or hydrothermal fluids. The presence of carbonatite veins in the TIC provide insights into the magmatic and processes that generated the TIC in the mid-Cretaceous. The TIC carbonatites represent the second carbonatite occurrence in New Zealand after the Haast Alpine Schist carbonatites and a new site to the list of the 527 globally distributed carbonatite occurrences.

SOMMAIRE

Les carbonatites sont des roches ignées rares contenant une grande proportion de minéraux carbonatés. Au Mont Tapuaenuku, dans les massifs intérieurs de Kaikoura, en Nouvelle Zélande, est localisée une série de dykes de lamprophyres fortement basiques, associés à des veines de carbonatites riches en calcite et dolomite, qui forme une intrusion dans le complexe igné de Tapuaenuku (TIC). La cristallisation de ce complexe de roches ignées a produit des résidus des fluides volatils -et très alcalins- qui sont présents sous la forme d'une série de lamprophyres dans le complexe. Traversant transversalement ces filons se trouvent des veines de carbonatites stratifiées à surface plane et des trainées de carbonatites chaotiques multidirectionnelles. Les recherches antérieures sur le champ de roches ignées de Tapuaenuku ont identifié ces veines comme des carbonatites; cependant l'analyse approfondie de la pétrographie, de la géochimie et de la pétrogenèse de ces veines n'est pas terminée. Dans notre travail, pour étudier la pétrogenèse des veines de carbonatites de Tapuaenuku, nous nous appuyons sur la minéralogie, la chimie et la stabilité des isotopes dans les veines de carbonatites. Dans les lamprophyres, les veines présentent des textures en peigne et des textures cruciforme et sont principalement constituées de calcite pure rhomboédrique limpide et de calcite trouble d'origine magmatique. Les résultats de la diffraction X montrent que le carbonate présent dans ces veines est un mélange composé principalement de calcite et dans une moindre mesure de dolomite ; les analyses pétrographiques révèlent la présence fréquente de quartz accessoire, d'épidote et d'ægyrine dans les veines de carbonatites. Les carbonatites de Tapuaenuku ont un large éventail de valeurs de $\delta^{13}C_{PDB}$ (-1.88 à -4.32‰) et de $\delta^{18}O_{SMOW}$ (6.09 à 16.75‰). Le type de veine et la composition minéralogique affectent les valeurs de $\delta^{18}O$; pour les strates de calcite limpides elles vont de 12.00 à 13.99 ‰, et pour les veines de calcites stratifiées troubles elles vont de 7.35 à 8.53 ‰ ; les strates limpides et les troubles affichent des valeurs de $\delta^{13}C$ comparables, alors que les veinules en araignée chaotiques affichent une variation plus forte de leur rapport $\delta^{18}O$ qui peut aller de 11.41 à 15.15‰ ainsi que de leur valeur $\delta^{13}C$ qui va de -4.00 à -4.32‰. La présence d'isotopes carbone ($\delta^{13}C$) et oxygène ($\delta^{18}O$) dans les veines et veinules de carbonatites associées aux filons de lamprophyre est typique de la fusion magmatique des roches carbonatées / carbonates hydrothermaux fluides, avec une variation du rapport isotopique $\delta^{18}O$ attribuée aux différences isotopiques minéralogiques, aux échanges isotopiques d' ^{18}O avec les

fluides magmatiques ou hydrothermaux ainsi qu'à de la cristallisation fractionnée. L'apparition des veines de carbonatites au sein du complexe de roches ignées de Tapuaenuku apporte des contraintes additionnelles aux conditions magmatiques du manteau terrestre qui ont abouti à la formation de ce complexe au milieu du Crétacée et offre également un second exemple de présence de carbonatites en Nouvelle Zélande qui vient s'ajouter aux 527 gisements de carbonatites dans le monde.

ACKNOWLEDGEMENTS

Firstly a big thank you to my supervisors Dr Travis Horton, Dr Chris Oze, Dr James Pope and Dr Jacqueline Dohaney. Travis' oversight for the general direction for my research has been invaluable throughout the year. The impromptu meetings at the gym in between sets have got to be some of the most bizarre thesis meetings. Chris' guidance, time and effort especially in the finally months has been priceless. His tireless efforts editing and teaching me academic writing and his ability to take complex ideas and break them down into relatable ideas that lead to the overall picture has been fundamental for this research. James, thank you for keeping me employed at CRL Energy whilst I carried on with my studies. The help and guidance throughout the year regarding academic study and professional life have been critical in keeping the big picture in view. Jacqueline, words cannot describe how thankful I am for the time, the effort and the knowledge that you have imparted. Throughout the year the direction and information Jacqueline gave me has been immense. That you were able to help with the field work and keep tabs throughout the research on not only my progress on this thesis but my learning and development to be a better scientist has been amazing. Travis, Chris, James and Jacqueline your input and combined knowledge has been immeasurably helpful over the last 12months.

I am indebted to the many technicians who helped me gather data; Rob Spiers helped via the preparation of the polished thin sections; Matt Cockcroft for the generator that was used during the field work. Stephen Brown aided with X-Ray Diffraction and X-Ray Fluorescence analysis and the insight on the methods and results obtained. Dr Kerry Swanson, your advice on the petrography photography has been invaluable. Chris Grimshaw, thank you for all of your help with the microscopes. My colleagues at CRL Energy Ltd in Christchurch, you have all been helpful with keeping the eye on the bigger picture. The discussions and advice regarding different techniques and sample preparation has been hugely appreciated. Nigel Newman and Trevor Dine thank you for the assistance regarding the heavy liquid separation and laboratory techniques. I also need to thank Dr David Craw from the University of Otago for the usage of the Portable XRF when the CRL Energy machine became unavailable at the last minute.

I would like to thank Bevan and Alan Pits of Gladstone Downs for allowing access to the Mt Tapuaenuku field area and for allowing me to sample rocks from their farm. A big thank you to the Department of Conservation for granting me permission to sample rocks on the DOC estate. The New Zealand Branch of AusIMM for the Education Endowment scholarship, without it the thesis would have been a lot harder to manage.

My office mates, Mattilda, Scott, Cam, Mitch, Gina and Sammy along with my classmates Matt, Josh, Jo, Fraser and Emma the coffee dates were always needed to feed the caffeine addiction. They have always been thoughtful and constructive and I have learnt a lot from you all. I would like to also express appreciation to the Mason Trust for the financial support that went towards the helicopter, fieldwork and laboratory testing. Matt Hanson deserves a massive thank you for taking time away from his thesis and coming out into the field and helping with the sampling and mapping. Your banter and sampling at each of the outcrops is greatly appreciated.

My family, without you my studies would not have occurred, so thank you. My parents have always supported any decision I made regarding my studies and the continued support is greatly appreciated. And finally, Katrina Woolf. The stability, love and food you brought to my life have been really appreciated. For your encouragement to follow my dreams, I will be eternally grateful.

Table of Contents

List of Figures

List of Tables

CHAPTER 1: INTRODUCTION

1.1 OVERVIEW

The Tapuaenuku Igneous Complex (TIC), Inland Kaikoura, New Zealand, is a complex multiphase layered igneous intrusion from the mid-Cretaceous. Highly alkaline lamprophyre dykes cross-cut the layered intrusives of the TIC. Within these lamprophyre dykes, a series of carbonate-rich veins appear to cross-cut the dykes. Previous work on the TIC has been limited, due to its relatively inaccessible location. Prior to this thesis, there was limited detailed outcrop to hand sample investigation of the TIC carbonatite veins. Thus, the processes and conditions that led to their formation were therefore unknown. Carbonatites are rare carbonate-rich igneous rocks that may occur in small intrusive complexes together with alkaline silicate rocks primarily in divergent tectonic settings. Limited prior field and petrographical descriptions of the TIC of these carbonate-rich veins suggested these veins were primary igneous carbonatites (Jongens et al. 2012). These field classified carbonatites represent an opportunity for an in-depth study into the geochemistry of the carbonatites, the associated mineralogy, timing relationships and stable isotopic composition.

Carbonatites are intrusive carbonate-mineral enriched igneous rocks that are known from only 527 localities worldwide. Carbonatites are subdivided into magmatic carbonatites and carbohydrothermal carbonatites (Woolley & Kjarsgaard 2008b; Woolley & Kjarsgaard 2008a). The majority of carbonatite occurrences are magmatic and are defined as primary igneous carbonatite formed from diverse mantle-derived magmas (Woolley & Kjarsgaard 2008b; Woolley & Kjarsgaard 2008a). Carbohydrothermal carbonatites are defined as those precipitated at sub-solidus temperatures from a mixture of CO_2-H_2O fluids that is either CO_2-rich (carbothermal) (Mitchell 2005), or H_2O-rich (hydrothermal) (Woolley & Church 2005;

Woolley & Kjarsgaard 2008b). Major and trace element analysis along with interpretation of the carbon and oxygen isotopic composition is used to classify the paragenesis of carbonatites (Bell 1989). The variation in the ^{13}C:^{12}C and ^{18}O:^{16}O ratios of carbonatite minerals is due to differences in the isotopic composition of magma sources, isotopic fractionation processes during magma formation, crystallisation and post magmatic alteration (Deines 1989). Oxygen ratios are presented in standard delta-notation as $\delta^{18}O_{V.SMOW}$ and carbon ratios as $\delta^{13}C_{PDB}$. The $\delta^{18}O$ values of carbonatites range from +5 to +25 ‰ with $\delta^{13}C$ values between -2 and -8 ‰ (Deines 1989). Most carbonatites are associated with at least one other alkaline lithology that commonly was emplaced earlier than the carbonatite unit itself (Woolley & Kjarsgaard 2008b; Woolley & Kjarsgaard 2008a). Carbonatite bodies associated with lamprophyres are in the form of dykes, sills, veins and small plugs (Woolley & Kjarsgaard 2008a) such as the carbonatite dykes associated with the lamprophyres dykes in the Haast Schist.

In north-western Otago and south Westland, New Zealand, Haast Schist basement is intruded by a regional dyke swarm of late-Oligocene to early-Miocene (32-20 Ma) ultramafic and feldspathic lamprophyres that contains carbonatite dykes (Cooper 1971, 1986; Cooper et al. 1987; Paterson 1993; Cooper & Paterson 2008). These Haast Schist hosted carbonatite dykes were previously considered to be the only classified carbonatites in New Zealand. The possibility of Tapuaenuku carbonatites would provide important constraints on the mechanisms of differentiation through the interaction of the mildly alkaline to highly alkaline magmas with carbonate enriched fluids in an alkaline intraplate rift system due to crustal thinning during the mid-Cretaceous extension and the magmatic conditions that formed the Tapuaenuku Igneous Complex.

This thesis presents: outcrop-scale field observations from the Little Gut stream, detailed hand sample descriptions, petrography and the geochemistry of the TIC lamprophyre dykes

and associated carbonatite veins. The key contribution of this thesis is the first classification of TIC carbonatite veins and their chemical and stable isotopic compositions.

1.2 RESEARCH AND OBJECTIVES

The objective of this research is to complete an evidence-based petrochemical classification of the carbonate-rich veins associated with the lamprophyric dykes present in the Tapuaenuku Igneous Complex. To achieve this primary objective, the following questions were used as a guide:

1) Are the TIC carbonate-rich veins: primary igneous carbonatite dykes, veins, secondary igneous (carbothermal) or secondary hydrothermal carbonate veins?
2) What types of mineralogy is present in the host and carbonate-rich veins?
3) What is the paragenetic sequence of the TIC and associated dykes and veins systems?

Table 1.1. Approaches taken to achieve research aims

Aims	Approach taken
Classify the carbonate veins associated with the lamprophyre dykes	Stable isotope analysis, XRD, XRF and polished thin section analysis for mineralogy
Determine the major and trace element chemistry of the carbonatites	pXRF and XRF analysis
Compare TIC $\delta^{13}C$ and the $\delta^{18}O$ isotopic values to the results of previously documented carbonatites	Stable isotope analysis; and review previous works
Document the mineralogy of the carbonatites	Interpret samples in polished thin sections for mineralogy under a transmitted light and reflected light microscope; XRD
Interpret the timing and relationships that the "carbonatite" dykes have with the other lithologies in the TIC	Detailed maps of the outcrop and polished thin section analysis for textures and structure
Describe the secondary alteration effects of the carbonatite intrusive have on the host rock lithologies	Interpret samples in polished thin sections for mineralogy and alteration under a transmitted light and reflective light microscope

To understand the geochemical and spatial relationships of the carbonatites in the lamprophyres; field work, laboratory and petrographical analysis were undertaken. The mineralogy was investigated using petrography in order to assess mineralisation, alteration and crystallinity. X-ray diffraction (XRD) was used to determine the carbonate mineralogy present in the sample suite. A portable X-ray fluorescence's spectrometer (pXRF) and in laboratory X-ray fluorescence spectrometer (XRF) were used to provide bulk rock chemical composition. Stable isotope analysis was used to determine whether the fluids that the carbonates were deposited from are primary or secondary source

1.3 THESIS STRUCTURE

Chapter 1 Introduction: This chapter provides an overview, the research aims, objectives and the outline of the thesis.

Chapter 2 Background information: Location, background geology, geochemistry and mineralogy of the TIC, specifically the lamprophyres are covered in this section. Additionally, an introduction to carbonatites, metasomatism, stable isotopes and the Alpine Haast Schist dyke swarm carbonatites is presented in this chapter.

Chapter 3 Materials and Methods: This chapter describes the methods used for sample collection, sample preparation, petrographical techniques and the geochemical analyses used to gain the data central to this thesis.

Chapter 4 Results: The results are divided into four sections: 1) petrography and hand sample descriptions and observations of spatial relationships. The alteration and the mineralisation present in the samples is described. 2) Whole rock geochemistry and comparisons of pXRF with XRF analysis. 3) Analysis of the crystalline structure of the carbonates by XRD. 4) Stable Isotope analysis of $\delta^{13}C$ and $\delta^{18}O$ to test the origin of the fluids that the carbonatites deposited from.

Chapter 5 Discussion: Results from chapter 4 are discussed in the context provided by mineralogical composition observed at outcrop-scale and through petrography, interpretation of the influence the intruding fluids had on the host rocks, presentation of the XRF geochemical variability at the outcrop-scale. This chapter also discusses the timing and the spatial relationships of the carbonatite veins have within the lamprophyre dykes. The results of the stable isotope data is evaluated and compared with the modal mineralogy percentages to classify the "carbonatite" dyke system.

Chapter 6: This chapter presents a summary of the thesis and some concluding statements regarding this research with an emphasis on the original contributions this thesis makes to our understanding of the mid-Cretaceous TIC.

CHAPTER 2: BACKGROUND

2.1 CARBONATITES

The classification of carbonatites varies, based on either their mineralogy and/or chemistry. The International Union of Geological Sciences (IUGS) define carbonatites as intrusive and extrusive igneous rocks in which the amount of primary carbonate is greater than 50 vol. % and containing less than 20 wt. % SiO_2 (Streckeisen 1979; Streckeisen 1980; Le Bas & Streckeisen 1991; Le Maitre et al. 2002). The IUGS carbonatite classification system is based on the mineralogical composition subdivided into four classes: calcite-carbonatite, dolomite-carbonatite, ferro-carbonatite (composed of Fe-rich carbonate minerals) and natro-carbonatite (composed of Na-K-Ca carbonates) (Streckeisen 1979; Streckeisen 1980; Le Bas & Streckeisen 1991; Le Maitre et al. 2002). The geochemical classification of carbonatites uses the weight percent of MgO-CaO-FeO+Fe_2O_3+MnO in the carbonate minerals and is subdivided into three classes: calcio-carbonatite (where CaO/(CaO+MgO+(FeO+Fe_2O_3+ MnO)) >80 wt. %), magnesio-carbonatite (where CaO/(CaO+MgO+(FeO+Fe_2O_3+MnO)) < 80 wt. % if Mg>F) and ferro-carbonatite (where CaO/(CaO+MgO+(FeO+Fe_2O_3+MnO)) < 80 wt. % if Mg<F) (Woolley & Kempe 1989; Lee et al. 2000). Where possible carbonatite classification is based on mineralogy (e.g. calcite-) and, if this is not possible, the chemistry of the carbonates is used to classify the carbonatite.

The carbonate content of an igneous rock is indicated by a prefix. If the carbonate content is less than 10 wt. % these rocks are deemed to be calcite-bearing/dolomite-bearing and between 10 and 50 wt. % are given the prefix modifiers calcitic/dolomitic (Streckeisen 1979; Streckeisen 1980; Woolley & Kempe 1989; Le Bas & Streckeisen 1991; Woolley et al. 1996; Le Maitre et al. 2002). The term carbonatite both refers to a name for a specific rock type and

a group name for a suite of genetically related rock types that is encompassed by wide range of primary igneous rocks that an carbonate enriched (Mitchell 2005; Tappe et al. 2006; Woolley & Kjarsgaard 2008b; Woolley & Kjarsgaard 2008a; Jones et al. 2013). As the IUGS carbonatite classification system is non-genetic system that is inadequate for diverse undersaturated potassic and plutonic rocks (Mitchell 2005; Woolley & Kjarsgaard 2008b; Woolley & Kjarsgaard 2008a; Mitchell 2012; Jones et al. 2013). Thus, the IUGS system is imprecise in its definition of carbonatites. In this system, any rock, regardless of its origin, with > 50% primary igneous carbonate is called a carbonatite. Consequently, the classification may include a wide spectrum from plutonic calcite (Mitchell 2005; Woolley & Kjarsgaard 2008a) or dolomite rich rocks (Mitchell 2005; Woolley & Kjarsgaard 2008a) to calcite veins formed by hydrothermal processes in the later stages of crystallisation of many types of magma (Deines 1989; Mitchell 2005; Woolley & Kjarsgaard 2008b; Woolley & Kjarsgaard 2008a; Jones et al. 2013). Grouping these modally similar, yet genetically distinct rock types has the potential to lead to misleading petrogenetic hypotheses (Mitchell 1979; Mitchell 1984; Mitchell 2005; Jones et al. 2013).

Mitchell (2005) proposed that any rock containing >30 wt.% of primary igneous carbonate regardless of silica content be classified as a carbonatite. This proposition recognises that through the chemical process of melting, separation of material, and outgassing, carbonatite-forming magma can generate a suite of genetically-related rocks in which the carbonate content varies significantly. Hence, an arbitrary amount of igneous carbonate present is less important than the fact that a suite of carbonate-bearing rocks are derived from same magma. The method proposed by Mitchell (2005) recognises that a wide variation in the modal percentages of the constituent minerals over small distances can be expected in the field and that a geographic domain can consist of a broad range of genetically related rocks types (Tappe et al. 2006; Woolley & Kjarsgaard 2008b; Woolley & Kjarsgaard 2008a). An

example is a rock composed of 30 wt. % calcite and 70 wt. % pyroxene is no less a carbonatite than the rock in close proximity composed of 51 wt. % calcite and 49 wt. % pyroxene. Variation of this magnitude is common in many plutonic carbonatite complexes (Mitchell 2005). Most authors agree, every carbonatite complex should be considered as a suite of rocks that are modally diverse but are derived from a common magmatic origin (Mitchell 2005; Tappe et al. 2006; Woolley & Kjarsgaard 2008b; Woolley & Kjarsgaard 2008a; Jones et al. 2013).

In an effort to provide a system for sub-classification, the concept of petrological 'clans' has been applied to carbonatites (Mitchell 2005). A petrological clan is defined when a particular magma type can be repeatedly produced in space and time and that a group of rocks with diverse mineralogy and textures can form through the differentiation of this parent magma (Woolley et al. 1996; Mitchell 2005, 2012). Two broad petrological clans of carbonatites are recognised globally using a mineralogical-genetic approach for the sub-classification of carbonatites: (1) magmatic carbonatites predominantly calcite and/or dolomite that are primary and are genetically related to nephelinite, melilitite, kimberlite and other mantle derived magmas and (2) carbohydrothermal (carbothermal residua (Mitchell 2005)) carbonatites derived from a wide variety of magmas. Carbothermal residua refer to low temperature fluids derived from magma dominated by CO_2-H_2O with some fluorine in variable proportions that precipitate at sub-solidus temperatures (Mitchell 2005; Woolley & Church 2005; Woolley & Kjarsgaard 2008b). Intrusive carbonatites associated with melilitite clan rocks are typically important sources of Nb, Ti and P, but not Rare Earth Elements (REE) (Le Bas et al. 1997; Mitchell 2005; Tappe et al. 2006; Jones et al. 2013). Carbothermal fluids typically concentrate the REE, Sr, Ba, but not Nb (Mitchell 2005; Tappe et al. 2006; Jones et al. 2013).

Experimental studies of synthetic carbonated upper mantle source rock have been used to provide insights into the genesis of primary carbonatitic magmas and carbonate liquid immiscibility and fractionation (Le Bas 1989; Mitchell 2005; Woolley & Kjarsgaard 2008a; Klein-BenDavid et al. 2009; Mitchell 2012; Jones et al. 2013; Kaminsky et al. 2013). Isotopic studies have corroborated that athenospheric and/or lithospheric mantle sources play a role in the genesis of carbonatites but has confused the relationship with associated silicate rocks (Mitchell 2005; Woolley & Kjarsgaard 2008a; Jones et al. 2013). A lack of clarity regarding the paragenesis of carbonatites is in part due to the common consideration that all carbonatites are a single rock type of derivation from a common parent magma, rather than a diverse group of rocks that come from a variety of origins (Mitchell 2005; Woolley & Kjarsgaard 2008a; Bell & Simonetti 2010; Jones et al. 2013). Mitchell (2005) suggests that an approach that regards not all carbonatites as petrographically synonymous rock but instead regards carbonatites as petrologically distinctive rocks with respect to their antecedents and descendents.

In light of these earlier works, the three main theories for the petrogenesis of carbonatites are:

1. Residual melts of fractionated carbonate nephelinite or melilitite (Gittins 1989; Gittins & Jago 1998; Jones et al. 2013)
2. Immiscible melt fractions of CO_2 saturated silicate melts (Freestone & Hamilton 1980; Amundsen 1987; Kjarsgaard & Hamilton 1988, 1989; Brooker & Hamilton 1990; Kjarsgaard & Peterson 1991; Church & Jones 1995; Lee & Wyllie 1997; Dawson 1998; Halama et al. 2005; Brooker & Kjarsgaard 2010; Jones et al. 2013).
3. Generation of primary mantle melts from partial melting of CO_2 bearing peridotite (Wallace & Green 1988; Sweeney 1994; Harmer et al. 1998; Ying et al. 2004; Jones et al. 2013).

The origin of the parental melt of carbonatites is complex with the majority of carbonatites restricted to continental areas (Bell & Simonetti 2010). Constraints imposed from carbonatites worldwide by both radiogenic and stable isotopic data is consistent with a sub-lithospheric source for the parental melts (Bell & Simonetti 2010). These may be associated with either asthenospheric 'upwellings' or more deep seated, plume related activity (Bell & Simonetti 2010). Conversely, lithospheric controls in the recent global compilation of carbonatite ages argues against the mantle plume theory (Woolley & Bailey 2012). In at least three carbonatite-bearing provinces, carbonatite emplacement has repeated with up to five episodes from the late Archean to relatively recent times. Over this time, the drift of the plates precludes any direct role for mantle plumes in carbonatite genesis (Woolley & Bailey 2012).

Carbon and oxygen isotope compositions are used to distinguish the paragenesis of the carbonatites and can be used to determine differences in magmatic conditions. Initial carbon and oxygen isotope studies of carbonatites suggested that they were homogenous with a $\delta^{18}O$ and $\delta^{13}C$ range of 6.0 to 8.5‰ and -5.1 to -7.3‰, respectively (Taylor et al. 1967). Later studies have corroborated values within the range specified by Taylor et al. (1967) but also included a significant number of carbonatites with higher $\delta^{13}C$ and $\delta^{18}O$ values (Deines & Gold 1973; Pineau et al. 1973; Nelson et al. 1988; Censi et al. 1989; Deines 1989; Le Bas 1989; Santos et al. 1990; Santos & Clayton 1995; Jones et al. 2013). Although $\delta^{18}O$ values of carbonates in carbonatites range from 5 to 25‰, about 50% of intrusive carbonatites range between 6 to 9‰. In contrast, carbonatite veins and dykes have a wider range of $\delta^{18}O$ with only 4% and 26% of $\delta^{18}O$ values between 6 to 9‰, respectively (Deines 1989). The $\delta^{13}C$ values are more constrained than $\delta^{18}O$ values; about 90% of $\delta^{13}C$ values fall between -2 and -8‰ (Deines 1989; Woolley & Kjarsgaard 2008b; Woolley & Kjarsgaard 2008a). A large number of the carbonatites worldwide are associated with central type alkaline complexes

(Woolley & Kjarsgaard 2008a). These complexes can range from deep-seated plutonic complexes right through to volcanic complexes (Deines 1989; Reid & Cooper 1992; Santos & Clayton 1995; Woolley & Church 2005; Woolley & Kjarsgaard 2008a). In the latter case, pervasive hydrothermal alteration to the country rock is common (Deines 1989; Woolley & Church 2005).

Oxygen and carbon isotopic composition variation is indicative of variety of processes including loss of fluids during emplacement, emplacement level, secondary and low-temperature interaction of carbonate with meteoric fluids, or assimilation and magmatic Rayleigh fractionation effects (Figure 2.1) (Blattner & Cooper 1973; Deines & Gold 1973; Deines 1989; Santos et al. 1990; Santos & Clayton 1995; Tappe et al. 2006; Jones et al. 2013). Shallower complexes and dykes and veins can have a wider range in $\delta^{13}C$ and $\delta^{18}O$ isotopic composition in comparison to deep seated complexes due to greater surface area of carbonatite and the proximity to near surface processes (Blattner & Cooper 1973; Deines & Gold 1973; Deines 1989; Santos et al. 1990; Santos & Clayton 1995; Tappe et al. 2006; Jones et al. 2013). The degree of secondary isotope exchange in carbonatite dykes and veins can partially explain the $\delta^{18}O$ isotope variation (Deines & Gold 1973; Deines 1989). The origins of the magmatic melt or the carbohydrothermal fluids also play an important role in the isotope variance (Deines 1989; Santos & Clayton 1995; Mitchell 2005; Tappe et al. 2006; Woolley & Kjarsgaard 2008b; Woolley & Kjarsgaard 2008a; Jones et al. 2013) as does the carbonate mineralogy (Deines 1989; Le Bas et al. 1997; Le Roex & Lanyon 1998; Lee et al. 2000; Lee & Wyllie 2000).

In order to divide carbonatites into three categories based on isotopic composition Pineau and others (1973) proposed: (1) carbonatites that have $\delta^{13}C$ and $\delta^{18}O$ values typical of mantle rock, (2) carbonatites which have variations in $\delta^{18}O$ values which can be correlate with the

variations in $\delta^{13}C$ values, and finally (3) carbonatites that $\delta^{18}O$ values which do not correlate with the variations in $\delta^{13}C$ values. Pineau et al. (1973) suggested that the variations in the $\delta^{13}C$ and $\delta^{18}O$ isotopic composition from groups 2 and 3 can be explained by late magmatic and deuteric processes. However, Nelson and others (1988) argued that variations in the $\delta^{13}C$ and $\delta^{18}O$ isotopic compositions may be, partly at least, related to the isotopic heterogeneity of the mantle source. Deines (1989) hypothesised after his review of $\delta^{13}C$ and $\delta^{18}O$ isotopic composition of carbonatites that magmatic processes related to the formation of carbonatite magma or the nature of the primary reservoir within the mantle can be attributed to isotopic variations.

Figure 2.1. Isotopic composition of carbonatite bodies worldwide. Oxygen ratios are measured relative to Vienna Standard Mean Ocean Water (SMOW) and carbon isotopes are measured against Vienna Pee Dee Belemnite (VPDB). Modified from Taylor et al. (1966) and Blattner and Cooper (1973).

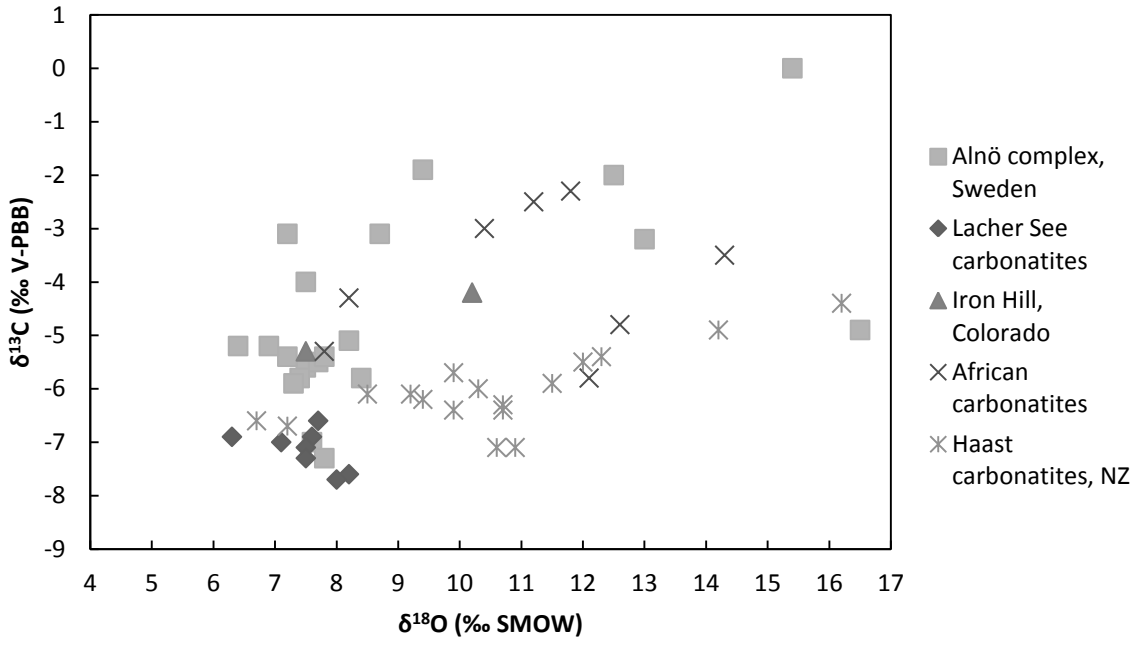

The interactions of hydrothermal fluids mostly explain variations in $\delta^{18}O$, whilst $\delta^{13}C$ variations can be explained as both primary (i.e., isotopic composition of the carbonatites parental magma) and secondary (i.e., hydrothermal alteration) processes (Taylor et al. 1967; Pineau et al. 1973; Deines 1989; Santos & Clayton 1995). The determination to the extent of the variations in $\delta^{13}C$ and $\delta^{18}O$ and whether they are primary related or crustal processes has

major implications in the evaluation of the isotopic composition of their mantle source (Deines 1989; Santos & Clayton 1995; Mitchell 2005; Tappe et al. 2006; Woolley & Kjarsgaard 2008b; Woolley & Kjarsgaard 2008a; Jones et al. 2013). These variations also give valuable insight into the mantle isotopic heterogeneity, recycling of crustal material into the magma, and the relationships between parental magma of the carbonatite and magmas associated with the host complex (Barker 1989; Deines 1989; Santos & Clayton 1995; Mitchell 2005; Tappe et al. 2006; Woolley & Kjarsgaard 2008b; Woolley & Kjarsgaard 2008a; Jones et al. 2013).

2.2 CARBONATITE OCCURENCES IN NEW ZEALAND

In north-western Otago, a late-Oligocene to early-Miocene (32-20 Ma) regional dyke swarm (Haast Alpine Dyke Swarm) intrudes the Haast Schist basement (Cooper 1971, 1986; Barreiro & Cooper 1987; Cooper et al. 1987; Cooper & Paterson 2008). The Haast Alpine Dyke Swarm is predominantly composed of lamprophyres and also contains carbonatite dykes that are typically <30 cm wide. These carbonatite dykes are currently considered to be the only correctly classified carbonatites in New Zealand (Cooper 1971, 1986; Cooper et al. 1987; Cooper & Paterson 2008; Woolley & Kjarsgaard 2008b; Woolley & Kjarsgaard 2008a). This thesis introduces and classifies the second occurrence of carbonatites in New Zealand and an additional instance of carbonatites associated with lamprophyres at the Tapuaenuku Igneous Complex.

2.3 TAPUAENUKU IGNEOUS COMPLEX

The Tapuaenuku Plutonic Complex (TPC) is a sub-circular alkaline igneous layered intrusion approximately 7 km in diameter outcropping in the Inland Kaikoura range, northeast Marlborough at the north-eastern end of the South Island of New Zealand (Fig. 2.3). Mt

Tapuaenuku, at 2,885 m asl, is amongst the highest peaks in the Inland Kaikoura Range (Challis 1961; Nicol 1977; Baker 1990; Baker et al. 1994; Rattenbury et al. 2006). A radial dyke swarm, centered on the TPC, cuts Torlesse Group greywacke and is Jurassic-Early Cretaceous age (201.3-100.5 Ma) and younger strata up to Ngaterian age (99.5-95.2 Ma) (Grapes 1972, 1975; Baker 1990; Baker et al. 1994; Baker & Seward 1996). Together the TPC and the radial dyke swarm form the Tapuaenuku Igneous Complex (TIC) (Baker 1990; Baker et al. 1994). Faulting coeval with the TIC creates a number of unconformities (Challis 1961; Nicol 1977; Baker 1990; Baker et al. 1994; Rattenbury et al. 2006; Timm et al. 2010). The Torlesse Group greywacke (210 ± 10 Ma) is the oldest rock that is exposed in the region (Lensen 1962; Nicol 1977; Baker 1990; Adams 2003; Rattenbury et al. 2006; Timm et al. 2010). The greywacke is complexly deformed and is comprised of massive sandstone and alternating greywacke/argillite (Lensen 1962; Baker 1990; Rattenbury et al. 2006).

Figure 2.2. Looking down the Hodder River from the staircase ridge. Photo-Matt Hanson, 17/5/2014.

Table 2.1. Geochronological data of the Tapuaenuku Igneous Complex (TIC) and associated igneous rocks. Modified from Baker (1994)

Igneous suite	Rock description and locality	Age (Ma)	Dating technique	Source
Tapuaenuku Plutonic Complex	Kaersutite mineral separate from a pegmatite dyke	101.2±1.4	K-Ar	Nicol (1977)
	Suite of plutonic rocks from the TPC	90±8	Rb-Sr	Baker (1990)
	Zircon (quartz syenite)	93±10	fission track	Baker (1990)
	Titanite (phonotephrite)	103±11	fission track	Baker (1990)
Radial dyke swarm	21 basanite and trachybasalt dykes, Awatere Valley	59.8±1.1 to 100±1.4	K-Ar	Grapes et al. (1992)
	Trachybasalt dyke, Awatere Valley	98.9±3.2	K-Ar	George (1988)
Lookout Volcanics	Six trachybasalt flows, Awatere Valley	90.3±1.6 to 99.9±0.7	K-Ar	Nicol (unpublished)
Gridiron Volcanics	Trachybasalt flows, Clarence Valley	93.5±2.0 to 98.3±1.3	K-Ar	Reay (1993)
Mandamus Igneous Complex	Suite of plutonic and volcanic rocks plus mineral separates.	97.2±1.2	Rb-Sr	Weaver and Pankhurst (1991)
Mt Somers Volcanic Group	Suite of rhyolites, Mt Somers	89.3±2.0	Rb-Sr	Barley et al. (1988)
	Suite of volcanics, Banks Peninsula	80.9±1.9	Rb-Sr	Barley et al. (1988)
	Whole rock and mineral ages	85-98	K-Ar	Oliver and Keene (1989)
Chatham Island Cretaceous volcanics	Basaltic dyke and flows	68.6-79.4	K-Ar	Grindley et al. (1977)

Outside of the TIC the basement is unconformably overlain by marine shale and glauconitic sandstone of Motuan age (99.5-103.3 Ma), which grade upwards into shallow water marine or terrestrial sediments of Ngaterian age (Challis 1961; Allen 1962; Nicol 1977; Challis 1978; Baker 1990; Baker et al. 1994; Baker & Seward 1996; Rattenbury et al. 2006; Bartholomew 2012). The Awatere and Clarence Faults to the west and east, respectively, confine the Inland Kaikoura Range. This faulting dominates the landscape, the Awatere and Clarence Rivers follows the course of the fault angle compression. The TIC geology has created steep topography causing drainage to flow although steep streams and rivers into the

two major rivers. The lack of vegetation and high climate has accelerated the erosion rates of this steep country (Fig. 2.2). This erosion coupled with extensive Quaternary glaciation, has created a landscape of steep bluffs and rocky peaks. At the foot of Mt Tapuaenuku are large scree slopes and valleys (Fig. 2.2).

Table 2.1 summarises geochronological data for the TPC, radial dyke swarm and other associated Cretaceous igneous rocks from Marlborough, Canterbury and the Chatham Rise. Dating of the TIC has been completed by a number of authors and the dates appear to correlate well (Nicol 1977; Challis 1978; Baker et al. 1994). Nicol (1977) used K-Ar analysis on a kaersutite (sample R6184 in his thesis) from a Tapuaenuku pegmatite to date 98.9 Ma. Baker (1990) recalculated the decay constants as per Steiger and Jager (1977) and dated the complex to 101.2 ± 1.4 Ma (Baker 1990; Weaver & Pankhurst 1991). The TIC is both geographically and compositionally associated with the mafic volcanics of the Lookout Formation, Awatere Valley (Baker 1990; Weaver & Pankhurst 1991; Baker et al. 1994; Rattenbury et al. 2006) and the Gridiron Formation, Clarence Valley (Weaver & Pankhurst 1991; Rattenbury et al. 2006).

2.4 GEOLOGY

The TIC is subdivided into eight major intrusive units (Baker 1990; Baker et al. 1994). The intrusion has an irregular elliptical shape and is comprises of an area of 35 km^2 (Fig. 2.3). In order of age based on cross-cutting relationships (Baker 1990; Baker et al. 1994) the TIC is comprised of:

1. Radial dyke swarm composed of basanite, trachybasalt, and shoshonite/latite dykes(Baker 1990; Baker et al. 1994).

2. Layered Series (LS) includes cumulate rocks forming the Lower Layered Series (LLS) and the Upper Layered Series (ULS) (Nicol 1977; Baker 1990; Baker et al. 1994). The LLS is principally gabbro, melanogabbro and pyroxenite layers with a thickness *c.* 1,700 m. Layers vary between *c.*200-500 m of monotonous layers of pyroxenites and melanogabbro to section of smaller scale alternations (*c.*10 m) of gabbro and leucogabbro. The ULS is a mixture of layered gabbro, leucogabbro monzogabbro and monzonite. The total thickness of the ULS is *c.*1,300 m (Baker 1990; Baker et al. 1994).
3. The Staircase Intrusives comprised of cumulate gabbro, noncumulate gabbro and monzogabbro. An extensive cone sheet intrusion along at the contact of the Staircase Intrusives and the Layered Series is present (Nicol 1977; Baker 1990; Baker et al. 1994). This sheath is a discontinuous layered gabbro.
4. Lower Hodder Gabbro and minor gabbroic intrusives are small stocks of noncumulate gabbro, monzogabbro, and monzonite that outcrop in the lower and upper Hodder River (Baker 1990; Baker et al. 1994). The Lower Hodder gabbro outcrops differ from the more evolved upper Hodder minor intrusives (Baker 1990; Baker et al. 1994).
5. The Red Hills Breccia Pipe encompasses the heterolithic breccias emplaced in a pipe or diatreme (Baker 1990; Baker et al. 1994). Two outcrops in close proximity and their lithological distinctness indicates they were formed in the same event (Nicol 1977; Baker 1990; Baker et al. 1994).
6. Hodder Intrusives are monzonite and sodalite syenite laccolith which intrude into the LS. The Hodder Intrusives along with the strongly alkaline dykes are the only plutonic rocks that contain modal feldspathoid minerals (Nicol 1977; Baker 1990; Baker et al. 1994).

7. Monzonite, orthoclase syenite and quartz syenite sills and dykes. These lithologies are present in two large sills that are distinctly more felsic than the adjacent cumulates intrude the ULS.
8. Highly alkaline lamprophyre, phonotephrite, tephriphonolite, and phonolite dykes. Melano- to mesocratic lamprophyre dykes cut all the intrusive units of the TPC (Nicol 1977; Baker 1990; Baker et al. 1994). These lamprophyres are most abundant in the LS and SI near the western margin of the complex (Nicol 1977; Baker 1990; Baker et al. 1994). The lamprophyres are irregular or sinuous dykes and veinlets which vary in width from 0.1 to 5 m (Nicol 1977; Baker 1990; Baker et al. 1994; Baker & Seward 1996; Jongens et al. 2012). It is in these dykes in the Lower Layered Series that the carbonatites veins are outcropping.

Cross-cutting all the intrusive units of the Tapuaenuku Igneous Complex are a series of melano-mesocratic lamprophyre dykes, most abundant in the Layered Series (LS) and the Staircase Intrusives (Baker 1990; Baker et al. 1994). These dykes and veinlets are irregular or sinuous and vary in width from 0.1-5 m and some have indistinct chilled margins, more commonly in the LS (Baker 1990; Baker et al. 1994). Lamprophyres in the LS are sub-parallel to the layering, with the lamprophyre irregular and sinuous in the other lithologies. This is suggestive of plastic deformation in a still partially molten semi-plastic host (Baker 1990; Baker et al. 1994).

The lamprophyres are typically aphyric to porphyritic. Individual dykes have varied textures and mineralogy. Large euhedral clinopyroxene and kaersutite phenocrysts are characteristic of this suite (Baker 1990; Baker et al. 1994). Titian-aluminian (-subsilic) diopside, kaersutite, titanomagnetite, ilmenite and apatite generally make up the phenocrysts, which are set in a

ground mass, that can be partially isotropic, of analcite, nepheline, altered feldspar (andesine), amphibole (Baker 1990; Baker et al. 1994).

Figure 2.3 Orientation map of New Zealand with the location of Mt Tapuaenuku (A). Topographic and geologic map of the Tapuaenuku Igneous Complex and Little Gut Creek (LGC) carbonatite field area. Geologic map modified from Jongens et al. (2012). (Map data sources see Appendix A).

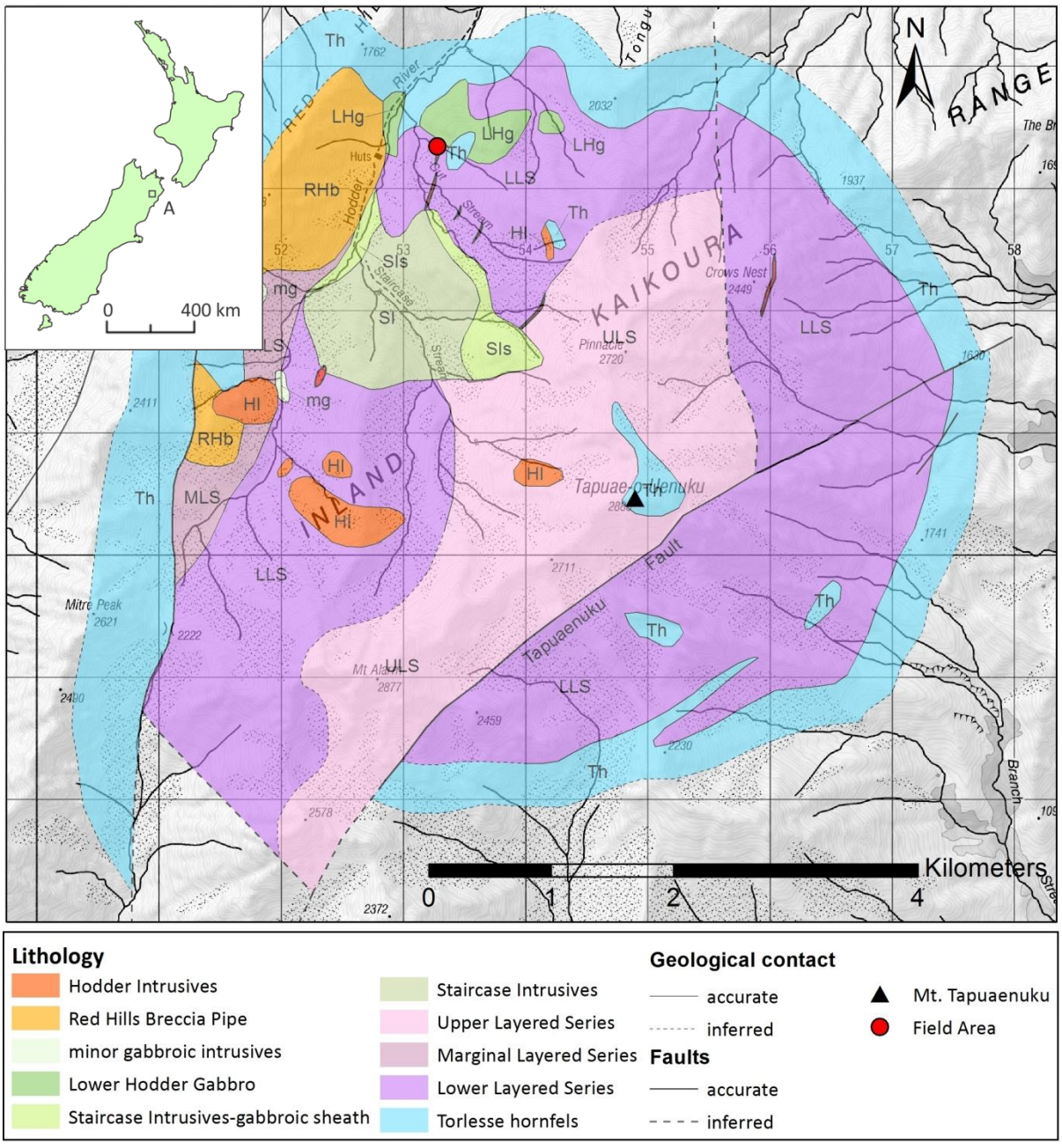

A trachytic texture seen in some of the dykes is due to numerous orientated micro-phenocrysts of kaersutite (Nicol 1977; Baker 1990; Baker et al. 1994). Clinopyroxene crystals commonly exhibit complex zoning and/or resorption textures (Baker 1990; Baker et

al. 1994). They can be up to 1 mm in size. Crystals commonly exhibit oscillatory zoning and continuous zoning from core to rim, sector zoning is also not uncommon (Baker 1990; Baker et al. 1994). Fe-Ti oxides are commonly grouped together with clinopyroxene phenocrysts to form glomeroporphyritic aggregates (Baker 1990). Amphibole is typically kaersutite (brown (X) to deep brown (Z) pleochroism) in the form of acicular crystals or basal sections with lengths and diameters of 0.3 mm and 0.05 mm respectively (Baker 1990). Fe-Ti oxides are 0.02 to 0.5 mm size and are scattered throughout the groundmass. Groundmass is composed of partially isotropic (glass) due to the replacement and alteration of the feldspathoid and feldspars by analcite (Baker 1990; Baker et al. 1994).

Petrographically as they contain phenocrysts of kaersutite and aluminous titanaugite in a groundmass of clinopyroxene, amphibole, plagioclase (andesine and labradorite), the lamprophyres can be classified as camptonites as per Rock (1987), Le Maitre et al. (2002), Streckeisen (1980) and Le Bas (2000). The camptonite lamprophyres signify alkali-enriched, volatile residual melts produced during crystallisation of the layered plutonic rocks (Baker et al. 1994). Crystallisation of amphibole rather than plagioclase was favoured due to the abundant alkalis and volatiles concentrated in the residual melt (Baker 1990; Baker et al. 1994). Extreme and intricate zoning of clinopyroxene and amphibole, coupled with the occurrence of large euhedral crystals, implies crystallisation from a volatile-enriched melt of rapidly changing composition (Baker et al. 1994). Thus the lamprophyre dyke melt could have served as the parental melt for the later emplacement of the cross-cutting carbonatites.

CHAPTER 3: METHODS AND MATERIALS

3.1 FIELDWORK AND SAMPLE COLLECTION

Fieldwork was undertaken in one period of 7 days in late May 2014 at Mount Tapuaenuku, Inland Kaikoura Range, South Island, New Zealand. Three sites were examined in the field; of these, the Little Gut Creek (LGC) site was examined in detail. Outcrop and hand sample descriptions, detailed mapping, field logs, sketches and photographs were used to record the structure, texture and composition of the TIC outcrops. Vertical and horizontal transects were used in order to provide a spatial reference frame work of the LGC outcrop. Fresh rock samples were collected along the vertical transect and analysed using an Olympus Innov-X Alpha Series Portable X-Ray Fluorescence (pXRF). Site investigation and sample transect line positions were logged using a Garmin GPSMAP62s (GPS). All samples are catalogued in the Department of Geological Sciences rock and mineral collection at the University of Canterbury.

The Inland Kaikoura Range experiences a wide range of weather conditions. During the summer, temperatures tend to be high, typically around 20-30° C, and rainfall is low with relatively stable weather patterns through mid-autumn. Heavy snowfalls in winter are common and snow will often settle in valleys. From mid-winter to late spring snow generally covers the range above 1500 m. During this period geological fieldwork is extremely difficult to not possible due to the extensive snow cover. In spring, the snow quickly melts and typically no permanent snow remains in the summer to early autumn, although snowfalls occur occasionally during periods of inclement weather.

Access to the field site is via a 15 km hike up the Hodder River with some 80 river crossings or by helicopter. Fieldwork for this study was based from the Hodder Hut (1470 m) (Fig.

3.1), located in the headwaters of the Hodder River, on the western margin of the Tapuaenuku intrusive site.

Figure 3.1 Hodder Hut located in the headwaters of the Hodder River below Mt Tapuaenuku. Photo Patrick Turner, 18/05/2014.

3.2 SAMPLE COLLECTION AND PREPARATION

Each hand sample at all three field sites (LGC, BGB and USC) were designated a number and its position within the vertical transect was recorded. Rock samples ranged from 20 to 250 grams. Some sampling locations were deemed 'not safe' due to exposure and terrain and only pXRF data was collected. Samples were labelled, photographed and bagged carefully to avoid breaking up any semi-consolidated or fragile samples during collection and sample preparation. These were then transported off of the mountain and back to the University of

Canterbury. Hand samples were photographed and cut with a rock saw for thin sectioning. A portion of each sample was retained for geochemical analysis and cataloguing. Polished thin sections were prepared in the Department of Geological Sciences at the University of Canterbury from all the hand samples taken. Using the Gilco LRM ring mill at CRL Energy Ltd in Christchurch all LGC samples were crushed and sieved into powders for whole rock geochemical analysis. Sample powders were then analysed by X-ray Fluorescence (XRF) and X-Ray Diffraction (XRD) by Stephen Brown from the Department of Geological Sciences, University of Canterbury. Note the mill head of the ring mill is made from Cr-Mo alloy and may contribute some trace elements to the sample.

3.3 PORTABLE X-RAY FLORESCENCE SPECTROMETER (pXRF)

Single spot readings of 1 minute using an Olympus Innov-X Alpha Series Portable X-Ray Fluorescence (pXRF) (Corporation 2015) from the University of Otago were conducted both in the field and on freshly cut hand samples in the lab. Freshly cut surfaces of the leftover samples were then analysed with the pXRF in the lab in order to perform a direct comparison of pXRF datasets. These devices return the most accurate results when performed on a flat clean surface. In the field this was not possible due to the roughness of the outcrop. Single spot readings greatly reduce the accuracy of the chemical abundances potentially present in the sample due to the lack of coverage in the analysis (Mackay & Simandl 2013; Mackay 2014; Simandl et al. 2014b; Simandl et al. 2014a). Averaged spot readings of the same sample give a far more representative chemistry of the rock (Mackay & Simandl 2013; Mackay 2014; Simandl et al. 2014b; Simandl et al. 2014a). Core scanning with the pXRF (Mackay & Simandl 2013; Mackay 2014; Simandl et al. 2014b; Simandl et al. 2014a) is another method to reduce the degree of variation associated with spot analyses. Core scanning provides a broader and more representative chemical analyses but the data is limited

by the inability of the operator to maintain constant scanning speed (Mackay & Simandl 2013; Mackay 2014; Simandl et al. 2014b; Simandl et al. 2014a). In this research multiple spot readings and core scanning methods were not utilised as all samples were analysed by conventional XRF techniques instead. This enabled comparative analyses of trace element data from the pXRF relative conventional XRF spectrometer data.

3.4 X-RAY FLORESCENCE SPECTROMETER (XRF)

Powdered samples were analysed by XRF in the Department of Geological Sciences, University of Canterbury. Data were using a Phillips PW2400 Sequential Wavelength Dispersive X-ray Fluorescence Spectrometer. The preparation of the glass fusion beads for major element analysis included fusing together 1.3 g of rock powder with 6.98 g of flux ($Li_2B_4O_7$, Li_2O and La_2O_3 mixture) and a few grains of oxidant (NH_4NO_3) at 1030 ˚C for at least 15 minutes in Pt/Au crucibles. After fusion the loss on ignition was calculated. The molten material was then poured into Pt/Au moulds which are cooled rapidly forming glass beads. The major elemental chemistry is determined on the glass fusion beads using a rhodium tube set at 50KV/55mA. Major element compositions including SiO_2, TiO_2, Al_2O_3, Fe_2O_3T, MnO, MgO, CaO, Na_2O, K_2O, and P_2O_5 were analysed. The pressed powder pellets for the trace element analysis were formed by pressing in a hardened steel die at 3,000 psi for 10 seconds approximately 8 g of rock powder with a polyvinyl alcohol solution as the binder. These pellets are approximately 32 mm in diameter. A rhodium tube set at 60KV/46mA is used to determine the trace element chemistry. Trace elements include; Vr, Cr, Ni, Zn, Zr, Nb, Bz, La, Ce, Nd, Ga, Pb, Rb, Sr, Th and Y.

3.5 X-RAY DIFFRACTION (XRD)

Hand sample mineralogy was determined by XRD at the Department of Geological Sciences, University of Canterbury. Oriented mounts were created by mixing the thirteen finely crushed powder samples with ethanol to form slurry which was then transferred to a half a microscope slide as a thin layer (orientated mount) using a disposable pipette and allowed to dry at room temperature. Each sample was ground in agate mortar and pestle with the addition of ethanol to form a slurry. The slurry was transferred to half a microscope slide as a thin layer (orientated mount) using a disposable pipette and allowed to dry at room temperature. XRD analyses were performed using a Philips W1729 X-ray generator (50kV/40mA) with a PW2273/20 Long fine focus 2.2kW Cu anode x-ray tube followed by a PW1752/00 monochromator, a PW1711/10 Sealed Gas (Xe) filled proportional detector and finally the PW 1710 Diffractometer control, which was connected to a computer with Visual XRD controller software. Traces (Version 4) search-match software using the Hanawalt search-match algorithm was applied to each XRD spectrogram. The samples were scanned from 3° to 70° (2Θ) with a step size of 0.02° (2Θ) and scan speed of 0.02 degrees (2Θ) per second.

3.6 OPTICAL PETROGRAPHY

Polished thin sections of samples were analysed for petrographic analysis using a Meiji Techno MT9420 compound, polarising microscope. Diagnostic properties were used to designate major and minor mineral species. Modal mineralogy percentages were estimated, and textures identified in thin section. The samples were viewed in plane polarised transmitted and reflected light settings of the microscope. Digital images of the thin sections were taken with a Leica DM 2500P petrological microscope with a Leica DFC295 camera and Lieca Application Suite software package (Microsystems 2015).

3.7 STABLE ISOTOPE

Approximately 500 µg of powdered carbonate was required for carbonate $\delta^{13}C$ and $\delta^{18}O$ determinations. Each of the thirteen cut samples were drilled in several locations. These samples were then designated with their root sample name and the number of the drill sample (Appendix E), corresponding to the matching thin sections. The location of the drill locations were photographed using a Nikon P600 digital camera (Appendix E, Fig. E2). Carbonate minerals and host minerals were powdered and separated from host-rocks using a standard dentist's drill. A standard weighing paper funnel was used to capture the carbonate powder and placed into a glass vial that was sealed with a rubber septum lined screw-top.

Sample powders were analysed for $\delta^{13}C$ and $\delta^{18}O$ as per the procedure of Horton and others (2003). Approximately 500 µg of carbonate powder were reacted for at least 12 hrs with anhydrous phosphoric acid (103%) at 25 °C. After 12 hrs the sample vessels were flushed. Carbon dioxide gas generated in the acid-carbonate reaction was analysed at the University of Canterbury Stable Isotope Laboratory using a Thermo Scientific Gas Bench II connected to a Delta V Plus gas Isotope Ratio Mass under continuous flow conditions. The precision of stable-isotopic analyses is ± 0.2‰ for oxygen and carbon, based on replicate analysis of NBS-18 and NBS-19 certified reference materials.

CHAPTER 4: RESULTS

4.1 FIELD RELATIONSHIPS

The Little Gut Creek outcrop is on the western margin of the Tapuaenuku Igneous Complex. Little Gut Creek is a steep alpine tributary of Gut Stream, a tributary stream flowing into the Hodder Stream (Fig. 2.3). The outcrop is stream-cut in the centre of the Little Gut Creek located at New Zealand Map Grid (NZGM) reference Easting 1653246 and Northing 5353368 (Fig. 2.3). All field observations and hand sample data reported in this chapter were collected at this site. Thirteen samples were taken from a 3 metre vertical transect of the outcrop spanning structural features across the outcrop see Figure 4.1. The outcrop is composed of two lamprophyre dykes (bearing of 160°) contacting the olivine gabbro host one metre above the transect and between LGC samples 11 and 12 (Fig. 4.1). The two lamprophyre dykes are cross-cut by a series of carbonate veins and veinlets (Fig. 4.2 and 4.3). The transect lithologies were subdivided into four main groups (Fig. 4.1; olivine gabbro, lamprophyre with adjacent chilled margin, and carbonatite veins and veinlets). Each of these groups will be discussed in more detail below.

4.1.1 Olivine Gabbro

At the LGC site, the Lower Layered Series (LLS) is the predominant lithology of area with several samples from the surrounding collected. An unaltered sample from above the vertical transect is a phaneritic, massive, black and white peppered mafic rock, with fine to medium-grained (0.1-5 mm) crystals. Layering of this unit strikes at 160° and dips 40°. Plagioclase (~40 vol. %) phenocrysts are well developed and show interlocking texture.

Figure 4.1. A: The LGC transect with locations of sample and pXRF analyses indicated. B: Cut hand specimens with black circles indicating stable isotope analysis drill locations.

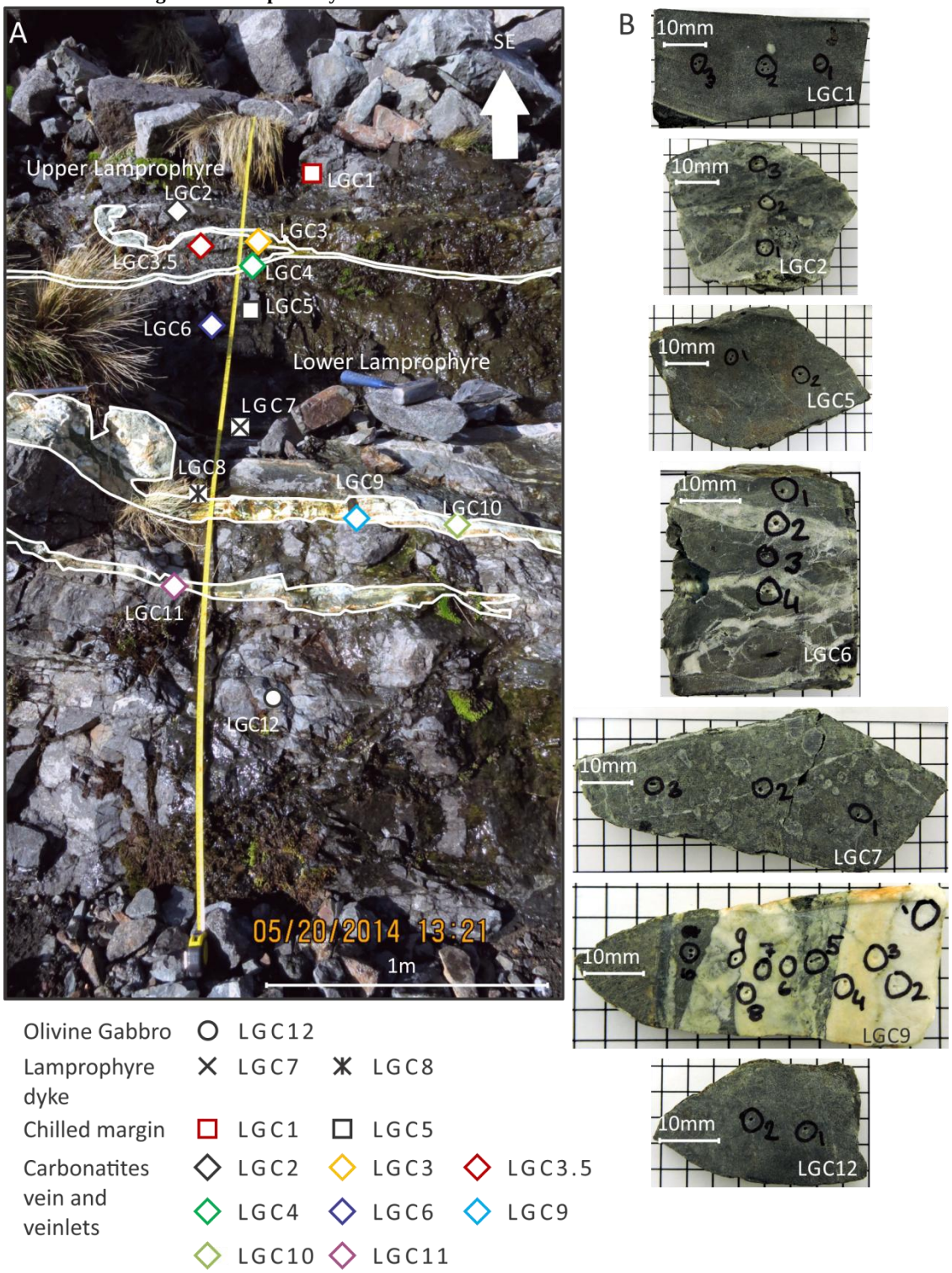

Clinopyroxene (~30 vol. %) crystals are euhedral to subhedral with subhedral olivine (~15 vol. %). LGC 12 is a more fine-grained sample of the layered mafic host which is also locally pervasively altered to clays. One metre above LGC 1 (i.e., the top most sample of the

transect) more layered olivine gabbro outcrops (Fig. 4.1). LGC 12 also includes occasional chaotic spider veinlets of carbonate

4.1.2 Lamprophyre

The majority of the transect is comprised of the lamprophyre suite which cross-cuts the LLS olivine gabbro along a strike of ~160° in conjunction to the layering of the LLS. Two lamprophyre (upper and lower) dykes contact each other, forming the dyke suite (Fig. 4.1). Both of these dykes exhibit distinct, very fine-grained to glass chilled margins. Where the upper lamprophyre contacts the olivine gabbro a gradational chilled margin is present. The contact is sharp and linear. A second chilled margin is present at samples LGC 5 and 6 between the two dykes (Fig. 4.1). In contrast, the lower lamprophyre's contact with the olivine gabbro between LGC 11 and 12 does not display a chilled margin. Both of these dykes exhibit distinct gradational chilled margins which are comprised of very fine-grained crystals to glass. Both dykes are porphyritic, massive, dark greyish to black in colour, with coarse-grained phenocrysts in a fine-grained groundmass. The samples contain coarse-grained (2-5 mm) euhedral amphibole and clinopyroxene phenocrysts within a glassy groundmass containing microcrystalline feldspar and pyroxenes. The samples taken from within the chilled margins of the dykes (i.e., LGC 1, 5 and 6) is aphanitic, dark greenish grey and appears slightly weathered with occasional feldspar and amphibole phenocrysts.

4.1.3 Carbonatite veins and veinlets

The carbonatites appear as veins and veinlets that range from 0.5 to 50mm thick (Fig. 4.2 and 4.3). Carbonatite veins cross-cut the mafic units parallel to the orientation of the lamprophyre. In the upper part of the dyke suite, spider, chaotic and thinner carbonate veins and veinlets are typical (Fig. 4.2). The carbonate in these veins predominantly appears chalky, brittle and ‘turbid’ with the occasional clean, pure, ‘limpid’ veinlet (See Fig.4.3 and

4.7) (de Oliveira Cordeiro et al. 2011). The carbonate veins in the lower lamprophyre have both turbid and limpid carbonate (Fig. 4.2). The veins appear as planar laminates with the centre limpid, clean euhedral carbonate and the outer edges of the laminates are turbid, iron stained and brittle (Fig. 4.3). The lateral extent of the carbonate veins in the area was not fully investigated due to time and weather constraints.

Figure 4.2. Chaotic, oxidized, carbonate veinlets and veins , cross-cutting the top lamprophyre dyke. Host lamprophyre exhibits large euhedral amphibole phenocrysts in a groundmass of feldspar and pyroxenes.

Figure 4.3. Photograph of a planar, laminate of turbid and limpid calcite vein in the lower lamprophyre dyke.

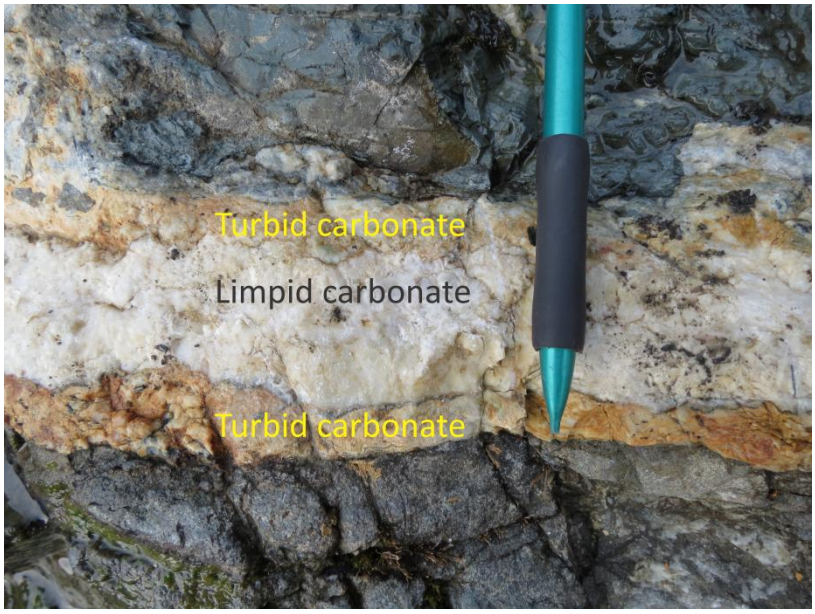

4.2 PETROGRAPHY

Polished thin sections of the 13 hand samples from the Little Gut Creek outcrop transect were used for petrographic analysis to distinguish the lithology and alteration present in each sample (Fig.4.1). Based on the minerals and textures identified through thin section analysis, four lithologies are present along the transect line. These are an olivine gabbro, glassy foidite (the chilled margin of the lamprophyre), camptonite lamprophyre and calcite carbonatites. This section presents a condensed description of the mineralogy and alteration present in the samples with a summary of the petrographic description present in Table 4.1. For detailed descriptions of each sample see Appendix B and for photomicrographs of the polished thin sections see Appendix C.

Table 4.1. Summary of the petrographic descriptions of the LGC samples

Symbol	Sample	Description
□	LGC 1	**Glassy foidite**. Trachytic texture amphibole phenocrysts and calcite veinlets
□	LGC 5	**Glassy foidite**. Trachytic texture amphibole phenocrysts and calcite veinlets
◇	LGC 2	**Calcite carbonatite veins in lamprophyre**. Carbonate veinlets with ghosts of mafic minerals. Quartz lenses in carbonate. Carbonate occurs as veins.
◇	LGC 3	**Calcite carbonatite**. Carbonatised mafic rock with ghosts of mafic minerals altering to clay. Epidote veinlets. Quartz lenses in carbonate. Host completely pseudomorphed to clays. Carbonate occurs as veins.
◇	LGC 3.5	**Calcite carbonatite**. Carbonatised mafic rock with ghosts of mafic minerals altering to Clay and chlorite. Epidote veinlets. Quartz lenses in carbonate. Host completely pseudomorphed to clays. Carbonate occurs as veins.
◇	LGC 4	**Calcite carbonatite veins in lamprophyre**. Carbonatised mafic rock (riebeckite and olivine) with ghosts of mafic minerals altering to clay and chlorite. Epidote veinlets. Quartz lenses in carbonate. Host completely pseudomorphed to clays. Carbonate occurs as veins.
◇	LGC 6	**Calcite carbonatite veins in glass lamprophyre chilled margin**. Bimodal rock glassy host and carbonate-rich veins and veinlets. Carbonatised mafic rock that exhibits no optical properties, brownish grey glass. Epidote and quartz lenses in turbid calcite veins.
◇	LGC 9	**Calcite carbonatite**. 6 primary carbonatite layers intermingled with Carbonatised mafic rock with ghosts of mafic minerals altering to clay

		and chlorite. Quartz lenses in carbonate.
◇	LGC 10	**Calcite carbonatite**. 4 primary carbonatite layers intermingled with Carbonatised mafic rock with ghosts of mafic minerals altering to clay and chlorite. Quartz lenses in carbonate.
◇	LGC 11	**Calcite carbonatite veins in lamprophyre**. Carbonatised lamprophyre with ghosts of mafic minerals altering to clay and chlorite either side of carbonate veins. Quartz lenses in carbonate.
×	LGC 7	**Lamprophyre**. Fine grained ground mass of plagioclase, amphibole, opaques and epidote. Phenocrysts of riebeckite, plagioclase, olivine and pyroxene pervasively altered to clay, serpentine, biotite, chlorite, sericite. Calcite veins throughout.
✳	LGC 8	**Lamprophyre**. Fine grained ground mass of plagioclase, amphibole, opaques and epidote. Phenocrysts of riebeckite, plagioclase, olivine and pyroxene pervasively to completely altered to clay, serpentine, biotite, chlorite, sericite. Calcite veins throughout.
○	LGC 12	**Olivine gabbro**. Plagioclase dominant groundmass coarse and fine grained. Amphibole, pyroxene and olivine pervasively to completely altered to serpentine, chlorite and clays. Calcite and quartz veins throughout.

4.2.1 Olivine gabbro: LGC 12

LGC 12 is a fine-grained, moderately altered olivine gabbro with coarse plagioclase crystals (Fig. 4.4). Amphibole (primarily kaersutite; 10 vol. %) are fine-grained, equant crystals which typically display concentric zoning with opaque inclusions of magnetite and is commonly pervasively altered to clay minerals. Fine-grained clinopyroxene (primarily augite with the occasional titan-augite; 10 vol. %) crystals are present. and show a range of alteration mineralogy and textures. Crystals adjacent to carbonatite veinlets are typically altered to clays, whereas clinopyroxene crystals further from the veinlets display either uralitisation to secondary actinolite (through network replacement textures) or chloritisation to secondary chlorite through rim alteration. Unaltered clinopyroxene grains are a rare occurrence. The clinopyroxene crystals are commonly altered in a sequence of augite (i.e., augite displays primary textures with secondary amphibole occurring along rim boundaries), to amphibole. Plagioclase (40 vol. %) is in the form of both coarse-grained (stubby and elongate) and fine-grained (elongate) crystals. Sericitisation of both fine and coarse

plagioclase is common. Coarse grains show andesine centres and bytownite rims with oscillatory zoning. Cleavage planes of coarse phenocrysts can be bent. Olivine (15 vol. %) phenocrysts are euhedral, orthorhombic crystals displaying pervasive serpentinisation in network alteration textures and rim alteration to iddingsite (common alteration mineral of olivine).

Figure 4.4. Photomicrographs of LGC 12 in cross polarized light (CPL) setting. A: Interstitial, fine-grained groundmass of amphibole, olivine, clinopyroxene, plagioclase and opaques with coarse plagioclase crystals. Alteration of amphibole and pyroxenes to dark brown clay mineral is shown. B: Large, coarse-grained plagioclase minerals with interstitial magnetite and ilmenite.. Plag-plagioclase, Ilm-ilmenite. Mag-magnetite.

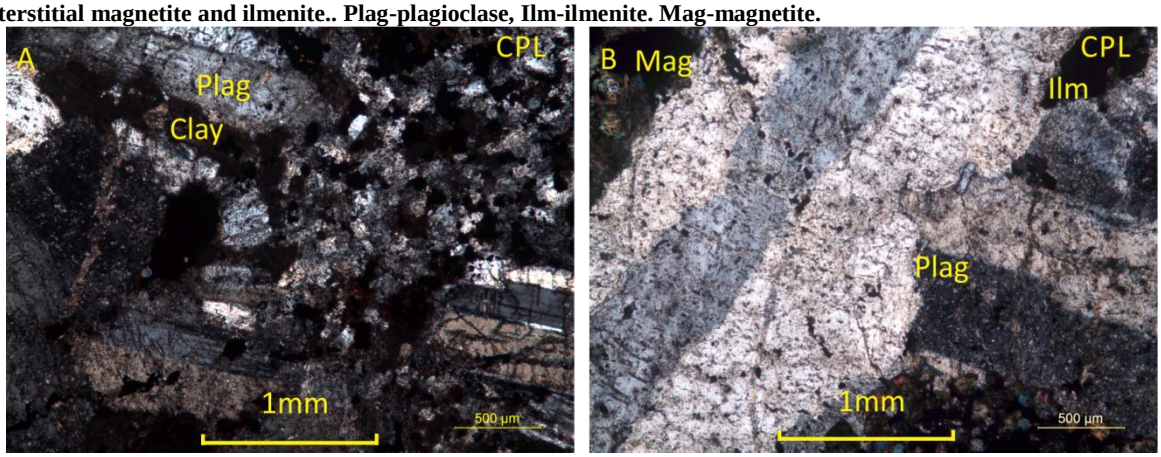

Evolved phases (alkali feldspar and orthoclase) form a minor constituent (<5 vol. %) of the overall mineralogy of the olivine gabbro. Alteration in the form of partial, acicular chloritisation, partial serpentinisation and formation iddingsite is common in the olivine crystals. An alteration front, which lessens with distance, emanates from the secondary turbid calcite veinlets. Calcite ocelli (any eyelike structure) are present within the minerals that have completely altered to clays. Overall, metasomatism of the olivine gabbro host is evidenced by clay alteration, sericitisation, serpentinisation, chloritisation and the introduction of calcite ocelli and veinlets.

4.2.2 Glassy foidite: LGC 1; LGC 5

The chilled margin of the lamprophyre (Samples LGC 1 and 5) consists of grey to black, aphanitic, very fine-grained, elongate phenocrysts (i.e., microlites). The chilled margin

samples both consist of black, partially to completely isotropic glass (55 vol. %; Fig. 4.5). The samples are predominantly composed of glass, making an accurate petrographic classification difficult, hence the classification of these samples was made using the Total Alkalis and Silica (TAS) diagram (Le Maitre et al. 2002) based on the XRF major element compositions of these samples. According to the IUGS Sub-commission glass bearing and glassy rocks classification, these samples are "glassy" (Table 4.1) (Streckeisen 1980; Le Bas & Streckeisen 1991; Le Bas 2000; Le Maitre et al. 2002).

Figure 4.5. Cross polarised and plane polarised transmitted light (CPL and PPL) photomicrographs. A: LGC 1- Euhedral, blocky magnetite (Mag) in a groundmass of partially isotropic groundmass that displays trachytic textures through acicular brown amphibole and stubby plagioclase phenocrysts. B: LGC 5-Alteration front between opaque rich clay (right side of image), acicular brown amphibole and stubby plagioclase phenocrysts displays trachytic textures in a partial to completely isotropic glass. C and D: LGC 1- Skeletal textures of the microcrystalline amphibole and occasional plagioclase in the partially isotropic glass groundmass. Opq – opaque minerals

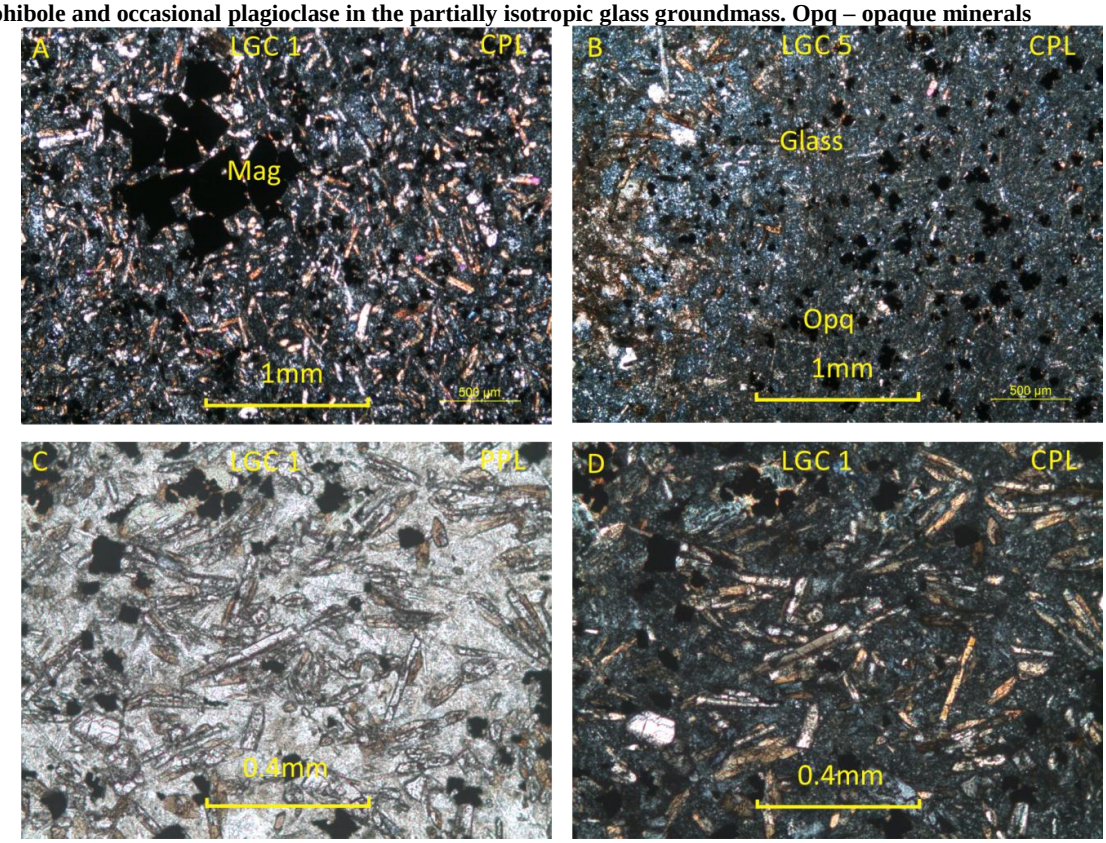

Both LGC 1 and 5 are primarily composed of black partially to completely isotropic glass. The dominant phenocryst phase is elongate, brown, amphibole (primarily kaersutite (< 1 mm); 30 and 15 vol. %, respectively) and plagioclase (< 1 mm) phenocrysts are very fine-grained and elongate. There is an absence of evolved (e.g., quartz and alkali feldspar) and

hydrous minerals (e.g., micas). At closer inspection, the kaersutite phenocrysts display non-directional trachytic textures and concentric zoning with magnetite inclusions and minor amounts of ilmenite with well defined cleavages which is interstitial to the glassy groundmass (Fig. 4.5). Skeletal plagioclase phenocrysts exhibit undulose extinction and is pervasively altered to clays. Both samples display chaotic, non-directional limpid calcite veinlets. These veinlets cross-cut the chilled margin. Emanating from the veinlets is an apparent alteration front (~2-5 cm; Fig. 5 B). Within the alteration front plagioclase and kaersutite phenocrysts are altered to clays. The alteration front also introduces the magnetite and ilmenite mineral inclusions to the kaersutite phenocrysts (Fig. 4.5). Alteration to amphibole is at its greatest within the alteration front in the vicinity of the veins with the severity of the alteration dissipating with distance (~2-5 cm) from the veinlets.

Table 4.2. IUGS Sub-commission glass bearing and glassy rocks classification (Streckeisen 1980; Le Bas & Streckeisen 1991; Le Bas 2000; Le Maitre et al. 2002).

Glass content (in modal vol. %)	
0-20	glass-bearing
20-50	glass-rich
50-80	glassy
80-100	special names such as obsidian, pitchstone, etc.

LGC 1 and 5 exhibit some minor yet distinct mineralogical and textural differences. LGC 1 is composed of 30 vol. % micro-amphiboles in an ophitic groundmass whereas, LGC 5 shows bimodal textures, with a boundary between fine-grained material (glassy, opaque-rich), and coarser material of micro-amphiboles (24 vol. %) and micro-plagioclase in an ophitic groundmass. The fine-grained glassy and opaque-rich groundmass of LGC 5 also includes interstitial, dark grey clays. The microamphibole (kaersutite) crystals of both samples are

fine-grained, elongate and acicular with the LGC 5 kaersutite appearing slightly finer and are more readily altered to clay. LGC 1 contains a cluster of medium-grained, cubic, euhedral magnetite

4.2.3 Lamprophyre: LGC 7 and 8

Samples LGC 7 and 8 display typical porphyritic lamprophyre textures and mineralogy. LGC 7 and 8 consists of coarse phenocrysts (total 30 and 35 vol. %, respectively) of riebeckite, augite, olivine and nepheline within in a fine-grained groundmass (63 and 52 vol. %, respectively) of microcrystalline plagioclase, amphibole, clinopyroxene and opaques. Texturally, the two samples are similar with minor mineralogical differences but the degree of alteration to the two samples differs slightly.

LGC 7 displays coarse (2-5 mm), euhedral, riebeckite phenocrysts (24 vol. %) that show network and rim alteration (completely or pervasively altered) to a clay, chlorite, serpentine or biotite. Olivine phenocrysts (3 vol. %) are coarse (2-3 mm) and display characteristic orthorhombic crystal shapes and but have undergone complete serpentinisation (i.e., occurring as pseudomorph). Heavily fractured augite phenocrysts (2 vol. %) are equant, stubby and display oscillatory zoning. The augite phenocrysts occur in glomeroporphyritic clusters. It is common that network and rim alteration occurs along the fractures within the crystals in the form of partial uralitisation to secondary amphibole. Alteration to clay minerals occurs more commonly adjacent to carbonate veinlets. “Laminar trains” of magnetite occur within the clay. Nepheline (1 vol. %) occurs as equant intergranular grains up to 4 mm in size and is extensively fractured and altered to cancrinite. The groundmass of LGC 7 is composed of fine-grained, green amphibole (15 vol. %), acicular clinopyroxene (10 vol. %), blocky nepheline (5 vol. %), plagioclase (20 vol. % labradorite and andesine) and magnetite (3 vol. %). The plagioclase is heavily altered to sericite and to partially isotropic

analcime. Alteration of the groundmass is less obvious in comparison to the coarse phenocrysts. LGC 8 contains slightly higher concentrations of coarse phenocrysts in comparison to LGC 7. Minor mineralogic differences are seen in the modal percentages. The macrocrysts of LGC 8 display lighter alteration with the same alteration products and alteration textures. Euhedral riebeckite phenocrysts (20 vol. %) are fractured and moderately altered through network and rim alteration to clay, biotite and/or chlorite.

Figure 4.6. Cross polarised transmitted light photomicrographs. A:LGC 7- Pseudomorphed olivine to clay with calcite ocelli within the clay. Serpentinisation occurs along the rim of the olivine. B: LGC 8-Limpid calcite veinlet with a groundmass of plagioclase, ampibole and clay. Radial cracks in nepheline from the apparent volume increase associated with serpentinisation of olivine. Coronitic textures are moderately well developed in plagioclase. C: LGC 7-Complete serpentinisation of an olivine crystal. D: LGC 8- Limpid calcite veinlet with a groundmass of plagioclase, ampibole and clay. Bottom left the complete serpentinisation of an olivine crystal. Plag-plagioclase, amphi-amphibole, and gm-groundmass.

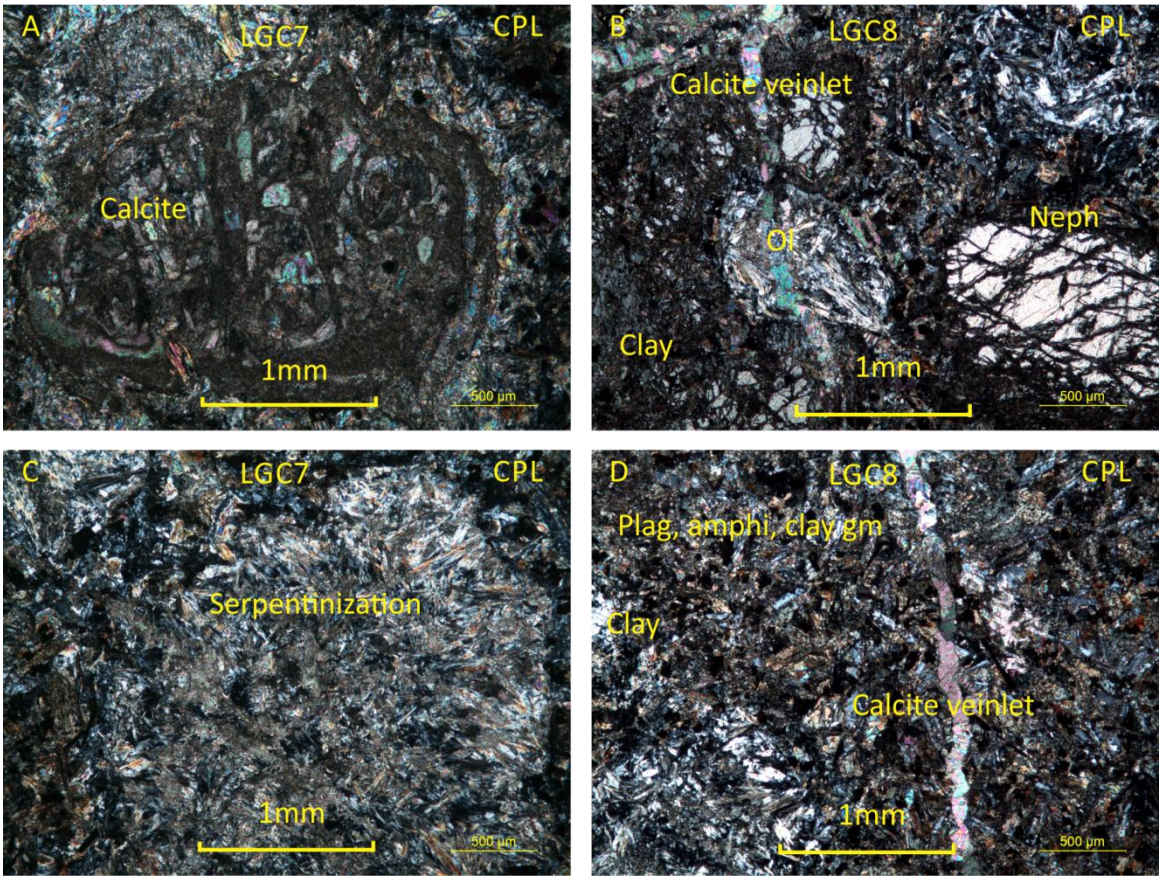

In comparison, LGC 8 contains slightly higher concentrations of coarse phenocrysts (i.e., macrocrysts) than LGC 7 and minor differences in overall modal percentages. The macrocrysts of LGC 8 display weaker alteration however with the same alteration products

and textures. Euhedral riebeckite phenocrysts (20 vol. %) are fractured and moderately altered through network and rim alteration to clay, biotite and/or chlorite. Augite phenocrysts (4 vol. %) occur in glomerophyric clusters and display partial uralitisation (network and rim alteration) along fractures to form secondary amphiboles. Olivine phenocrysts (1 vol. %) are less common in LGC 8 and show either complete serpentinisation or complete clay pseudomorphism. Elevated proportions of nepheline (>10%) are present and are extensively fractured and altered to cancrinite. The LGC 8 groundmass contains fine grained green amphibole (15 vol. %), blocky nepheline (2 vol. %), plagioclase (23 vol. % labradorite and andesine) and magnetite (2 vol. %). Both the groundmass and the coarse phenocrysts of LGC 8 display higher clay content than LGC 7.

Table 4.3 IUGS subcommission lamprophyre classification table. Shaded area likely to be lamprophyre classification, shaded cell indicates LGC 7 and 8 classification (Streckeisen 1980; Le Bas & Streckeisen 1991; Le Bas 2000; Le Maitre et al. 2002).

light-coloured constituents		**predominant mafic minerals**			
feldspar	feldspathoid	biotite, diopside augite, (±olivine)	hornblende, diopside augite, (±olivine)	amphibole (barkevikite, kaersutite), titanaugite, olivine, biotite	melitite, biotite, ± titanaugite, ± olivine, ±calcite
ortho>plag	-	minette	vogesite		
plag>ortho		kersantite	spessartite		
ortho>plag	felds>foid			sannaite	
plag>ortho				camptonite	
-	glass or foid			monchiquite	pozenite
-	-				alnöite

Adjacent to veins in both LGC and 8, alteration to clay minerals is prevalent. The tendency to alter to clay is greatest in the groundmass of both LGC 7 and 8 with the coarse phenocrysts preferentially altering to their successive alteration constituents (e.g., olivine to serpentine). The clays are appear as a brown turbid material that demonstrates no changes in optical properties in both plane polarised and cross polarised light. Using the criteria set out by the

IUGS subcommission on lamprophyre classification, both samples LGC 7 and 8 can be classified as camptonite (Table 4.2; Streckeisen 1980; Le Bas & Streckeisen 1980; Le Bas & Streckeisen 1991; Le Bas 2000; Le Maitre et al. 2002) consistent with previous work by Baker (1990) (sample H8).

4.2.4 Carbonatite: LGC 2, 3, 3.5, 4, 6, 9, 10 and 11

At least seven distinct carbonatite veins were identified in the lamprophyre dykes (Fig. 4.1). These veins range from 1-50mm in thickness. A separate hand sample of each of the veins (except for LGC 9 and 10 where the samples are of the same vein) was made into polished thin sections and petrographically analysed. The majority of the seven thin sections contain veins of >50% modal carbonate minerals (n.b. predominantly calcite) thereby classifying them as calcite carbonatite veins. In LGC 2, 4, 6 and 11 the total modal carbonate percentage of the sample is not >50%. Between each of these carbonatite veined samples is the host lamprophyre as seen in LGC 7 and 8. The seven thin section samples can be subdivided into two subsections:

1. Chaotic calcite veinlets - LGC 2, 3, 3.5, 4 and 6.
2. Laminar calcite veins - LGC 9, 10 and 11.

LGC 2, 3, 3.5 and 4 are hosted by a pervasively to completely altered very fine-grained lamprophyre. The lamprophyre is altered to clays and exhibits little of the original and unaltered mineral facies. Clay minerals appear as a yellow-brown turbid material that demonstrates no changes in optical properties in both plane polarised and cross polarised light. Limpid calcite ocelli appear within the clay-altered lamprophyre. Calcite is the predominant carbonate vein mineral in samples LGC 2, 3, 3.5 and 4 but the modal percentage varies in each sample. Both LGC 2 and 4 contain less than <50 modal volume percentage of carbonate within the entire hand sample with 40 and 20%, respectively. However LGC 3 and

3.5 both contain 60 and 65% modal percentages of carbonate, respectively. The calcite in these four samples is a mixture of clean, pure, limpid, rhombohedral calcite and turbid calcite appears as calcite that is heavily assimilated with the host lithologies. In the veins and veinlets of LGC 2 lenses of accessory quartz (14%), illustrating sutured grain boundaries, are present. LGC 3 also has elevated levels of accessory minerals in the form of quartz (20%) and epidote (5%) in the carbonate veins and veinlets. LGC 3.5, however, has only a minor amount of quartz (5%) in the form of lenses within the calcite veinlets. Within the turbid calcite and clay of LGC 4, accessory quartz (29%) is in clusters in the clay and lenses in the veinlets.

LGC 6 is composed of a grey-green-brown glass (chilled margin) that exhibits no change in optical properties that has three major veins with numerous veinlets (30%) of both limpid and turbid calcite (Fig. 4.7). The contacts between the calcite and the glassy host are sharp and quartz (15%) is present in many places and has adhered to this contact, forming comb textures. These comb textures are only present in the turbid calcite veinlets. Accessory epidote (5%) occurs in small clusters and lenses within the core of the calcite veins.

Carbonate veins and veinlets (0.5 mm width) cross-cut both LGC 7 and 8. Calcite phenocrysts in these veins and veinlets exhibit limpid, perfect, euhedral rhombohedral form and fourth order birefringence. Accessory aegirine (<1 vol. %) forms in lenses within the core of the carbonate veins. Limpid calcite ocelli appear throughout both samples, especially in macrocrysts that have altered to clays, see figure 4.7.

Samples LGC 9 and 10 each have two distinct veins of carbonate. A laminar carbonate vein with a core of clean unaltered, rhombohedral limpid calcite contacts the turbid carbonate laminate (Fig. 4.3). Adjacent to the turbid vein contacts is the lamprophyre host. LGC 9 and 10 both include coarse limpid calcite phenocrysts within thicker (2-10 mm) laminations in the

veins. LGC 11 has seven separate veins, with six veins consisting of turbid calcite and the remaining vein exhibiting limpid calcite. The lamprophyre host rock is pervasively altered to clay in all three samples however remnants of the original textures and minerals of the lamprophyres are displayed. The clay minerals present in the altered lamprophyre host are a brown turbid material that demonstrates no changes in optical properties and contains occasional calcite microphenocrysts and opaques (Fig. 4.7).

Figure 4.7. Cross polarised transmitted light photomicrographs. A and B: Polycrystalline texture mainly displayed by limpid calcite with turbid calcite/pseudomorphed carbonate clay. C: Polycrystalline texture quartz and lipid calcite veins in carbonate clay and metasomatised host lamprophyre groundmass. Quartz display comb textures. D: Directional spider veins in mafic glass. Turbid and limpid calcite in veins with the occasional ocelli. Quartz comb texture. Polycrystalline texture mainly displayed by limpid calcite E: Turbid calcite with quartz lenses and ocelli F: Turbid calcite with quartz lenses and comb textures.

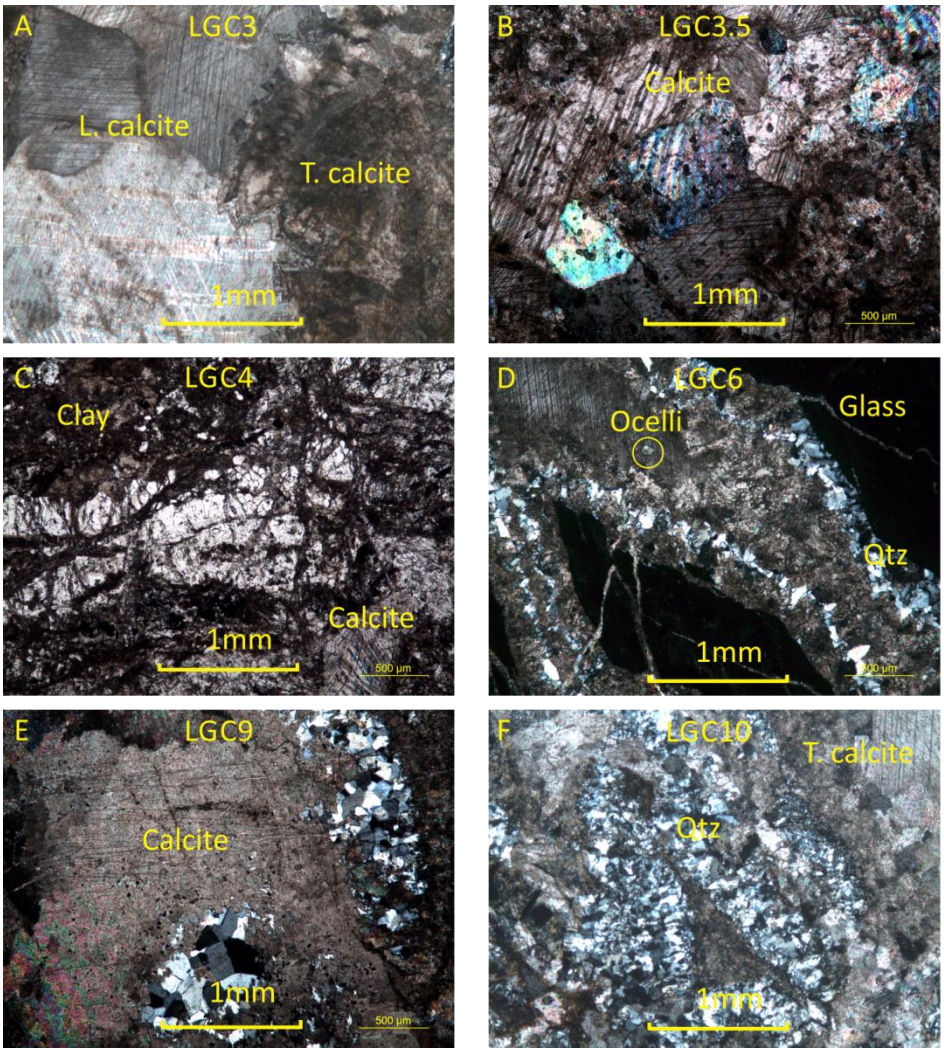

The mineralogy of the LGC 9, 10 and 11 is comparable with some variance in modal percentages. The calcite (70 vol. %) of LGC 9 is predominantly turbid with the one planar vein laminate consisting of limpid calcite. Accessory quartz (10%) appears as lenses and clusters in or near the limpid and turbid carbonate veins. LGC 10 is similar as the majority of the carbonate (60%) of the sample is turbid with minor limpid calcite veining. Comb textures of quartz (10%) along with lenses and clusters are also present. Neither LGC 9 nor 10 petrographically exhibit dolomite in the limpid carbonate. However LGC 11 has a mixture of both calcite (30%) and dolomite (20%). The carbonate in LGC 11 is distributed across the 7 separate veins. A mixture of calcite and dolomite can be found in these veins. Accessory quartz (15%) is present in the form of lenses and clusters in LGC 11.

4.1.3 XRD

X-ray diffraction (XRD) was used to further refine mineral compositions of the Little Gut Creek samples. The XRD results are summarised in Table 4.4 and the full data set are included in Appendix D. Figure 4.8 is a binary plot showing a diagrammatical representation of the mineralogical modal percentage of the types of carbonate minerals present in the samples. The carbonate mineral in LGC 2-4 and LGC 7, 8 and 11 is calcite. However dolomite minerals are present in LGC 6, 9 and 10. LGC 6 remains a calcite carbonatite as it only has a modal percentage of dolomite of 5%. The XRD analysis of LGC 9 shows that 40% of the total modal mineralogical percentage of the sample is dolomite, with 50% as calcite. LGC 10 (the same vein as LGC 9) however only has 10% dolomite. LGC 7 and 8 have a modal mineralogy of 45 and 50% calcite, respectively but no dolomite. This is significantly higher than the modal percentage estimates suggested by the petrographic analysis. LGC 2, 3, 3.5, 4, 6, 9, 10 and 11 all indicate high levels of carbonate especially calcite with LGC 6, 9, 10 and 11 exhibiting elevated levels of dolomite in comparison to LGC 2, 3, 3.5 and 4.

XRD analysis of the glassy foidites (LGC 1 and 5) describes the mineralogy detailed in the above petrographic descriptions. The XRD analysis shows that LGC 12 is an olivine gabbro that contains 15 vol. % calcite carbonate and equivalent levels in quartz. The classification of the samples using petrographic analysis combined with the XRD results is not possible due to the significant difference between the petrographic description modal percentages and the XRD modal percentages. Clay minerals and/or glass are present in all of the thirteen samples. As the original mineralogy of the clay minerals and the glass has not been determined, petrographic classification as per the IUGS carbonatite classification is only possible in LGC 3, 3.5, 9 and 10 as these samples are of the carbonate vein with ghosts of the lamprophyre.

Figure 4.8. Binary representation of the XRD analysis carbonates modal percentages.

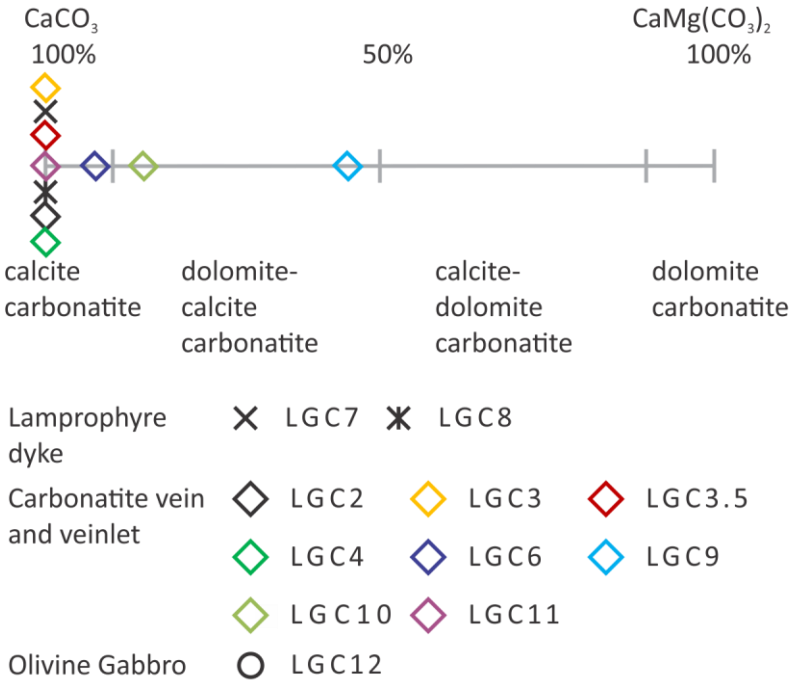

Samples LGC 2, 4, 6 and 11 are lamprophyre samples that are cross-cut by carbonatite veins. If the IUGS classification was applied to the XRD results, the carbonatite veined samples of LGC 2-4, 6, 9 and 10 would be classified as calcite or calcite-dolomite carbonatites with LGC 11 classified as a calcitic-lamprophyre. Petrographic modal percentages would classify

the LGC 3, 3.5, 9 and 10 as calcite carbonatites with samples LGC 2, 4 and 11 due to their lower than 50% modal carbonate as calcitic lamprophyre.

Table 4.4 XRD modal percentage results. 'Trace' indicates values of <1%. See Appendix F for XRD counts.

Sample	Calcite	Dolomite	Quartz	Albite	Clay minerals	Augite	Mg-Riebeckite
LGC 1	-	-	-	50	-	40	5
LGC 2	80	trace	20	-	trace	-	-
LGC 3	60	trace	40	-	trace	-	-
LGC 3.5	65	trace	35	-	trace	-	-
LGC 4	60	trace	35	-	5	-	-
LGC 5	-	-	-	15	10	75	-
LGC 6	60	5	20	-	5	10	-
LGC 7	45	-	35	-	10	-	10
LGC 8	50	-	20	-	15	-	15
LGC 9	50	40	10	-	trace	-	-
LGC 10	60	10	30	-	trace	-	-
LGC 11	30	-	15	20	trace	-	-
LGC 12	15	-	15	-	trace	-	5

4.2 GEOCHEMISTRY

X-ray florescence (XRF) analyses of the thirteen samples are tabulated in Table 4.5 with major and trace element Harker diagrams (Harker 1909) presented in Fig.4.9. Note that LGC 2, 3, 3.5, 4, 6, 9, 10 and 11 are primarily carbonatite veins and also contain varying amounts of the lamprophyre host that will alter the chemical nature of the samples.

4.3.1 Major and Minor Elements

The olivine gabbro (LGC 12) contains 46.34 wt. %. SiO_2 and 2.52 wt. % MgO. The CaO abundances of the olivine gabbro is elevated (9.22 wt. %) due to the carbonatite veinlets present in the sample. Using the major element chemistry, samples LGC 1 and 5 plot on the TAS as foidites. These samples contain SiO_2 concentrations (39.88 to 40.95 wt. %.) along with the combined Na_2O (2.43 and 4.73wt. %, LGC 1 and 5, respectively) and K_2O (3.23 and 1.22 wt. %, LGC 1 and 5, respectively) concentrations (Table 4.5 and Fig. 4.10). The glassy

foidites have MgO concentrations of 4.76 to 5.93 wt. % and slightly elevated CaO (9.56 to 10.16 wt. %) concentrations (Section 4.2.1).

The camptonite lamprophyre dykes (LGC 7 and 8) contain SiO_2. wt. % concentrations that range from 36.90 to 38.53 wt. % and have Na_2O concentrations (0.86 and 0.88wt. %, LGC 7 and 8 respectively) when combined with the K_2O (1.09 and 1.33 wt. %, LGC 7 and 7 respectively) concentrations plot on the TAS as foidites as well, albeit with much lower Na_2O and K_2O abundances. The MgO range of the camptonites is from 9.38 to 10.55 wt. %, with Al_2O_3 concentrations between 8.23 to 8.86 wt. %. CaO enrichment (14.69 to 15.64 wt. %) is notably higher than the glassy foidites (LGC 1 and 5; Table 4.5 and Fig. 4.10).

The carbonatite veins and veinlets hosted by metasomatised lamprophyre (LGC 2, 3, 3.5,4, 6, 9, 10, and 11) displays a range of undersaturated SiO_2 (12.2- 37.1 wt. %) values (Table 4.5). LGC 1, 3, 3.5,4, 6 and 11 all have greater than 20 wt. % SiO_2. This is above the IUGS carbonatite classification criteria (Streckeisen 1979; Streckeisen 1980; Le Bas & Streckeisen 1991; Le Maitre et al. 2002). LGC 2, 3, 3.5, 4, 6, 9, 10 and 11 show a range of 1.5 to 7.08 wt. % MgO. LGC 10 (2.50 wt. % MgO) in XRD contains dolomite ($CaMg(CO_3)_2$) and plots in the major element carbonatite classification diagram (Woolley & Kempe 1989) as a magnesio-carbonatite. However LGC 9 (7.08 wt. % MgO) contains higher levels of dolomite (XRD results Section 4.1.3) plots as calcio-carbonatite due to its extremely high CaO ratio to MgO and total Fe+MnO content. LGC 3, 4, 6, and 11 plot as ferro-carbonatites due to their elevated Total Fe+MnO contents in comparison to their CaO and MgO concentrations (Fig. 4.9) Al_2O_3 concentrations of the carbonatites are typically below 6.08 wt. % with anomalous results from LGC 6 and 11 exhibiting 10.54 and 8.14 wt. %, respectively. These anomalous results are more in line with the host lithologies. Strong Ca enrichment is characteristic of the LGC samples (Table 4.5 and Fig. 4.10). There is a wide range of CaO values within the carbonatites with LGC 2 containing 39.00 wt.% and LGC 6 containing 16.86 wt. % CaO.

Figure 4.9 Major element ternary carbonatite classification diagram (Woolley & Kempe 1989).

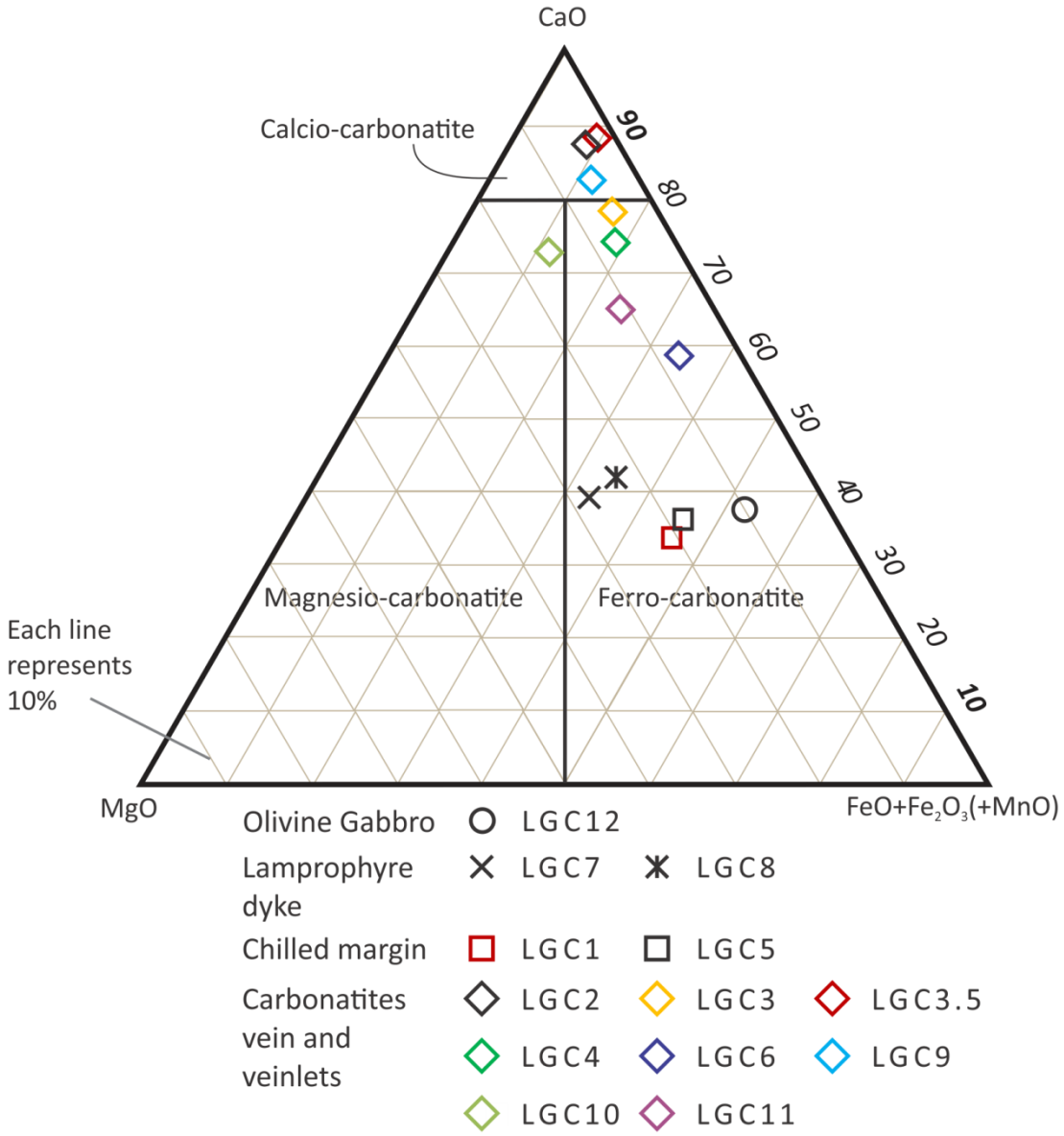

The Harker diagrams (Fig. 4.10) show that TiO_2, P_2O_5 and Al_2O_3 concentrations increase with the increasing SiO_2 content. In contrast, CaO concentrations decrease with SiO_2 wt. % (Fig. 4.10). N_2O abundances in the carbonatite veined samples is very low with exception of LGC 11. The total iron oxide content (Fe_2O_3T) is variable in the carbonatite veined samples with elevated iron content in the host lithologies. MgO is elevated in LGC 9 which can be attributed to the dolomite content of this sample, it is also elevated in the LGC 7 and 8 (lamprophyre) due to the predominance of mafic minerals in these samples.

Trace element analyses are tabulated in Table 4.5. Most of the samples show low abundances of Ba, Th, Ce, Nd, Nb, Zr and Y with the notable exception of LGC 6 which possesses significantly higher levels of these elements. Samples LGC 1 and 5 have virtually no Cr. However, these two samples have far higher quantities of Ba, Th, Ce, Nd, Nb, Zr and Y. These elevated abundances are also present to a certain degree in the lamprophyre LGC 7 and 8 samples and the olivine gabbro of LGC 12.

Zr/Nb trace element ratios remain stable with the increasing of SiO_2 wt. %. The relatively low Zr/Nb ratios (3.2 to 5.l6) suggest strong incompatible trace element enrichment. The glassy foidites (LGC 1 and 5) and LGC 6 are both predominantly glass samples, have the lowest Zr/Nb ratios, and highly variable trace element concentrations (Table 4.5). Cr and Ni contents are higher in the carbonatites (Cr 20-1049 ppm, Ni 31-248 ppm) than in the foidite and olivine gabbro (Cr <3-83 ppm, Ni <3-25ppm; Table 4.5). The lamprophyres are consistently higher in Cr and Ni than the other lithologies with 932-1146 ppm Cr and 340-435ppm Ni. Rare Earth Element chemical analyses are an integral part to the majority of carbonatite studies however in this study a complete suite of REE abundances was not undertaken. Portable XRF (pXRF) data taken from both in the field and of the cut hand samples is tabulated in Appendix E.

Figure 4.10. Harker Diagrams showing major element oxide and trace element ratios vs SiO_2 for the LGC samples (Harker 1909).

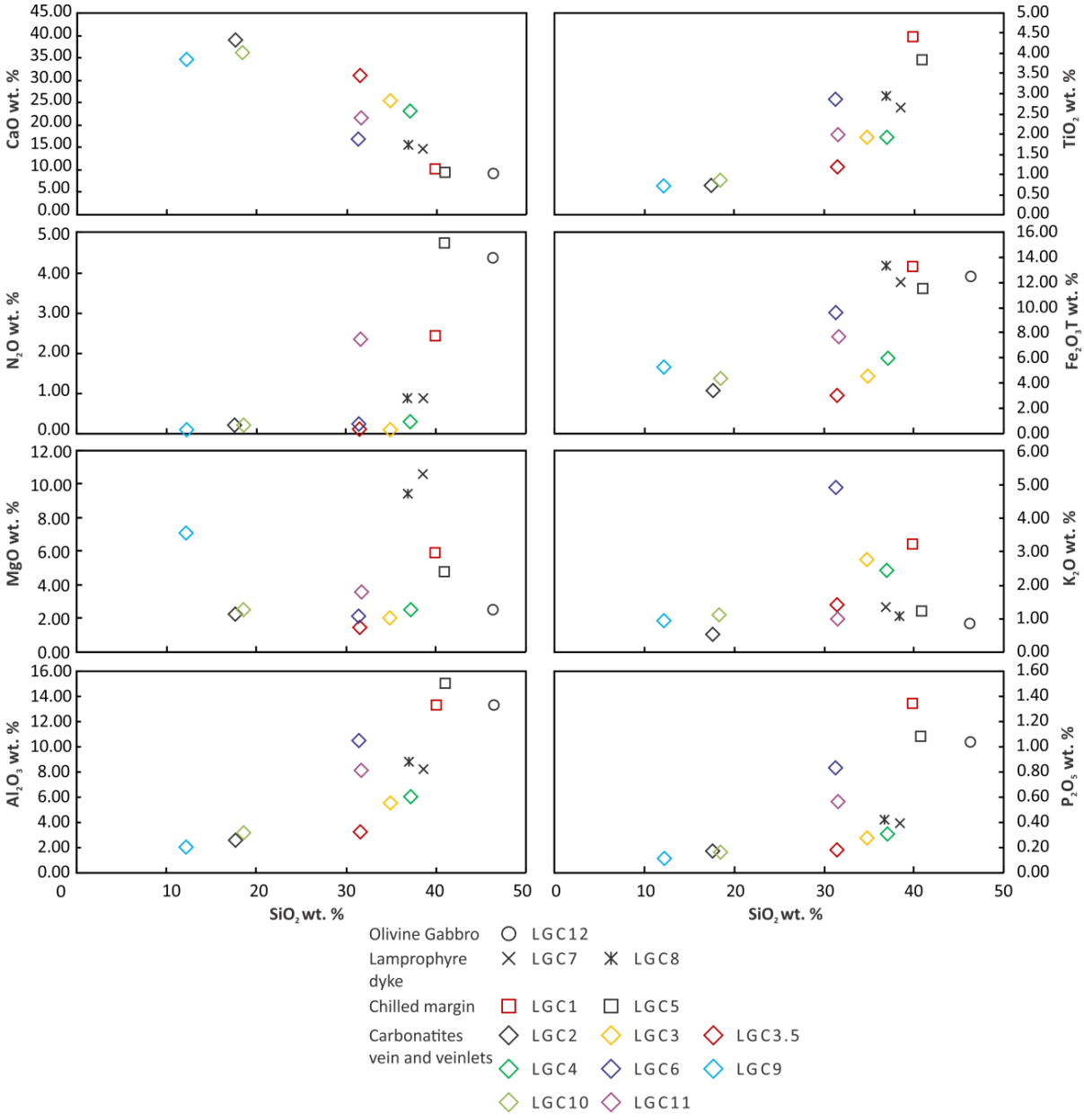

Table 4.5. Major and trace elements composition of the collected samples.

Sample Rock type	LGC 1 glassy foidite	LGC 2 calcite carbonatite	LGC 3 calcite carbonatite	LGC 3.5 calcite carbonatite	LGC 4 calcite carbonatite	LGC 5 glassy foidite	LGC 6 calcite carbonatite	LGC 7 lamprophyre	LGC 8 lamprophyre	LGC 9 dolomite-calcite carbonatite	LGC 10 dolomite-calcite carbonatite	LGC 11 dolomite-calcite carbonatite	LGC 12 olivine gabbro
SiO_2	39.88	17.63	34.87	31.51	37.08	40.95	31.36	38.53	36.90	12.19	18.50	31.60	46.34
TiO_2	4.41	0.70	1.90	1.18	1.91	3.83	2.84	2.77	2.99	0.71	0.87	1.99	2.34
Al_2O_3	13.31	2.64	5.57	3.30	6.08	15.09	10.54	8.23	8.86	2.02	3.21	8.14	13.36
Fe_2O_3T	13.36	3.48	4.60	3.03	6.07	11.62	9.71	12.05	13.35	5.32	4.36	7.74	12.53
MnO	0.15	0.32	0.24	0.30	0.12	0.36	0.19	0.18	0.16	0.22	0.19	0.19	0.15
MgO	5.93	2.28	2.00	1.47	2.52	4.76	2.06	10.55	9.38	7.08	2.50	3.56	2.52
CaO	10.16	39.00	25.55	31.02	23.27	9.56	16.86	14.69	15.64	34.70	36.23	21.63	9.22
Na_2O	2.43	0.22	0.12	0.11	0.33	4.73	0.22	0.86	0.88	<0.1	0.23	2.35	4.37
K_2O	3.23	0.51	2.77	1.41	2.44	1.22	4.95	1.09	1.33	0.91	1.10	0.99	0.85
P_2O_5	1.35	0.15	0.27	0.17	0.30	1.08	0.83	0.38	0.41	0.10	0.15	0.55	1.04
LOI	5.30	32.38	22.02	25.56	19.34	6.04	11.05	9.94	10.07	36.25	32.29	21.21	1.67
Total	99.50	99.30	99.90	99.05	99.45	99.24	90.61	99.27	99.95	99.51	99.62	99.94	94.38
Trace Elements													
V (ppm)	289	73	203	119	229	221	175	258	286	87	98	191	195
Cr (ppm)	<3	129	1049	662	1031	<3	20	1146	932	150	115	131	83
Ni (ppm)	14	31	264	121	248	<3	33	435	340	40	27	22	25
Zn (ppm)	141	46	59	35	62	133	100	112	119	27	27	65	106
Zr (ppm)	591	70	134	87	146	790	540	191	204	62	67	241	307
Nb (ppm)	146	15	27	19	33	224	166	40	42	11	15	55	56
Ba (ppm)	851	51	108	65	162	702	758	149	215	22	87	106	332
La (ppm)	74	<5	12	14	14	104	90	14	16	9	12	33	46
Ce (ppm)	178	27	26	25	39	224	217	29	54	34	21	78	104
Nd (ppm)	89	42	30	52	48	121	98	41	37	36	41	62	72
Ga (ppm)	25	8	11	7	13	28	28	16	16	7	7	17	24
Pb (ppm)	<1	<1	1	<1	3	5	8	3	3	<1	<1	2	6
Rb (ppm)	64	6	57	28	58	60	134	21	30	18	19	23	20
Sr (ppm)	1499	665	355	352	240	697	1377	295	378	565	491	547	827
Th (ppm)	13	<1	2	<1	4	18	14	3	2	<1	2	5	7
Y (ppm)	47	12	15	12	16	62	40	22	23	11	11	33	49

4.2.3 Stable Isotopes

The carbonate minerals within the LGC samples were drilled and analysed for stable carbon and oxygen isotope compositions. Oxygen and carbon isotopes ratios from the Tapuaenuku carbonatite samples are given in Figure 4.11, 4.11, 4.13 and Table 4.6. $\delta^{18}O$ values range from 5.35 and 16.75‰, and $\delta^{13}C$ values range between -1.4 to -7.88‰ (Table 4.6). Veins in the LGC 1 and 5 samples (i.e., Lamprophyre dyke chilled margins) exhibit the most primitive stable isotope compositions and they are closest to that of the probable primary igneous carbonatite (PIC) $\delta^{13}C$- $\delta^{18}O$ ratios (Reid & Cooper 1992). LGC 9, 10 and 11 display stable $\delta^{13}C$ compositions yet have two distinct groups of $\delta^{18}O$ values which can be attributed to the condition the calcite is in (Fig. 4.11, 4.12 and Table 4.6).

Figure 4.11. Carbon and oxygen isotopes of samples LGC 9 and 10.

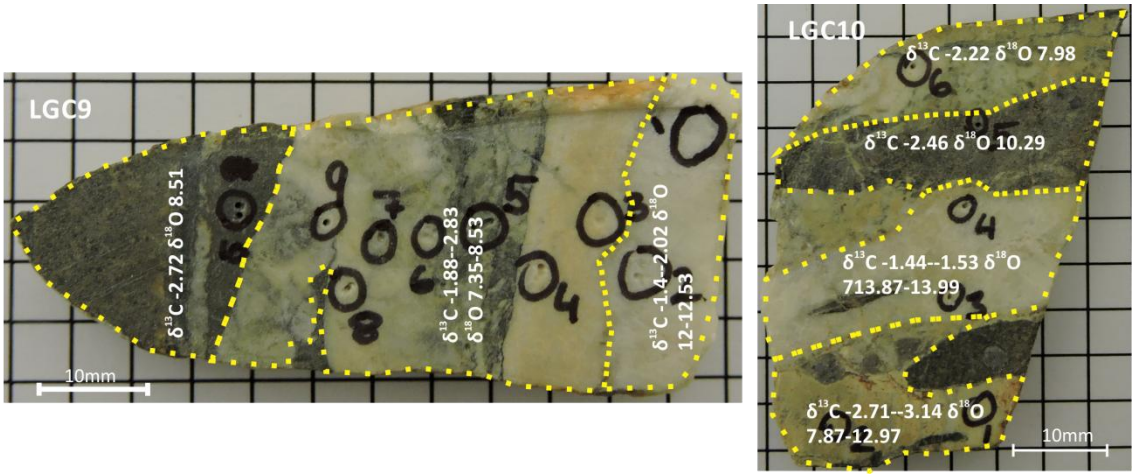

Limpid calcite laminate veins in LGC 9, 10 and 11 have $\delta^{18}O$ values that range from 12 and 13.99 ‰ where as the turbid calcite veins range from 7.35 to 8.53 ‰ (Fig. 4.11, 4.12).The thinner carbonate vein hosted samples (LGC 2, 3, 3.5, 4, and 6) exhibit a larger variation in their $\delta^{18}O$ values and lower but also more constant $\delta^{13}C$ values. LGC 6 $\delta^{18}O$ values range from 10.24 to 13.94 ‰ with their $\delta^{13}C$ ratios relatively constant at -2.77 to -4.32 ‰. LGC 3 displays larger variation within its $\delta^{18}O$ ratios, 11.41 to 15.15 ‰ and has near constant $\delta^{13}C$

values of -4.00 to -4.32 ‰. The veinlets within the olivine gabbro, glassy foidite and lamprophyre $\delta^{13}C$- $\delta^{18}O$ values range from -3.13 to -7.88 ‰ and 5.35 to 11.77 ‰. The lamprophyre sample LGC 7 contains a calcite veinlet that has more positive $\delta^{18}O$ values at 15.85 ‰ consistent with the other calcite veinlets of the carbonatite spider veinlet samples.

Table 4.6. Stable isotope composition of the LGC samples.

Sample	$\delta^{13}C$ (‰ V-PDB)	$\delta^{18}O$ (‰ SMOW)	Sample	$\delta^{13}C$ (‰ V-PDB)	$\delta^{18}O$ (‰ SMOW)
LGC 1	-4.90	6.36	LGC 8	-4.04	7.57
	-5.48	5.35		-3.65	8.32
	-6.41	8.76		-3.13	9.21
LGC 2	-2.84	7.74	LGC 9	-2.02	12.00
	-2.94	14.36		-1.40	12.53
	-3.62	10.88		-1.88	7.72
LGC 3	-4.32	15.15		-2.21	7.88
	-4.19	14.56		-2.50	8.53
	-4.00	11.41		-2.83	7.36
LGC 3.5	-2.82	12.80		-2.33	7.64
	-2.71	12.73		-2.72	7.89
	-4.25	13.53		-2.66	7.35
LGC 4	-4.15	15.91		-2.72	8.51
	-3.85	15.36	LGC 10	-2.71	7.87
	-3.85	16.75		-3.14	12.97
LGC 5	-6.32	9.81		-1.44	13.87
	-7.88	12.25		-1.53	13.99
LGC 6	-4.32	13.94		-2.46	10.29
	-2.81	13.93		-2.22	7.98
	-2.77	10.40	LGC 11	-2.48	8.40
	-2.83	11.45		-1.65	12.00
	-3.10	10.24		-2.51	6.09
LGC 7	-4.65	10.61		-2.23	11.38
	-4.38	15.85	LGC 12	-4.20	6.84
	-4.76	11.77		-3.95	8.45

Figure 4.12 Carbonatite stable isotope composition of the Tapuaenuku Igneous Complex. Shading indicates the type of mineralogical source. No shading-host rock, light grey-calcite veinlets, dark grey- Turbid calcite with host rock and black-limpid calcite veins.

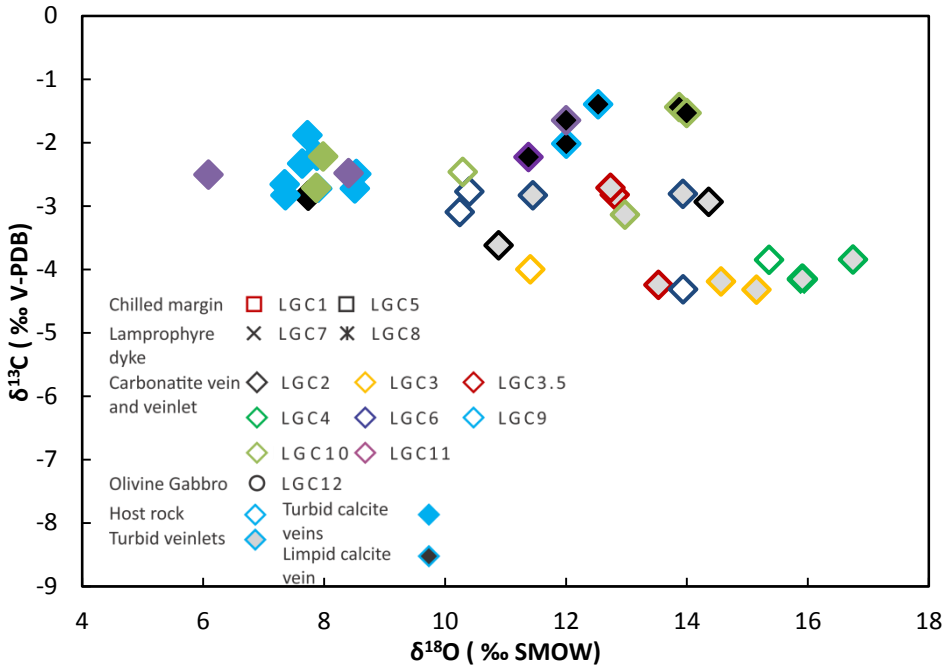

Figure 4.13. Stable isotope composition of carbonate minerals within the Little Gut Creek samples. A: The thirteen LGC samples oxygen and carbon isotope composition B:Close up of the box, indicated. Shading indicates the type of mineralogical source (i.e., host rock, veinlets and limpid or turbid veins same as Figure 4.12).

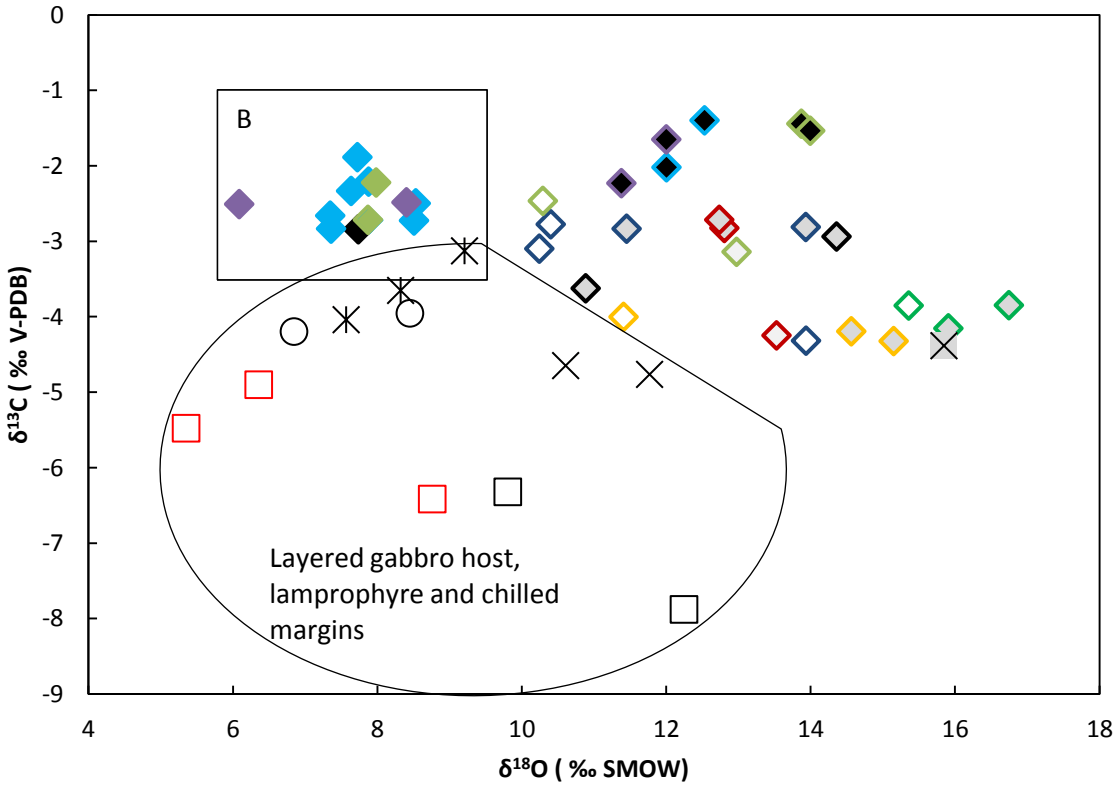

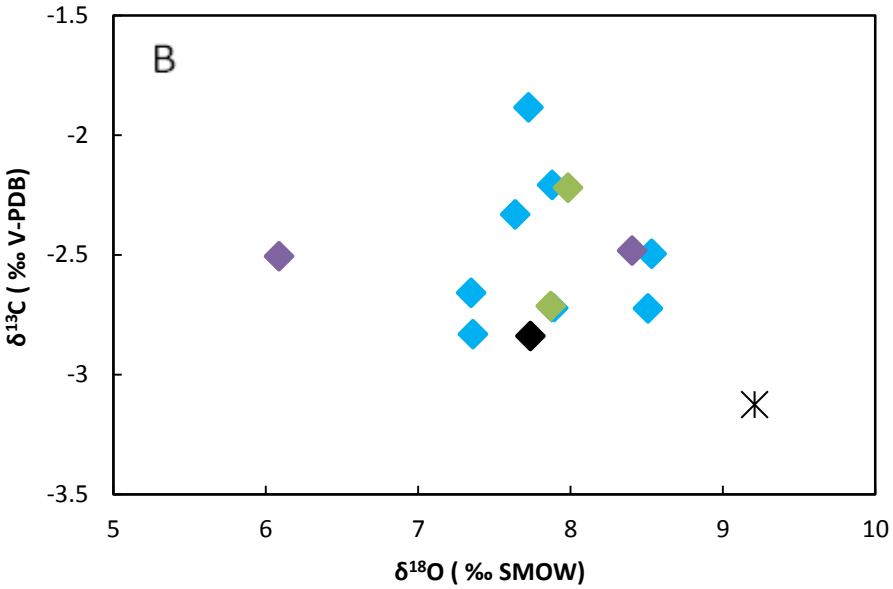
B
-1.5
-2
-2.5
-3
-3.5
δ13C (‰ V-PDB)
5
6
7
8
9
10
δ18O (‰ SMOW)

CHAPTER 5: DISCUSSION

The primary goal of this thesis was to complete a comprehensive petrochemical classification of the carbonate-rich veins that are associated with the lamprophyric dykes present in the Tapuaenuku Igneous Complex. In order to complete this goal; the timing, field relationships, mineralogy and alteration of carbonatites associated with the lamprophyre dykes were described and documented. Additionally, I determine the processes involved in the formation of the Tapuaenuku Igneous Complex and the associated mineralisations the mineralogy, major, trace element and stable isotope chemistry were investigated. Chapters three and four present the methods and results used to achieve these goals. This chapter presents an integrated analysis of the mineralogy and geochemical data in an effort to establish a robust geological evolution for the Tapuaenuku carbonatites. By discussing the alteration, textural, chemical and stable isotope relationships with the timing and temperatures it is possible to ascertain the paragenesis of the TIC and its carbonatite veining.

5.1 FIELD RELATIONSHIPS AND PETROGRAPHY

Previous research of the TIC has been limited due to its remote and at times inaccessible location. However, the TIC is a potential source of platinum group element mineralisations and, with the potential for carbonatite occurrences, a potential source of rare earth elements (Jongens et al. 2012). The TIC occurs during a period of major tectonic change from a convergent to an extensional plate boundary system creating a complex igneous structure that has been described broadly by Nicol (1977) and (Baker 1990). More in-depth outcrop scale research, as discussed below, elucidates and expands our understanding of the geological evolution of this rare mildly alkaline, mafic igneous complex (Baker 1990; Winter 2014). The TIC dyke suite includes a novel series of consanguineous (i.e., of the same origin) members of highly alkaline lamprophyre, phonotephrite, and phonolite (Nicol 1977; Baker

1990; Baker et al. 1994). The field site of this study contained two highly alkaline lamprophyres separated by a chilled margin (glassy foidite) that are hosted by olivine gabbro of the Lower Layered Series of the main Layered Series present in the complex (Fig. 4.1).

The igneous textures and mineral assemblages present in the Tapuaenuku host rocks, lamprophyres and carbonatites provide key evidence of the geological evolution of the system. The olivine gabbro (LGC 12) located within the field site is mineralogically and texturally similar to descriptions of the LLS olivine gabbro from Baker (1990) (Fig. 4.1, 4.4, Table 4.1 and Appendix B). The crystallisation order of the olivine gabbro is likely to have followed the normal mildly alkaline mafic crystallisation sequence (i.e., olivine-clinopyroxene-plagioclase). The olivine gabbro exhibits a mixture of both coarse and fine grained phenocrysts. Fine grained phenocrysts are typically a mixture of plagioclase, clinopyroxene, olivine and biotite whilst the coarse phenocrysts are altered plagioclase (oligoclase and bytownite). Bent coarse grained plagioclase phenocrysts are indicative of mechanical deformation. This suggests mechanical deformation in a partially molten semi-plastic host (Fig. 4.4, Table 4.1 and Appendix B and C). Oscillatory zoning coupled with the large phenocryst crystal phases suggest crystallisation from a volatile enriched melt with a relatively stable melt composition (Fig. 4.4, Table 4.1 and Appendix B and C) (Baker 1990; Baker et al. 1994). Apart from slight changes in mineral (and whole rock) Mg/Fe ratios and compatible trace element contents, influxes of fresh magma appear to have had little effect on the overall chemistry of the magma chamber (Nicol 1977; Baker 1990; Baker et al. 1994). Later stage influxes of carbonate rich fluids have altered the whole rock chemistry significantly along with mineral alteration through metasomatism (see Section 5.2).

Highly alkaline lamprophyre dykes are common throughout the TIC. Volatile- and alkali-enriched residuals melts that were produced during the crystallisation of the plutonic rocks

(Baker 1990; Baker et al. 1994) are represented by these lamprophyres. Crystallisation of amphibole is favoured over plagioclase due to the abundance of alkalis and volatiles concentrated in the residual magma (Baker 1990; Baker et al. 1994). Intricate and extreme zoning of the amphiboles and clinopyroxene is seen in LGC 8 and in LGC 7 by the oscillatory and patchwork pseudomorphism, coupled with the large euhedral crystals, suggests that the crystallisation occurred in a volatile rich melt that was rapidly changing in composition (Baker 1990; Baker et al. 1994). The chilled margin above the upper lamprophyre (LGC 1) and between the upper and lower lamprophyre (LGC 5 and 6) contains >50% glass. This is indicative of rapid cooling during the emplacement of the lamprophyres in contact with the host rocks. The trachytic texture of the amphibole phenocrysts forming in a euhedral manner is consistent with previous descriptions of chilled lamprophyre margins in Baker (1990).

The carbonatite veins and veinlets cross-cut the lamprophyre dykes and present their own later stage primary textures and mineralogy. These carbonatite veins have introduced fluids to the host lamprophyre evident by the heavily metasomatised ground mass and coarse phenocrysts seen in the LGC 2, 3, 3.5, 4, 9, 10, and 11 samples (Fig. 4.6 and 4.7) and discussed in Section 5.2. The textures of the carbonatites in the LGC samples are commonly allotriomorphic granular veins, with banding defined by variations of grain size, vein widths and the assimilation with the lamprophyre to form turbid calcite. The carbonate veins may contain clusters and veinlets of quartz, epidote and aegirine whereas altered feldspars, nepheline, along with destabilized micas, clinopyroxene, olivine and amphiboles are found in the silicate parts. Carbonate rich veins are almost entirely composed of calcite. The grain size of the calcite is constrained by the size of the dilatant fractures. Primary vein textures of colloform, comb quartz textures, calcite ocelli and the limpid coarse rhombohedral calcite crystal are indicative of incremental infill of open space structures by carbonate rich, low

alkali fluids (Dong et al. 1995; Alvin et al. 2004; Chauvet et al. 2006; de Oliveira Cordeiro et al. 2011). The quartz comb textures require slow changing fluid conditions in an open void space during crystal growth (Dong et al. 1995). Turbid coarse calcite crystals in the larger veins of LGC 9 and 10 are commonly twinned and highly interlocking which results in a granular texture with rare interstitial veinlets and patches of aegirine and quartz. These textures are a result of partial recrystallisation of the primary magmatic calcite crystals to form the granular aggregates similar to those of other carbonatite vein systems (Barker 1989; Wagner et al. 2003). This irregular vein network reflects late-stage carbonate fluid circulation (Barker 1989; Wagner et al. 2003; Alvin et al. 2004).

5.2 ALTERATION AND METASOMATISM

Along the margins of the carbonatite veins and veinlets, the country rock (i.e., olivine gabbro), the host lamprophyre dykes and the glassy foidites are distinctly altered through fenitization, a form of carbonate fluid metasomatism. This metasomatism has partially to completely altered components of the host olivine gabbro, the lamprophyre dykes and the chilled margin.

Primary minerals of the olivine gabbro (LGC 12) exhibit alteration by carbonate fluid induced metasomatism. Mechanical deformation and radial cracks in some plagioclase can be interpreted as resulting from the apparent volume increase associated with serpentinisation of olivine and the sericitisation of adjacent plagioclase. Clay is prevalent throughout and is indicative of the metasomatism of the primary minerals by the carbonate fluids that formed the calcite veins. In contrast to the primary assemblages, intercumulus kaersutite in the olivine gabbro may have been the product of metasomatism by volatile-rich residual melts (Baker 1990; Baker et al. 1994). These melts are likely to have been derived by the crystallisation of numerous smaller intrusive units that intruded into the LLS, including the

lamprophyres as suggested by Baker (1990). This intercumulus kaersutite and the pervasive metasomatism from the influx of carbonate fluids suggest that two differing metasomatic sequences occurred; one which altered the mineralogy with little chemical mass-transfer and a second that changed the chemical composition of the olivine gabbro (Fig. 5.1).

The lamprophyre samples (LGC 7 and 8) maintain their primary textures despite being metasomatised. Nevertheless, the primary coarse phenocrysts are pervasively to completely pseudomorphed and altered. Calcite, quartz and aegirine are typical constituents that are pseudomorphed into the phenocrysts (i.e., olivine and clinopyroxene) of the lamprophyres. Partial serpentinisation and the degradation of the primary ground mass minerals is prevalent throughout the samples (Fig. 4.6 and Appendix B and C). In both LGC 7 and 8 the apparent scarcity of alteration to the groundmass suggests that the metasomatic fluids used the groundmass as a pathway, originating from the veins. Pervasively to completely metasomatised phenocrysts of kaersutite, riebeckite, olivine and nepheline are set in a distinctly less altered groundmass of nepheline, plagioclase (labradorite and andesine), titanaugite, ilmenite, titanomagnetite, analcite and green amphibole.

Secondary influxes of carbonate metasomatic fluid have pervasively pseudomorphed the phenocrysts and also introduced calcite carbonate that has precipitated out in fractures to form veinlets along with associated minor quartz and aegirine veinlets. The mafic phenocrysts present in LGC 7 are further away from large igneous carbonate pathways (Fig. 4.6 and Appendix B and C) than sample LGC 8, exhibiting higher levels of metasomatic alteration than the phenocrysts in LGC 8 whilst maintaining their phenocryst textures (Fig. 4.6 and Appendix B and C). This suggests that the mafic phenocrysts are more likely to be chemically altered by the influx of igneous carbonate fluids as the fluids slow down and cool. Field relationships imply that various magmatic and/or hydrothermal carbonatite veins as well as their associated aegirine, epidote and quartz inclusions are a coeval to later stage

intrusive of camptonite lamprophyre intrusives. Crucially the three lithologies, glassy foidite, camptonite and olivine gabbro (LGC 1, 5, 7, 8 and 12) are all carbonate bearing. As these samples were pervasively metasomatized by the carbonate fluids, their mineralogical composition changes as does their chemical composition.

Figure 5.1. Olivine crystal from sample LGC 12 exhibiting a serpentinised rim and pseudomorphed core to clay with calcite ocelli.

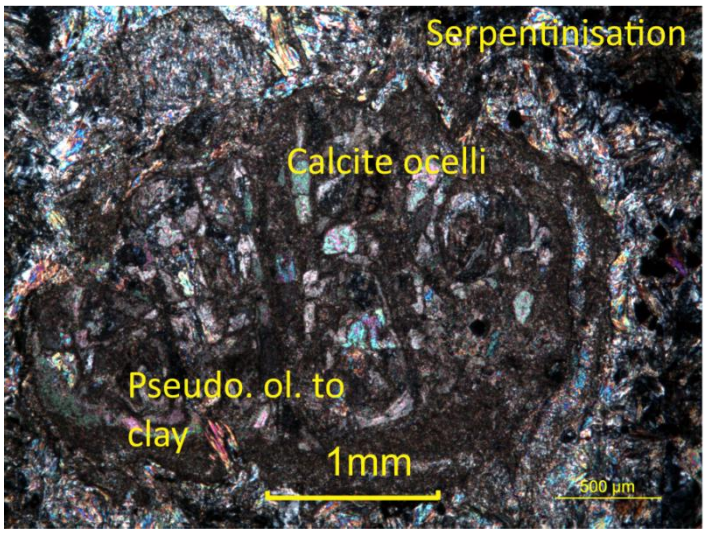

The chilled margin (glassy foidites; LGC 1 and 5) of the lamprophyres also exhibit textural and mineralogical alteration. The foidites are frequently mineralogically reconstituted to form a calcite-aegirine-quartz-magnetite alteration front (Fig. 4.5 and Appendix B). The metasomatic fluid source is likely to be the same source that led to the formation of the calcite veins. In thin section, the glassy foidite, shows an alteration front which is visibly seen emanating from the veins and the alteration weakens further from the veins and veinlets (Fig. 4.5). The influx of igneous carbonate introduced significant concentrations of magnetite, titanomagnetite and to a lesser extent ilmenite in the alteration front visible through microscopic analysis. This is not uncommon in igneous carbonate systems (Cooper 1971; Deines & Gold 1973; Mitchell 1984; Morogan & Woolley 1988; Santos et al. 1990; Santos & Clayton 1995; Harmer 1999; Wagner et al. 2003; Tappe et al. 2006).

Alteration of the minerals by the carbonate fluids follows the degradation sequence of each specific mineral. The degradation of the kaersutite and hornblende to chlorite and clays is indicative of intense metasomatic alteration. Undulose extinction and sericitisation are also key indicators of metasomatism. During this process branching and clean igneous calcite precipitated into fractures that formed as the original host lamprophyre magma chilled rapidly to form the chilled margin glassy foidite. Alteration appears more severe adjacent to the veins reinforcing the connection between metasomatism of primary igneous host rocks and the emplacement of carbonatite vein networks.

Figure 5.2. Chilled margin (LGC 5) photomicrograph displaying the alteration front that emanated from the calcite veinlets.

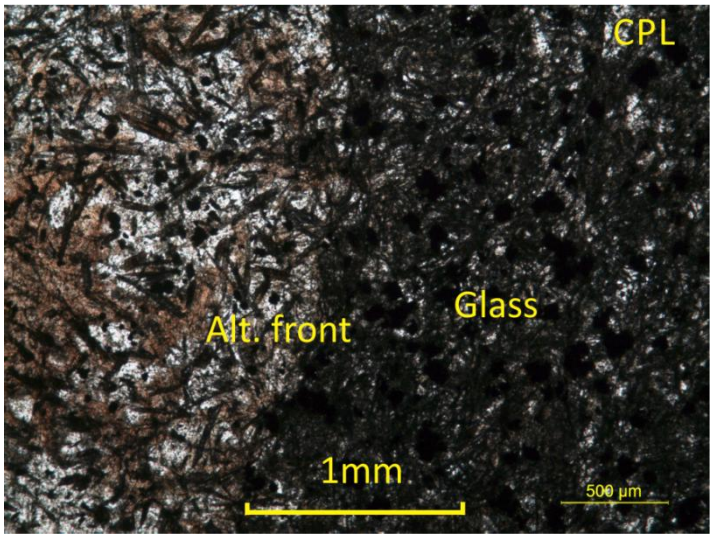

In order to correctly classify the chilled margin, chemically unaltered samples are required. Unfortunately, samples LGC 1 and 5 are geochemically compromised by the influx of carbonate fluids (Fig. 5.2). Chemically these glassy foidites contain higher levels of Na_2O and K_2O than the lamprophyres, yet contain similar levels of SiO_2. A similar result was reported by Baker (1990) with his samples exhibiting higher levels of SiO_2. This suggests that the influx of igneous carbonate fluids have chemically lowered the SiO_2 composition and possibly lowered the Na_2O and K_2O as well. The difference in Na_2O and K_2O compositions between the chilled margin and the lamprophyres may be attributed to the degree of chemical

alteration during the influx of carbonate fluids, as the carbonatite samples have lower Na_2O and K_2O compositions (Fig. 4.9 and 4.10).

Carbonatite samples LGC 3, 3.5, 9 and 10 exhibit high levels of metasomatism to the host lamprophyre with near complete removal of the primary textures and minerals (Fig. 4.7, Table 4.1 and Appendix B and C). Carbonate fluid metasomatism has produced significant amounts of clay minerals that need further study. The degree of metasomatic alteration appears to be irregular. Carbonate minerals form veins, veinlets, ocelli and pervasive patches which are heterogeneously distributed throughout the samples in a similar manner to what is seen at the alkaline lamprophyres from Taourirt, Morocco (Wagner et al. 2003) and the Haast carbonatites, New Zealand (Cooper 1971; Blattner & Cooper 1973; Cooper 1986; Cooper et al. 1987; Paterson 1993; Cooper & Paterson 2008). Mafic minerals, in particular olivine and kaersutite, have pseudomorphed into carbonate clays with conspicuous calcite ocelli. The metasomatic alteration from the igneous carbonate fluids is gradational and irregular with preferential access of the metasomatic fluids through the groundmass and fractures of the lamprophyres (Fig. 4.6 and 4.7, Table 4.1 and Appendix B and C). Intrusions by the metasomatic carbonate fluids into the glassy foidite and olivine gabbro appear to be less pervasive. In order to further elucidate these relationships microprobe analysis would be required. In summary, the findings presented in this thesis suggest at the LGC outcrop, a lightly to pervasively metasomatised camptonite lamprophyre cross-cut by xenolithic carbonatite veins was emplaced by a sub-solidus carbonate metasomatic process.

5.3 WHOLE ROCK GEOCHEMISTRY

Major and trace element compositions of the carbonatites and the silicate rocks provide an understanding of the parent melt characteristics and geological processes that occurred during the genesis of the complex. Trace element enrichment or depletion provides a glimpse of the

magmatic condition that occurred during paragenesis. The carbonatite veined samples are enriched in Sr (240-1377 ppm), which is typical of magmatic carbonatites, in contrast to replacement carbonate rich rocks which contain low Sr carbonates (Kapustin 1982; Ngwenya & Bailey 1990; Wagner et al. 2003). Depleted Rb, K and Ti are also indicative of magmatic carbonatites (Kapustin 1982; Ngwenya & Bailey 1990; Wagner et al. 2003; Dalsin 2013). However, contrary to magmatic carbonatites, La and Ce concentrations are anomalously low in the LGC samples. The source of the carbonatite veins is either carbohydrothermal fluids or magmatic carbonatite melt formed through either primary mantle carbonate magmas, or secondary magmas with carbonate differentiation by fractional crystallisation and/or liquid immiscibility of an evolved mantle-derived parental silicate melt (Blattner & Cooper 1973; Bell 1989; Deines 1989; Le Bas 1989; Woolley & Kempe 1989; Mitchell 2005; Jones et al. 2013)

In the case of the Tapuaenuku carbonatite veins, the MgO deficiency of the TIC carbonatites diverges from the primary mantle-derived magma model, as primary carbonatites are likely to be magnesiocarbonatites (Fig. 4.9) (Bailey 1993; Lee & Wyllie 1994; Wyllie & Lee 1998; Lee et al. 2000; Bell & Simonetti 2010). This low MgO content at the LGC site suggests that the carbonatites are derived from carbohydrothermal fluids (Gittins et al. 2005; Mitchell 2005; Tappe et al. 2006; Woolley & Kjarsgaard 2008b; Woolley & Kjarsgaard 2008a; Woolley & Bailey 2012; Jones et al. 2013). The carbonate veins (calcite ~85-95%) exhibit high $CaCO_3$ abundances and mineralogically low total alkalis in the veins, (note that LGC 9 and 10 contains 10-40 vol. % of $CaMg(CO_3)_2$). LGC 10 exhibits MgO concentrations that are consistent with magnesiocarbonatites (Fig 4.9), likely due to the dolomite mineral present in this sample (Table 4.5). Chemical variation in major and trace element abundances over short distances is a phenomenon that is not uncommon in carbonatites (Bailey 1993; Dalton & Wood 1993; Lee & Wyllie 1994; Wyllie & Lee 1998; Lee et al. 2000; Hoernle et al. 2002;

Wagner et al. 2003; Bell & Simonetti 2010). This variation is present in samples LGC 9 and 10. Both LGC 9 and 10 were taken 20 cm horizontally apart, from the same veins structure, and plot as ferro- and magnesio-carbonatites, respectively (Fig. 4.1 and 4.9). The carbonatite veins do not represent carbonate liquid formed through immiscibility, as immiscible carbonate liquids are rich in alkalis (Lee & Wyllie 1994, 1998; Wyllie & Lee 1998; Lee et al. 2000; Lee & Wyllie 2000; Wagner et al. 2003). The LGC carbonatite vein calcite abundances appear to sit between 65-90% suggesting that they may represent a calcio-carbonatite magma that is generated via metasomatism with the wall rock (Bailey 1993; Dalton & Wood 1993; Lee & Wyllie 1994; Wyllie & Lee 1998; Lee et al. 2000; Hoernle et al. 2002; Wagner et al. 2003; Bell & Simonetti 2010). This produces carbonate liquids containing <87% $CaCO_3$ (Dalton & Wood 1993; Lee & Wyllie 1994; Wyllie & Lee 1998; Wagner et al. 2003). Hydrous carbonate-rich liquids with compositions of both calcite ($CaCO_3$) and dolomite ($CaMg(CO_3)_2$) will precipitate the calcite-carbonatites out first, followed by the precipitation of calcite-dolomite-carbonatites (Dalton & Wood 1993; Lee et al. 2000; Lee & Wyllie 2000; Hoernle et al. 2002; Gittins et al. 2005; Tappe et al. 2006; Bell & Simonetti 2010). The precipitation of dolomite-carbonatites follows the calcite-dolomite-carbonatites but have a limited temperature window (Lee et al. 2000; Lee & Wyllie 2000). The inclusion of dolomite in the core of the carbonate veins of LGC 9 and 10 is indicative of the calcite-dolomite-carbonatite precipitation window and suggest at least two stages of carbonate precipitation process have occurred.

5.4 STABLE ISOTOPES

Stable isotopic proxies are invaluable indicators of geological processes and conditions. In carbonatite systems, stable isotope compositions of carbonate oxygen and carbon have been shown to demonstrate the source of the carbonate. This section presents an original

interpretation of the geological evolution of the TIC carbonatites based on the $\delta^{13}C$ and $\delta^{18}O$ values. The source of carbonatites likely originates within the convecting mantle, as their carbon and oxygen isotopic compositions are similar to those other mantle-derived carbonatites worldwide (Deines 1989; Le Bas 1989; Santos et al. 1990; Harmer 1999; Mitchell 2005; Jones et al. 2013). Although the carbonatite veins form a minor component (<1%) of the lamprophyric suite within the TIC, they give a rare insight into the geological processes that occurred during emplacement and alteration of the TIC.

An important finding of this thesis is the determination of distinct primary igneous carbonate $\delta^{13}C$ and $\delta^{18}O$ compositions recognised in the TIC. The carbonatites and the metasomatised rocks are the products of superimposed primary magmatic and hydrothermal processes. In the context of this study, the term magmatic includes processes such as liquid immiscibility, fractionational crystallisation and assimilation of country rock, whereas hydrothermal processes are defined as the interaction between rocks and fluids of differing compositions and temperatures. Metasomatism may accompany the hydrothermal interactions.

Carbon and oxygen in the mantle and crustal rocks play significant roles controlling the stable isotopic composition of primary igneous carbonates. The lower abundance of carbon in crustal rocks, when compared to oxygen, prohibits large carbon isotopic variations even during extrusive contamination by country rocks. $\delta^{13}C$ of carbonates is also not strongly affected by low temperature alteration processes and weathering (Deines 1989; Santos & Clayton 1995). Hence, variation in the $\delta^{13}C$ isotopic composition can give insight into the heterogeneity of the mantle source region of the alkaline carbonatite magma (Deines 1989; Santos & Clayton 1995). In contrast, oxygen isotope compositions provide insight into the interactions involving carbonatites and the country rocks, as well as secondary processes

involving fluids and the temperature at which water-rock interaction occurs (Barker 1989; Bell 1989; Deines 1989; Santos & Clayton 1995).

A number of processes are known to cause variation in the $\delta^{13}C$ and $\delta^{18}O$ composition of carbonatites some of which are not relevant to the TIC carbonatites. Liquid immiscibility is unlikely to cause significant $\delta^{13}C$- $\delta^{18}O$ variations in carbonatite systems. Santos and Clayton (1995) rebuts the suggestion by Deines (1989) that oxygen and carbon isotopic variations in carbonatites are related to the extraction of the carbonatite melt from its mantle source. Liquid immiscibility would require unrealistic oxygen and carbon isotope fractionation factors and does not explain the preservation of the carbonatite melt isotopic composition during exhumation (Santos & Clayton 1995; Wagner et al. 2003). In the case of the Tapuaenuku, the lack of $\delta^{13}C$ variation within each sample implies liquid immiscibility is unlikely to have played a significant role in producing the variation seen in the $\delta^{18}O$ values. This interpretation is further reinforced by results discussed above (see Section 5.3).

Although not relevant to the Tapuaenuku carbonatites, it is worthwhile noting that contamination of the carbonatite magma by country rock containing limestone is readily recognisable using stable isotope proxies. An example of this is the Mato Preto carbonatite in Brazil (Santos et al. 1990; Santos & Clayton 1995). This complex intrudes Upper Proterozoic granites and limestones and has $\delta^{13}C$ values of -6.0 to +0.5‰ and $\delta^{18}O$ values ranging from 9.0 and 14.0‰ (Santos et al. 1990; Santos & Clayton 1995). Radiogenic isotopes are used to distinguish contamination by country rock that have similar $\delta^{13}C$- $\delta^{18}O$ values to that of the carbonatites' parental magma (Santos et al. 1990; Santos & Clayton 1995; Bell & Simonetti 2010).

The range of the oxygen and carbon isotope values in the Tapuaenuku carbonatites similar to the carbonatites world wide (Blattner & Cooper 1973; Deines & Gold 1973; Deines 1989;

Bailey 1993; Santos & Clayton 1995; Adams & Cooper 1996; Mitchell 2005; Tappe et al. 2006). The Tapuaenuku isotope dataset has an overall positive slope trend on the $\delta^{13}C$- $\delta^{18}O$ ‰ similar to data reported by Deines (1989), Reid and Cooper (1992) and Cooper and Paterson (2008) for low temperature carbonatites. Deines (1989) suggested that these positive co-variation trends could be attributed to a variety of processes. These processes include magmatic fractionation effects, during emplacement the loss of fluids, secondary low-temperature hydrothermal interaction between carbonate and meteoric fluids and/or assimilation with the host lithologies.

The Tapuaenuku carbonatites are characterised by mildly elevated $\delta^{13}C$ values (Fig. 2.1, 4.11 and 4.12 and 5.3). A number of samples exhibit $\delta^{18}O$ values that are consistent with mean primary mantle values (i.e., $\delta^{18}O$=6.0‰ total range from 5 to 25‰) whilst many samples are consistent with a mantle carbonate source based on their $\delta^{13}C$ values (i.e., $\delta^{13}C$=-6.5‰). Deines (1989) states that the $\delta^{18}O$ isotopic composition of carbonatite veins and dykes differ from carbonatite intrusions. Carbonatite systems have a clear peak of $\delta^{18}O$ values at +6 to 9‰ with 26% of all carbonatite intrusions worldwide falling in this range. However, only 4% of carbonatite veins and dykes have similar values. The variation in carbon isotope compositions of carbonatite intrusions has a narrow range between -2 and -8‰ with 91% of the $\delta^{13}C$ values falling within this range globally. The Tapuaenuku carbonatites lie within the -2 to -8‰ $\delta^{13}C$ expected of carbonatite intrusions, with some slightly elevated $\delta^{13}C$ values suggesting $\delta^{13}C$ variation typical of carbonatite veins and dykes (Fig. 5.3).

The positive values recognised in calcite veinlets (LGC 2, 3, 3.5, 4, and 6) are likely due to interaction between primary carbonatite and hydrothermal fluids, as similar oxygen isotope compositions have been observed in several other carbonatite systems (Bell 1989; Censi et al. 1989; Deines 1989; Le Bas 1989; Bailey 1993; Dalton & Wood 1993; Santos & Clayton

1995; Wagner et al. 2003; Mitchell 2005; Tappe et al. 2006). As the quantity of carbonate is lower in dykes and veins, the potential isotopic exchange is greater. Hence, dykes and veins are less likely to retain their original isotopic composition (Deines 1989). In contrast the $\delta^{18}O$ variation in the laminate veins of samples LGC 9 and 10 could also be due to their temperatures of formation.

Figure 5.3 Carbonatite and host rock stable isotope composition of the Tapuaenuku Igneous Complex. Shading indicates the type of mineralogical source. No shading-host rock, light grey-calcite veinlets, solid colour- turbid calcite with host rock and black-limpid calcite veins.

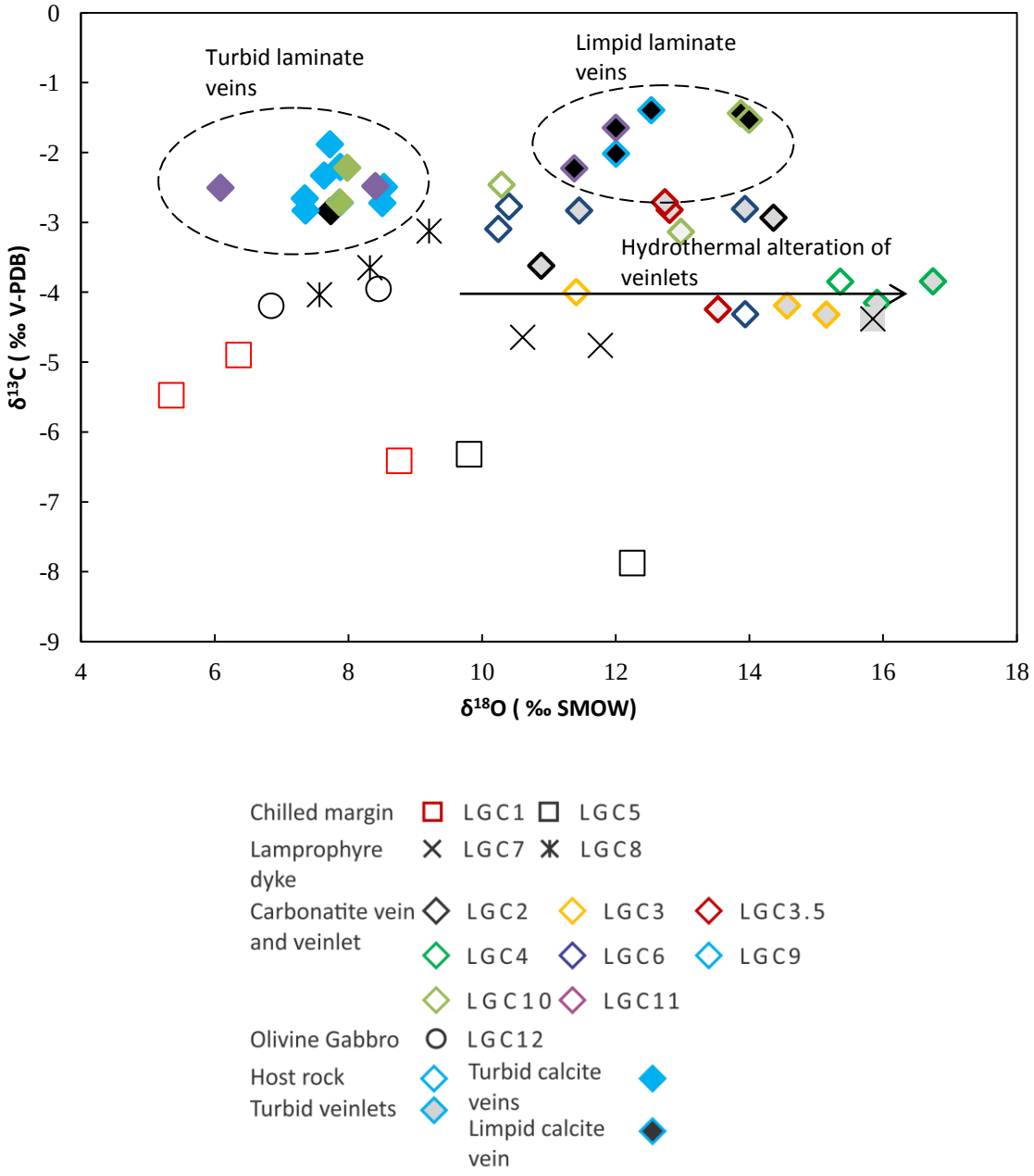

The limpid calcite that has precipitated in the centre of veins LGC 9 and 10 has $\delta^{18}O$ values between 12.00 and 12.53‰ and 13.87 and 13.99‰ (Fig. 4.1, 4.2, 4.3, 4.11, 4.12 and Table 4.6). The turbid planar laminates and chaotic veinlets of LGC 9 and 10 have lower $\delta^{18}O$ values ranging from 7.35 to 7.89‰ and 7.87 to 7.98‰, respectively. Differences in formation conditions and the likely assimilation of the carbonate with the lamprophyre is the probable cause behind the lower $\delta^{18}O$ values of the turbid planar laminate carbonate. Hydrothermal processes are the most likely source of variation of the chaotic spider veinlet carbonatites from samples LGC 2, 3, 3.5, 4, 6 and 11. As the significant variations of the $\delta^{18}O$ values are not accompanied by significant $\delta^{13}C$ variation suggest that the hydrothermal fluids were water rich (Censi et al. 1989; Santos et al. 1990; Santos & Clayton 1995; Lee et al. 2000; Lee & Wyllie 2000), and that the larger variation in $\delta^{18}O$ values of samples LGC 9 and 10 is indicative of oxygen disequilibrium between calcite and dolomite. Large ranges in carbonatites $\delta^{13}C$ and $\delta^{18}O$ values have been observed in other shallow complexes, dykes and veins (Deines 1989). Thus, it is possible that these variations result from a lower temperature hydrothermal alteration in which H_2O and CO_2 are important constituents of the fluid phase (Santos & Clayton 1995).

However, lower temperature hydrothermal alteration a likely cause of the variation in $\delta^{18}O$ values, recognised in the chaotic spider veinlet carbonatites in samples LGC 2, 3, 3.5, 4, and 6. The oxygen isotope values range from 5.35‰ to 16.75‰. Previous studies of meteoric water give $\delta^{18}O$ values c. -7.0 ‰ and that meteoric fluids are the only major source of fluids at temperatures below 270° (O'Neil et al. 1969; Friedman & O'Neil 1977). At these lower epithermal temperatures calcite-water fractionation exceeds 6.0‰ (O'Neil et al. 1969). Thus, water-rich fluids responsible for the high temperature alteration (i.e., >300° C) of carbonatite host rocks are likely to be of magmatic carbohydrothermal origin (Lee & Wyllie 1994; Santos & Clayton 1995; Bell & Simonetti 2010).

Based on the $\delta^{18}O$ results presented in this thesis, TIC carbonatites likely formed across a wide range in temperatures (c. 200° to >400° C). As lamprophyre melt cools, carbonate fluids will infill open void spaces and interact with the lamprophyre at high temperatures precipitating the turbid calcite/dolomite. This model is consistent with the LGC samples exhibiting lower $\delta^{18}O$ values. At a later stage, cooler carbohydrothermal fluids likely intruded or were injected into the centre of the turbid carbonate. Precipitating the limpid calcite/dolomite at lower temperatures likely between 135° to 225° C (O'Neil et al. 1969; Friedman & O'Neil 1977). These are the TIC carbonatites with the higher $\delta^{18}O$ values (Fig. 5.3). Such a two-stage process helps explain the boundary between the turbid and limpid calcite present in the LGC veins (Fig. 4.1, 4.2 and 4.3). In summary, the $\delta^{18}O$ values of the Tapuaenuku carbonatite veins and veinlets reinforce the complex primary igneous and secondary hydrothermal alteration processes that occurred in this system.

In the bigger picture, emplacement of the TIC is related the mid-Cretaceous extension manifest throughout the South Island of New Zealand (Baker et al. 1994; Baker & Seward 1996). The emplacement of carbonatites during the mid-Cretaceous is indicative of an enrichment of carbon and CO_2 volatiles in the parent melt through low degree partial melting of the upper mantle. A mantle source capable of producing carbonatite melts requires the conversion of CO_2 to CO_3^- (Deines & Gold 1973; Bell 1989; Bell & Simonetti 2010). Debate remains as where and at what depth this conversion occurs, and thus where carbonatitic melts are formed. However, recent radiogenic isotope data suggests that carbonatite melt generation is restricted to the lithosphere (Bell et al. 1982) and upper mantle (Nelson et al. 1988; Simonetti et al. 1998; Bell & Tilton 2002; Bell & Simonetti 2010).Based on the results and interpretation present in this thesis a conceptualised model of the formation of the TIC is presented in Figure 5.4.

Figure 5.4. Conceptualised model of the Tapuaenuku Igneous Complex, during its formation in the mid-Cretaceous. A: Representation of basement greywacke before mid- Cretaceous extension. B:Emplacement of the TIC as a layered intrusion as a result of phase of igneous activity due to the mid-Cretaceous extension. C: Volatile- and alkali-enriched residuals melts that were produced during the crystallisation of the plutonic rocks intrude the layered series in the form of lamprophyres. D: Carbon and CO_2 volatiles enrichment in the parental melt through low degree partial melting of the upper mantle occurs. Hydrothermal fluids mix with the carbon and CO_2 volatiles to form carbohydrothermal fluids that intrude the lamprophyres and precipitates in the form of primary igneous carbonatite veins. Subsequent exhumation in the early-Miocene allows the TIC to outcrop.

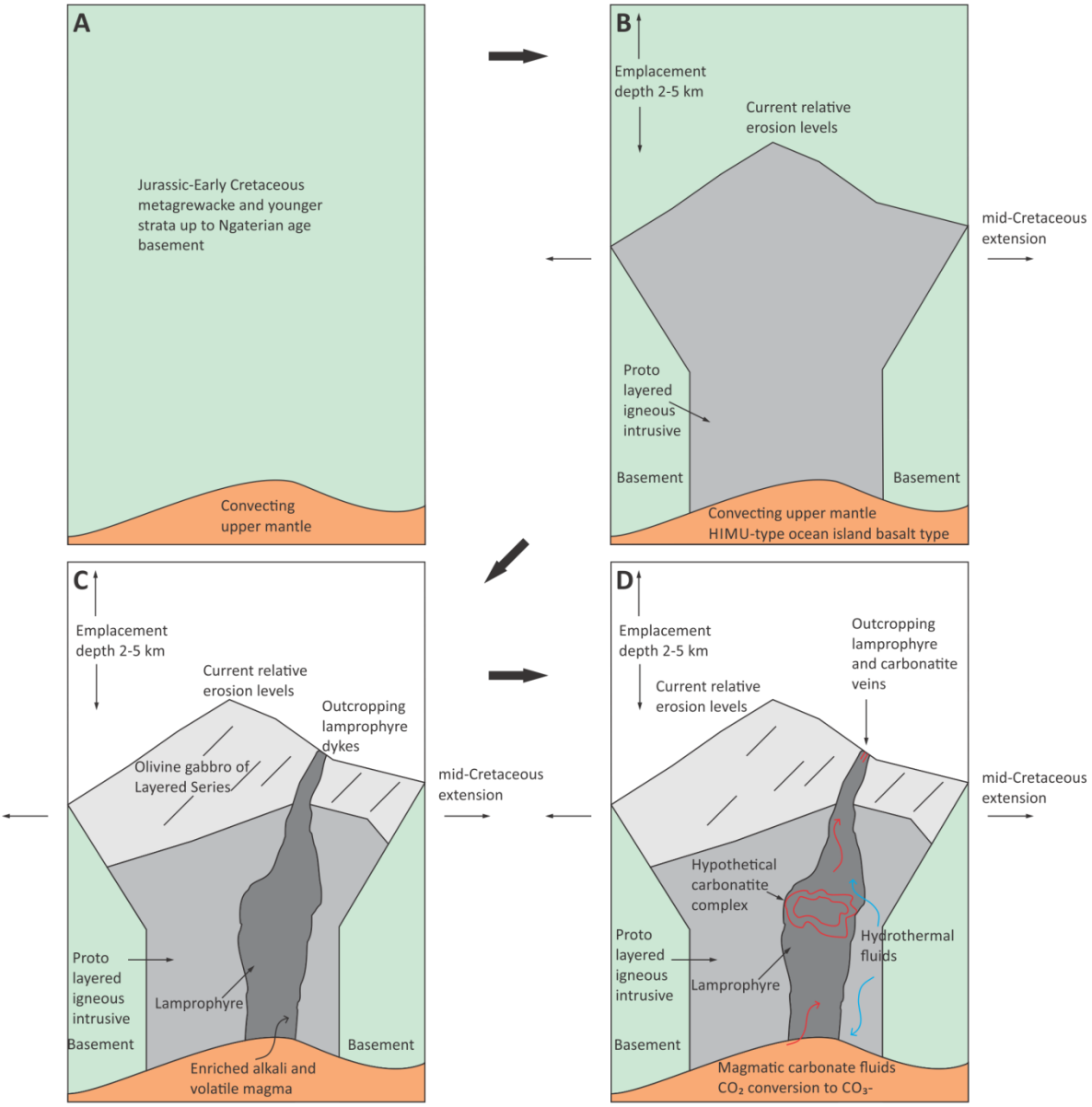

The model present in Figure 5.4 suggests the waning phase of igneous activity in the South Island, New Zealand, related to the mid-Cretaceous extension produced conditions conducive to the formation of carbohydrothermal metasomatic carbonatites. The documentation of carbonatites in the Tapuaenuku Igneous Complex provides further insights to the magmatic conditions present in this intra-continental rift system.

CHAPTER 6: CONCLUSION

6.1 CONCLUSION

This thesis present evidence consistent with the presence of carbohydrothermal carbonatite veins in the lamprophyre dykes of the Tapuaenuku Igneous Complex. The veins are primarily comprised of calcite, with two samples exhibiting a mixture of calcite and dolomite, quartz, epidote and aegirine. These veins likely formed by from a carbohydrothermal fluid that also altered the lamprophyre, glassy foidite and olivine gabbro host rocks. The geochemical processes leading to the formation of the carbonatite veins, carbon and oxygen isotopic variability and the alteration to the lamprophyres are complex and have been described in this thesis through detailed field, petrographical and geochemical investigations at the outcrop to sub-hand sample scale.

The mineralogy of the metasomatised upper and lower lamprophyre dykes and the carbonatite veins and veinlets at the LGC outcrop is relatively complex. The host dykes are primarily composed of two camptonite lamprophyres and its chilled margins glassy foidite. Both camptonites are predominantly composed of phenocrysts of kaersutite, riebeckite, and occasionally augite, olivine and plagioclase are found in a matrix of plagioclase, actinolite, nepheline and opaques. The glassy foidite is primarily glass with trachytic phenocrysts composed of elongate kaersutite. Coeval or perhaps later stage igneous carbonate fluids precipitated into fractures to from the carbonatite veins and veinlets. These carbonate fluids heavily metasomatised the host rock, whilst pervasively pseudomorphing the phenocrysts.

Carbonatite carbon and oxygen isotopic compositions are consistent with a mantle source. The significant variations in $\delta^{18}O$ values of the chaotic carbonatite veinlets are likely the

result of lower temperature hydrothermal alteration in which H_2O and CO_2 were important constituents of the fluid phase.

The over arching goal of this thesis was to produce an evidence-based petrochemical classification of the carbonate-rich veins cross-cutting the lamprophyric dykes present in the Tapuaenuku Igneous Complex. The mineralogical and geochemical results for TIC rocks exposed at the LGC outcrop confirm the presence of carbonatites in this area. These carbonatite veins precipitated into the LS gabbro hosted lamprophyres, heavily metasomatising them in the process.

The research aims and the results obtained in this research are summarised in Table 6.1. Due to limited time in the field the full lateral and spatial extent of the carbonatites was not pursued. Future research including, radiogenic dating, Sr, Nd and Pb isotopes to determine the mantle source region and the paragenesis of the carbonate fluids is recommended. A full suite Rare Earth Element composition by laser ablation ICP-MS will also aid in the determination on whether these carbonatites are in fact magmatic or carbohydrothermal origin. Electron microprobe analyses are also required to further document the mineralogy of the lamprophyres and their metasomatised mineralogies.

Table 6.1 Summary of conclusions obtained for the research aims of this thesis

Aims	Results obtained during this research
Classify the type of carbonatite associated with the lamprophyre dykes.	Calcite and calcite-dolomite carbonatites veins and veinlets are present in the lamprophyres.
Characterise the major and trace element chemistry of the carbonatites.	Sr and CaO is enriched within most of the samples, MgO is enriched in samples LGC 9 and 10 due to the presence of dolomite in the carbonatite veins, depleted SiO_2, Rb, K and Ti are also indicative of magmatic carbonatites.
Compare the δC^{13} and the δO^{18} isotope results of previously documented carbonatites.	The δC^{13} and the δO^{18} isotope of the Tapuaenuku carbonatite veins sit within the range expected for carbonatite veins, dykes and carbonatites from shallow complexes.
Ascertain the mineralogy of the "carbonatites".	Petrographic analyses indicate calcite, some dolomite and associated aegirine, quartz, magnetite and epidote are present in the carbonatite veins.
Assess the timing and relationships that the "carbonatite" dykes have with the host rock.	The carbonatites are in the form of veins and appear along the strike of the lamprophyres. These veins are coeval to later stage to the formation of the lamprophyre dyke suite.
Assess the alteration the "carbonatite" intrusive have on the host rock.	The carbonate fluids have heavily metasomatised the host lamprophyres using the ground mass as the fluid pathway. Phenocrysts are pervasively to completely pseudomorphed to clays with the calcite ocelli prevalent within pseudomorphed phenocrysts.

REFERENCES

Adams C 2003. K-Ar geochronology of Torlesse Supergroup metasedimentary rocks in Canterbury, New Zealand. Journal of the Royal Society of New Zealand 33(1): 165-187.

Adams C, Cooper AF 1996. K-Ar age of a lamprophyre dike swarm near Lake Wanaka, west Otago, South Island, New Zealand. New Zealand Journal of Geology and Geophysics 39(1): 17-23.

Allen AD 1962. The stratigraphy and structure of the Middle Awatere Valley. Unpublished thesis, Victoria University of Wellington, Unpublished. 62 p.

Alvin M, Dunphy J, Groves D 2004. Nature and genesis of a carbonatite-associated fluorite deposit at Speewah, East Kimberley region, Western Australia. Mineralogy and Petrology 80(3-4): 127-153.

Amundsen HE 1987. Evidence for liquid immiscibility in the upper mantle.

Bailey D 1993. Carbonate magmas. Journal of the Geological Society 150(4): 637-651.

Baker IA, Gamble JA, Graham IJ 1994. The age, geology, and geochemistry of the Tapuaenuku igneous complex, Marlborough, New Zealand. New Zealand journal of geology and geophysics 37(3): 249-268.

Baker J, Seward D 1996. Timing of Cretaceous extension and Miocene compression in northeast South Island, New Zealand: Constraints from Rb-Sr and fission-track dating of an igneous pluton. Tectonics 15(5): 976-983.

Baker JA 1990. The Geology of the Western Margin of the Tapuaenuku Plutonic Complex, Marlborough, New Zealand. Unpublished thesis, Univeristy of Wellington, Wellington. 215 p.

Barker D 1989. Field relations of carbonatites. Carbonatites: Genesis and Evolution. London: Unwin Hyman: 38-69.

Barley M, Weaver S, De Laeter J 1988. Strontium isotope composition and geochronology of intermediate-silicic volcanics, Mt Somers and Banks Peninsula, New Zealand. New Zealand journal of geology and geophysics 31(2): 197-206.

Barreiro BA, Cooper AF 1987. A Sr, Nd, and Pb isotope study of alkaline lamprophyres and related rocks from Westland and Otago, South Island, New Zealand. Geological Society of America Special Papers 215: 115-126.

Bartholomew TD 2012. Neotectonics, Kinematics, and Evolution of the Vernon, Awatere, and Cloudy Faults of the Marlborough Fault System, New Zealand.

Bell K 1989. Carbonatites, Unwin Hyman.

Bell K, Tilton GR 2002. Probing the mantle: the story from carbonatites. Eos, Transactions American Geophysical Union 83(25): 273-277.

Bell K, Simonetti A 2010. Source of parental melts to carbonatites–critical isotopic constraints. Mineralogy and Petrology 98(1-4): 77-89.

Bell K, Blenkinsop J, Cole T, Menagh D 1982. Evidence from Sr isotopes for long-lived heterogeneities in the upper mantle.

Blattner P, Cooper A 1973. Carbon and oxygen isotopic composition of carbonatite dikes and metamorphic country rock of the Haast Schist terrain, New Zealand. Contributions to mineralogy and petrology 44(1): 17-27.

Brooker R, Hamilton D 1990. Three-liquid immiscibility and the origin of carbonatites. Nature 346(6283): 459-462.

Brooker R, Kjarsgaard B 2010. Silicate-carbonate liquid immiscibility and phase relations in the system SiO_2-Na_2O-Al_2O_3-CaO-CO_2 at 0· 1-2· 5 GPa with applications to carbonatite genesis. Journal of Petrology.

Censi P, Comin-Chiaramonti P, Demarchi G, Longinelli A, Orué D 1989. Geochemistry and Carbon and Oxygen isotopes of the Chiriguelo carbonatite, northeastern Paraguay. Journal of South American Earth Sciences 2(3): 295-303.
Challis GA 1961. Post-intrusion deformation of a dyke swarm, Awatere Valley, New Zealand. Geological Magazine 98: 441-448.
Challis GA 1978. Cretaceous igneous rocks: Marlborough Province. In: Suggate RP, Stevens GR, Te Punga MT ed. The Geology of New Zealand. Wellington, EC Keating, Govt. Printer.
Chauvet A, Bailly L, André A-S, Monié P, Cassard D, Tajada FL, Vargas JR, Tuduri J 2006. Internal vein texture and vein evolution of the epithermal Shila-Paula district, southern Peru. Mineralium Deposita 41(4): 387-410.
Church AA, Jones AP 1995. Silicate—Carbonate Immiscibility at Oldoinyo Lengai. Journal of Petrology 36(4): 869-889.
Cooper A 1971. Carbonatites and fenitization associated with a lamprophyric dike-swarm intrusive into schists of the New Zealand geosyncline. Geological Society of America Bulletin 82(5): 1327-1340.
Cooper A 1986. A carbonatitic lamprophyre dike swarm from the Southern Alps, Otago and Westland. Late Cenozoic volcanism in New Zealand. Royal Society of New Zealand bulletin 23: 313-336.
Cooper A, Barreiro B, Kimbrough D, Mattinson J 1987. Lamprophyre dike intrusion and the age of the Alpine fault, New Zealand. Geology 15(10): 941-944.
Cooper AF, Paterson LA 2008. Carbonatites from a lamprophyric dyke-swarm, South Westland, New Zealand. The Canadian Mineralogist 46(4): 753-777.
Corporation O 2015. Handheld XRF Analyzers http://www.olympus-ims.com/en/xrf-xrd/delta-handheld/
Dalsin ML 2013. The mineralogy, geochemistry and geochronology of the Wicheeda Carbonatite Complex, British Columbia.
Dalton JA, Wood BJ 1993. The compositions of primary carbonate melts and their evolution through wallrock reaction in the mantle. Earth and Planetary Science Letters 119(4): 511-525.
Dawson J 1998. Peralkaline nephelinite–natrocarbonatite relationships at Oldoinyo Lengai, Tanzania. Journal of Petrology 39(11-12): 2077-2094.
de Oliveira Cordeiro PF, Brod JA, Santos RV, Dantas EL, de Oliveira CG, Barbosa ESR 2011. Stable (C, O) and radiogenic (Sr, Nd) isotopes of carbonates as indicators of magmatic and post-magmatic processes of phoscorite-series rocks and carbonatites from Catalão I, central Brazil. Contributions to Mineralogy and Petrology 161(3): 451-464.
Deines P 1989. Stable isotope variations in carbonatites. Carbonatites: Genesis and evolution, Unwin Hyman London. Pp. 301-359.
Deines P, Gold D 1973. The isotopic composition of carbonatite and kimberlite carbonates and their bearing on the isotopic composition of deep-seated carbon. Geochimica et Cosmochimica Acta 37(7): 1709-1733.
Dong G, Morrison G, Jaireth S 1995. Quartz textures in epithermal veins, Queensland; classification, origin and implication. Economic Geology 90(6): 1841-1856.
Freestone I, Hamilton D 1980. The role of liquid immiscibility in the genesis of carbonatites-an experimental study. Contributions to Mineralogy and Petrology 73(2): 105-117.
Friedman I, O'Neil JR 1977. Compilation of stable isotope fractionation factors of geochemical interest, USGPO.
George AD 1988. Accretionary prism rocks of the Torlesse terrane, western Aorangi Range-Cape Palliser, New Zealand. Unpublished thesis, Victoria University of Wellington.

Gittins J 1989. The origin and evolution of carbonatite magmas. Carbonatites: genesis and evolution. Unwin Hyman, London: 580-600.
Gittins J, Jago B 1998. Differentiation of natrocarbonatite magma at Oldoinyo Lengai volcano, Tanzania. Mineralogical Magazine 62(6): 759-768.
Gittins J, Harmer R, Barker D 2005. The bimodal composition of carbonatites: Reality or misconception? Lithos 85(1): 129-139.
Grapes RH 1972. Petrology of the Blue Mountain Igenous Complex. Unpublished thesis, Victoria University of Wellington, Unpublished. 236 p.
Grapes RH 1975. Petrology of the Blue Mountain Complex, Marlborough, New Zealand. Journal of petrology 16(1): 371-428.
Grapes RH, Lamb SH, Adams CJ 1992. K-Ar ages of basanitic dikes, Awatere Valley, Marlborough, New Zealand. New Zealand journal of geology and geophysics 35(4): 415-419.
Grindley G, Adams C, Lumb J, Watters W 1977. Paleomagnetism, K-Ar dating and tectonic interpretation of Upper Cretaceous and Cenozoic volcanic rocks of the Chatham Islands, New Zealand. New Zealand journal of geology and geophysics 20(3): 425-467.
Halama R, Vennemann T, Siebel W, Markl G 2005. The Grønnedal-Ika carbonatite–syenite complex, South Greenland: carbonatite formation by liquid immiscibility. Journal of Petrology 46(1): 191-217.
Harker A 1909. The natural history of igneous rocks, Cambridge University Press.
Harmer R 1999. The petrogenetic association of carbonatite and alkaline magmatism: constraints from the Spitskop Complex, South Africa. Journal of Petrology 40(4): 525-548.
Harmer R, Lee C, Eglington B 1998. A deep mantle source for carbonatite magmatism: evidence from the nephelinites and carbonatites of the Buhera district, SE Zimbabwe. Earth and Planetary Science Letters 158(3): 131-142.
Hoernle K, Tilton G, Le Bas MJ, Duggen S, Garbe-Schönberg D 2002. Geochemistry of oceanic carbonatites compared with continental carbonatites: mantle recycling of oceanic crustal carbonate. Contributions to Mineralogy and Petrology 142(5): 520-542.
Jones AP, Genge M, Carmody L 2013. Carbonate melts and carbonatites. Rev Mineral Geochem 75(1): 289-322.
Jongens R, Timm C, Christie A, Smith-Lyttle B, Leybourne M, Rattenbury M 2012. Mineral potential of the Tapuaenuku and Blue Mountain Igneous Complexes, Kaikoura: Desktop studies and Geochemical Survey. In: Minerals NZPa ed., GNS Science Report.
Kaminsky FV, Wirth R, Schreiber A 2013. Carbonatitic inclusions in deep mantle diamond from Juina, Brazil: new minerals in the carbonate-halide association. The Canadian Mineralogist 51(5): 669-688.
Kapustin YL 1982. Geochemistry of strontium and barium in carbonatites. Geokhimiya(3): 369-380.
Kjarsgaard B, Hamilton D 1988. Liquid immiscibility and the origin of alkali-poor carbonatites. Mineral Mag 52(364): 43-55.
Kjarsgaard B, Hamilton D 1989. The genesis of carbonatites by immiscibility. Carbonatites: genesis and evolution. Unwin Hyman, London: 388-404.
Kjarsgaard B, Peterson T 1991. Nephelinite-carbonatite liquid immiscibility at Shombole volcano, East Africa: Petrographic and experimental evidence. Mineralogy and Petrology 43(4): 293-314.

Klein-BenDavid O, Logvinova AM, Schrauder M, Spetius ZV, Weiss Y, Hauri EH, Kaminsky FV, Sobolev NV, Navon O 2009. High-Mg carbonatitic microinclusions in some Yakutian diamonds-a new type of diamond-forming fluid. Lithos 112: 648-659.
Le Bas M 1989. Carbonatites: genesis and evolution.
Le Bas M 2000. IUGS reclassification of the high-Mg and picritic volcanic rocks. Journal of Petrology 41(10): 1467-1470.
Le Bas M, Streckeisen A 1991. The IUGS systematics of igneous rocks. Journal of the Geological Society 148(5): 825-833.
Le Bas M, Spiro B, Yang X 1997. Oxygen, carbon and strontium isotope study of the carbonatitic dolomite host of the Bayan Obo Fe-Nb-REE deposit, Inner Mongolia, N China. Mineralogical Magazine 61(4): 531-541.
Le Maitre RW, Streckeisen A, Zanettin B, Le Bas M, Bonin B, Bateman P 2002. Igneous rocks: a classification and glossary of terms: recommendations of the International Union of Geological Sciences Subcommission on the Systematics of Igneous Rocks, Cambridge University Press.
Le Roex AP, Lanyon R 1998. Isotope and Trace Element Geochemistry of Cretaceous Damaraland Lamprophyres and Carbonatites, Northwestern Namibia: Evidence for Plume—Lithosphere Interactions. Journal of Petrology 39(6): 1117-1146.
Lee W-j, Wyllie PJ 1994. Experimental data bearing on liquid immiscibility, crystal fractionation, and the origin of calciocarbonatites and natrocarbonatites. International Geology Review 36(9): 797-819.
Lee W-j, Wyllie PJ 1997. Liquid immiscibility between nephelinite and carbonatite from 1.0 to 2.5 GPa compared with mantle melt compositions. Contributions to Mineralogy and Petrology 127(1-2): 1-16.
Lee W-J, Wyllie PJ 1998. Processes of crustal carbonatite formation by liquid immiscibility and differentiation, elucidated by model systems. Journal of Petrology 39(11-12): 2005-2013.
Lee W-J, Fanelli M, Cava N, Wyllie P 2000. Calciocarbonatite and magnesiocarbonatite rocks and magmas represented in the system CaO-MgO-CO_2-H_2O at 0.2 GPa. Mineralogy and Petrology 68(4): 225-256.
Lee W, Wyllie P 2000. The system CaO-MgO-SiO_2-CO_2 at 1 GPa, metasomatic wehrlites, and primary carbonatite magmas. Contributions to Mineralogy and Petrology 138(3): 214-228.
1962 Sheet 16 Kaikoura Map, New Zealand Department of Scientific and Industrial Research.
Mackay DA 2014. Indicator minerals and stream sediments in exploration for carbonatite-hosted Nb deposits, Aley, British Colombia, Canada. 2014 GSA Annual Meeting in Vancouver, British Columbia.
Mackay DA, Simandl GJ 2013. Portable x-ray fluorescence to optimize stream sediment chemistry and indicator mineral surveys, case 1: Carbonatite-hosted Nb deposits, Aley carbonatite, British Columbia, Canada. Geological Fieldwork: 2014-1.
Microsystems L 2015. Leica Application Suite 2015, from http://www.leica-microsystems.com/products/microscope-software/software-for-life-science-research/las-x/
Mitchell R 1984. Mineralogy and origin of carbonate-rich segregations in a composite kimberlite sill. Neus Jahrbuch fur Mineralogie-Abhandlungen 150(2): 185-197.
Mitchell RH 1979. The alleged kimberlite-carbonatite relationship; additional contrary mineralogical evidence. American Journal of Science 279(5): 570-589.
Mitchell RH 2005. Carbonatites and carbonatites and carbonatites. The Canadian Mineralogist 43(6): 2049-2068.

Mitchell RH 2012. Kimberlites, orangeites, and related rocks, Springer Science & Business Media.
Morogan V, Woolley AR 1988. Fenitization at the Alnö carbonatite complex, Sweden; distribution, mineralogy and genesis. Contributions to Mineralogy and Petrology 100(2): 169-182.
Nelson D, Chivas A, Chappell B, McCulloch M 1988. Geochemical and isotopic systematics in carbonatites and implications for the evolution of ocean-island sources. Geochimica et Cosmochimica Acta 52(1): 1-17.
Ngwenya B, Bailey D 1990. Kaluwe carbonatite, Zambia: an alternative to natrocarbonatite. Journal of the Geological Society 147(2): 213-216.
Nicol ER 1977. Igneous Petrology of the Clarence and Awatere Valleys, Marlborough. Unpublished thesis, University of Victoria, Wellington. 412 p.
O'Neil JR, Clayton RN, Mayeda TK 1969. Oxygen isotope fractionation in divalent metal carbonates.
Oliver P, Keene H 1989. Sheet K36 AC & part sheet K35–Mount Somers, Geological map of New Zealand 1: 50 000. Map (1 sheet) and notes. Wellington, New Zealand. Department of Scientific and Industrial Research.
Paterson AL 1993. A Study of Carbonatites and Associated Fenitisation at Haast River, South Westland, New Zealand: A Thesis Submitted for the Degree of Doctor of Philosophy in Geology at the University of Otago, Dunedin, New Zealand. Unpublished thesis, University of Otago.
Pineau F, Javoy M, Allegre CJ 1973. Etude systématique des isotopes de l'oxygène, du carbone et du strontium dans les carbonatites. Geochimica et Cosmochimica Acta 37(11): 2363-2377.
Rattenbury MS, Townsend DB, Johnston MR 2006. Geology of the Kaikoura area, Institute of Geological Nuclear Sciences.
Reay MB 1993. Geology of the middle Clarence valley, Marlborough, New Zealand, Institute of Geological and Nuclear Sciences.
Reid DL, Cooper AF 1992. Oxygen and carbon isotope patterns in the Dicker Willem carbonatite complex, southern Namibia. Chemical Geology 94(4): 293-305.
Rock NM 1987. The nature and origin of lamprophyres: an overview. Geological Society, London, Special Publications 30(1): 191-226.
Santos RV, Clayton RN 1995. Variations of oxygen and carbon isotopes in carbonatites: a study of Brazilian alkaline complexes. Geochimica et Cosmochimica Acta 59(7): 1339-1352.
Santos RV, Dardenne MA, Eiichimatsui E 1990. Geoquímica de isótopos de carbono e oxigênio dos carbonatitos do Complexo Alcalino de Mato Preto, Paraná, Brasil. Brazilian Journal of Geology 20(1): 153-158.
Simandl G, Stone R, Paradis S, Fajber R, Reid H, Grattan K 2014a. An assessment of a handheld X-ray fluorescence instrument for use in exploration and development with an emphasis on REEs and related specialty metals. Mineralium Deposita 49(8): 999-1012.
Simandl G, Paradis S, Stone R, Fajber R, Kressall R, Grattan K, Crozier J, Simandl L 2014b. Applicability of handheld X-Ray fluorescence spectrometry in the exploration and development of carbonatite-related niobium deposits: a case study of the Aley Carbonatite, British Columbia, Canada. Geochemistry: Exploration, Environment, Analysis 14(3): 211-221.
Simonetti A, Goldstein S, Schmidberger S, Viladkar S 1998. Geochemical and Nd, Pb, and Sr isotope data from Deccan alkaline complexes—inferences for mantle sources and plume–lithosphere interaction. Journal of Petrology 39(11-12): 1847-1864.

Steiger RH, Jager E 1977. Subcommission on geochronology: conventions on the use of decay constants in geo- and cosmochronology. Earth and planetary science letters 36: 359-362.
Streckeisen A 1979. Classification and nomenclature of volcanic rocks, lamprophyres, carbonatites, and melilitic rocks: Recommendations and suggestions of the IUGS Subcommission on the Systematics of Igneous Rocks. Geology 7(7): 331-335.
Streckeisen A 1980. Classification and nomenclature of volcanic rocks, lamprophyres, carbonatites and melilitic rocks IUGS Subcommission on the systematics of igneous rocks. Geologische Rundschau 69(1): 194-207.
Sweeney RJ 1994. Carbonatite melt compositions in the Earth's mantle. Earth and Planetary Science Letters 128(3): 259-270.
Tappe S, Foley SF, Jenner GA, Heaman LM, Kjarsgaard BA, Romer RL, Stracke A, Joyce N, Hoefs J 2006. Genesis of ultramafic lamprophyres and carbonatites at Aillik Bay, Labrador: a consequence of incipient lithospheric thinning beneath the North Atlantic craton. Journal of Petrology 47(7): 1261-1315.
Taylor HP, Frechen J, Degens ET 1967. Oxygen and carbon isotope studies of carbonatites from the Laacher See District, West Germany and the Alnö District, Sweden. Geochimica et Cosmochimica Acta 31(3): 407-430.
Timm C, Hoernle K, Werner R, Hauff F, van den Bogaard P, White J, Mortimer N, Garbe-Schönberg D 2010. Temporal and geochemical evolution of the Cenozoic intraplate volcanism of Zealandia. Earth-Science Reviews 98(1): 38-64.
Wagner C, Mokhtari A, Deloule E, Chabaux F 2003. Carbonatite and alkaline magmatism in Taourirt (Morocco): petrological, geochemical and Sr–Nd isotope characteristics. Journal of Petrology 44(5): 937-965.
Wallace ME, Green DH 1988. An experimental determination of primary carbonatite magma composition.
Weaver SD, Pankhurst RJ 1991. A precise Rb-Sr age for the Mandamus Igneous Complex, North Canterbury, and regional tectonic implications. New Zealand journal of geology and geophysics 34(3): 341-345.
Winter JD 2014. Principles of igneous and metamorphic petrology, Pearson.
Woolley A, Kempe D 1989. Carbonatites: nomenclature, average chemical compositions, and element distribution. Carbonatites: genesis and evolution. Unwin Hyman, London 619.
Woolley A, Church A 2005. Extrusive carbonatites: a brief review. Lithos 85(1): 1-14.
Woolley A, Bailey D 2012. The crucial role of lithospheric structure in the generation and release of carbonatites: geological evidence. Mineralogical Magazine 76(2): 259-270.
Woolley AR, Kjarsgaard BA 2008a. Paragenetic types of carbonatite as indicated by the diversity and relative abundances of associated silicate rocks: evidence from a global database. The Canadian Mineralogist 46(4): 741-752.
Woolley AR, Kjarsgaard BA 2008b. Carbonatite occurrences of the world: map and database, Geological Survey of Canada.
Woolley AR, Bergman SC, Edgar AD, Le Bas MJ, Mitchell RH, Rock NM, Scott Smith B 1996. Classification of lamprophyres, lamproites, kimberlites, and the kalsilitic, melilitic, and leucitic rocks. Canadian Mineralogist 34: 175-186.
Wyllie PJ, Lee W-J 1998. Model system controls on conditions for formation of magnesiocarbonatite and calciocarbonatite magmas from the mantle. Journal of Petrology 39(11-12): 1885-1893.
Ying J, Zhou X, Zhang H 2004. Geochemical and isotopic investigation of the Laiwu–Zibo carbonatites from western Shandong Province, China, and implications for their petrogenesis and enriched mantle source. Lithos 75(3): 413-426.

CHAPTER 7: APPENDICES

APPENDIX A: BASE MAP DATA SOURCES

DEM sourced from LINZ Data Service (https://koordinates.com/layer/3747-19-kaikoura-15m-dem-nzsosdem-v10/) and licenced for re-use under the Creative Commons Attribution 3.0 New Zealand Licence.

Geological Map sourced from the New Zealand Petroleum and Minerals Report MR5062 data pack.

APPENDIX B: PETROGRAPHY

Sample number: LGC1
Rock Name: Glassy Foidite

Hand Sample Description: Dark greenish grey, aphanitic. Strong slightly weathered. Fine grained with occasional plagioclase phenocryst. Inequigranular. Hypidiomorphic. Silver coloured metallic mineral presents in specks. Sample predominantly comprised of dark greenish grey ground mass with a small number of poorly developed amphibole and feldspar phenocrysts in an aphanitic groundmass.

Thin section description: Black and white speckled, aphanitic (0.01-0.02 mm), massive, trachytic, **Glassy foidite**. Subtrachytic groundmass of amphibole and plagioclase. Accessory alteration minerals include serpentine, biotite, chlorite, sericite and clay. Cumulophyric amphibole and feldspar. Alteration front from carbonate fluids present and alteration pathway through the sample. Opaques associated with the alteration front with higher density of opaques in altered ground mass.

Modal mineralogy	%	Diagnostic properties	Textures
glass	55	PPL-Colourless to brownish grey, no relief. CPL- Isotropic	Some weathering and iron oxide staining.
brown amphibole hornblende-kaersutite	28	PPL-green to greenish brown, moderately pleochroic, moderate to high relief, anhedral. CPL-2 perfect cleavages at 120°, extinction 10-30° from cleavage, 0.014 - 0.034 δ	Elongate acicular phenocrysts. Trachytic texture. Serpentinisation and alteration to clays and biotite, chlorite prevalent.
plagioclase-labradorite	3	PPL-Colourless, low relief, inclined extinction, elongate, euhedral to subhedral CPL-Carlsbad and polysynthetic twinning, 0.007 – 0.013 δ.	Predominantly altering to clays. Heavy sericite alteration. Plagioclase laths are elongate and apart. Undulose extinction.
opaques-magnetite and ilmenite	10	PPL and CPL black. Anhedral.	Interstitial. Stubby.
clinopyroxene-aegirine	3	PPL-Pale green to olive green, pleochroic, high relief, stubby to elongate, inclined extinction, subhedral-euhedral. CPL-	Clusters of aegirine adjacent to calcite veinlets and phenocrysts.
calcite	6	PPL-Colourless to pale pink, low pleochroism, low relief, subhedral, lamellar twinning, perfect rhombohedral cleavage at 74° 55'. CPL- 0.179-0.202 δ.	Veinlets cross cutting the groundmass with the occasional subhedral phenocryst or cluster of phenocrysts.

Sample number: LGC2
Rock Name: Calcite carbonatite veins in lamprophyre

Hand Sample Description: Medium greenish whitish grey. Crystallised, phaneritic. Strong, unweathered. Fine to medium grained. Inequigranular, Hypidiomorphic. Carbonate-blocky, euhedral and subhedral, white translucent and fizzes to HCl acid - 40%. Epidote-corroded, subhedral. Light green, weathered -10%. 7 carbonate veins and veinlets throughout the sample. Clusters of calcite and quartz throughout. Chaotic non directional brecciation and spider veinlets. Some brassy yellow metal sulphide- Pyrrhotite?

Thin section description: Moderate greenish grey and white, fine to medium grained (0.5-1 mm), massive, hypidiomorphic to idiomorphic, bimodal, porphyritic, CALCITE CABONATITE VEINS in a LAMPROPHYRE. Plagioclase phenocryst composed of andesine. Carbonate minerals throughout, sutured. Accessory quartz and plagioclase. Large veins and fingering of carbonate. Quartz is bimodal, medium and fine grained phenocrysts. Rare epidote and chalcedony in clusters. Pervasively altered host to clay. Varying layers of alteration. Alteration greatest adjacent to calcite veins and veinlets.

Modal mineralogy	%	Diagnostic properties	Textures
calcite	40	PPL-Colourless to pale pink, low pleochroism, low relief, subhedral, lamellar twinning, perfect rhombohedral cleavage at 74° 55'. CPL- 0.179-0.202 δ.	Vein structures that cross cut host rock. Carbonate veins cross cut one another. Traces of dolomite. Accessory aegirine and epidote in trace levels clustered adjacent and within veinlets.
clay	14	Brown to grey in both PPL and CPL.	Vague fragments of biotite, amphibole, plagioclase and their degradation products throughout. Cross cut by calcite veins.
quartz	14	PPL- Colourless, very low relief, subhedral to anhedral. CPL-0.009 δ	Clusters of quartz, sutured with varying extinctions.
opaques	2	PPL and CPL black. Anhedral, blebby.	Interstitial. Stubby.
brown amphibole	28	PPL-green to greenish brown, moderately pleochroic, moderate to high relief, anhedral. CPL-2 perfect cleavages at 120°, extinction 10-30° from cleavage, 0.014 - 0.034 δ	Pervasively altered to fibrous serpentine.
nepheline	1	PPL-Colourless, very low relief, uniaxial -ve, euhedral, blocky. CPL- 0.004 δ.	Blocky nepheline typically adjacent to feldspars. Partial alteration to analcime not uncommon. Undulose extiction
plagioclase	1	PPL-Colourless, low relief, inclined extinction, elongate, euhedral to subhedral CPL-Carlsbad and polysynthetic twinning, 0.007 – 0.013 δ.	Completely altered to sericite. Plagioclase laths are elongate and acicular. Undulose extinction.

Sample number: LGC3
Rock Name: Calcite Carbonatite

Hand Sample Description: Medium greenish grey. Crystallised, phaneritic, strong, unweathered. Fine grained with coarse crystals. Inequigranular, hypidiomorphic. Carbonate-Blocky, euhedral and subhedral. White Translucent and fizzes to HCl acid-50%. Quartz-glassy and transparent, appearing grey in hand specimen. White Translucent-5%. 4 carbonate veins throughout the sample with 5+ veinlets. Heavy epidote weathering emanating from a carbonate vein areas. Some metallic mineral, magnetite?

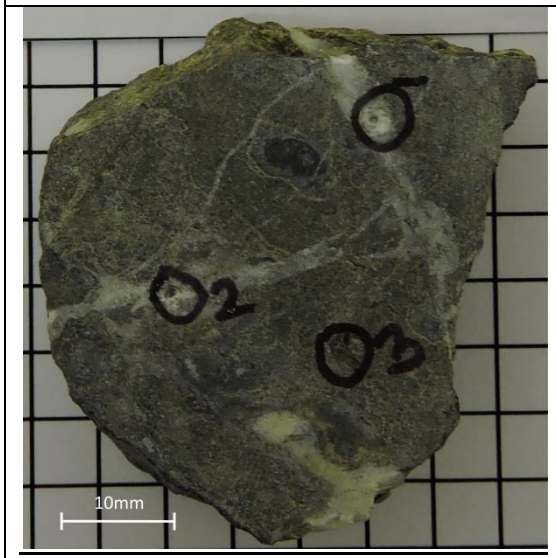

Thin section description: Moderate greenish grey and white, fine to medium grained (0.5-1 mm), massive, hypidiomorphic to idiomorphic, bimodal, porphyritic, CALCITE CABONATITE. Plagioclase phenocryst composed of andesine. Carbonate minerals throughout, sutured. Accessory quartz and plagioclase. Large veins and fingering of carbonate. Quartz is bimodal, medium and fine grained phenocrysts. Rare epidote and chalcedony in clusters. Pervasively altered host to clay.

Modal mineralogy	%	Diagnostic properties	Textures
calcite	60	PPL-Colourless to pale pink, low pleochroism, low relief, subhedral, lamellar twinning, perfect rhombohedral cleavage at 74° 55'. CPL- 0.179-0.202 δ.	Vein structures that cross cut host rock. Carbonate veins cross cut one another. Traces of dolomite. Accessory aegirine and epidote in trace levels clustered adjacent and within veinlets. Mixture of limpid rhombohedral calcite and indistinct, contaminated with clay carbonate.
clay	5	Brown to grey in both PPL and CPL. No optical properties	Vague fragments of biotite, amphibole, feldspar? and their degradation products throughout. Cross cut by calcite veins.
quartz	20	PPL- Colourless, very low relief, subhedral to anhedral. CPL-0.009 δ	Clusters of quartz, sutured with varying extinctions.
opaques	2	PPL and CPL black. Anhedral to subhedral.	Interstitial in the clay (altered host rock). High density of opaques in host. Predominantly magnetite with some ilmenite.
brown amphibole	8	PPL-green to greenish brown, moderately pleochroic, moderate to high relief, anhedral. CPL-2 perfect cleavages at 120°, extinction 10-30° from cleavage, 0.014 - 0.034 δ	Pervasively altered to fibrous serpentine, biotite and chlorite. Large phenocryst rim visible concentrically zoned by calcite, clay and opaques
epidote	5	PPL- Pale green to colourless, weakly pleochroic, high relief, subhedral. CPL- Parallel extinction and 0.004 – 0.049 δ	Small occasional clusters of epidote.

Sample number: LGC3.5
Rock Name: Calcite Carbonatite

Hand Sample Description: Medium greenish grey. Crystallised, phaneritic, strong, unweathered. Fine grained with coarse crystals, inequigranular, hypidiomorphic. Carbonate-Blocky, euhedral and subhedral. White translucent and fizzes to HCl acid-65%. Ghosts of host aphanitic and contaminated by carbonate. Chaotic non-directional brecciation and spider veinlets. Some metallic mineral, magnetite?

Thin section description: Moderate greenish grey and white, fine to medium grained (0.5-1 mm), massive, hypidiomorphic to idiomorphic, bimodal, porphyritic, CALCITE CABONATITE. Carbonate minerals throughout, sutured. Accessory quartz and plagioclase. Large veins and fingering of carbonate. Quartz is bimodal, medium and fine grained phenocrysts. Rare epidote and aegirine in clusters within the calcite veinlets. Pervasively altered host to clay.

Modal mineralogy	%	Diagnostic properties	Textures
calcite	65	PPL-Colourless to pale pink, low pleochroism, low relief, subhedral, lamellar twinning, perfect rhombohedral cleavage at 74° 55'. CPL- 0.179-0.202 δ.	Vein structures that cross cut host rock. Carbonate veins cross cut one another. Traces of dolomite. Accessory aegirine and epidote in trace levels clustered adjacent and within veinlets. Mixture of limpid rhombohedral calcite and indistinct, contaminated with clay carbonate.
clay	15	Yellowish brown to grey in both PPL and CPL. No optical properties	Vague fragments of biotite, amphibole, feldspar and their degradation products throughout. Cross cut by calcite veins.
quartz	5	PPL- Colourless, very low relief, subhedral to anhedral. CPL-0.009 δ	Clusters of quartz, sutured with varying extinctions.
opaques	1	PPL and CPL black. Anhedral to subhedral.	Interstitial in the clay (altered host rock). High density of opaques in host. Predominantly magnetite with some ilmenite.
brown amphibole	3	PPL-green to greenish brown, moderately pleochroic, moderate to high relief, anhedral. CPL-2 perfect cleavages at 120°, extinction 10-30° from cleavage, 0.014 - 0.034 δ	Pervasively altered to fibrous serpentine, biotite and chlorite.

Sample number: LGC4
Rock Name: Calcite carbonatite veins in lamprophyre

Hand Sample Description: Medium greenish grey. Crystallised, phaneritic, strong, unweathered. Fine grained with coarse crystals, inequigranular, hypidiomorphic. Carbonate-Blocky, euhedral and subhedral. White Translucent and fizzes to HCl acid-60%. Quartz-glassy and transparent, appearing grey in hand specimen. White Translucent-5%.Carbonate veins throughout the sample. Heavy epidote weathering emanating from epidote rich areas. Chaotic non-directional brecciation and spider veinlets. Some metallic mineral, magnetite?

Thin section description: Moderate greenish grey and white, fine to medium grained (0.5-1 mm), massive, hypidiomorphic to idiomorphic, bimodal, porphyritic, CALCITE CABONATITE VEINS in a LAMPROPHYRE. Carbonate minerals throughout, sutured. Accessory quartz and plagioclase. Large veins and fingering of carbonate. Quartz is bimodal, medium and fine grained phenocrysts. Rare epidote and aegirine in clusters within the calcite veinlets. Pervasively pseudomorphed host to clay.

Modal mineralogy	%	Diagnostic properties	Textures
calcite	20	PPL-Colourless to pale pink, low pleochroism, low relief, subhedral, lamellar twinning, perfect rhombohedral cleavage at 74° 55'. CPL- 0.179-0.202 δ.	Vein structures that cross cut host rock. Carbonate veins cross cut one another. Traces of dolomite. Accessory aegirine and epidote in trace levels clustered adjacent and within veinlets. Mixture of limpid rhombohedral calcite and indistinct, contaminated with clay carbonate.
clay	40	Yellowish brown to grey in both plane PPL and CPL. No optical properties	Vague fragments of biotite, amphibole, feldspar? and their degradation products throughout. Cross cut by calcite veins.
quartz	29	PPL- Colourless, very low relief, subhedral to anhedral. CPL-0.009 δ	Clusters of quartz, sutured with varying extinctions. Intermingled quartz lenses in calcite veinlets.
opaques	7	PPL and CPL black and brown. Anhedral to subhedral.	Interstitial in the clay (altered host rock). High density of opaques in host and associated with clay. Predominantly magnetite with some ilmenite.
brown amphibole	3	PPL-green to greenish brown, moderately pleochroic, moderate to high relief, anhedral. CPL-2 perfect cleavages at 120°, extinction 10-30° from cleavage, 0.014 - 0.034 δ	Pervasively altered to fibrous serpentine, biotite and chlorite.
olivine	1	PPL- Colourless, moderate to high relief, 0° extinction, prismatic, sub to anhedral. CPL-0.035 - 0.052 δ.	Concentrically zoned with serpentinisation occurring inside with iddingsite rim replacement. Opaques concentrically zoned around the rim.

Sample number: LGC5
Rock Name: Glassy Foidite

Hand Sample Description: Dark greenish grey, aphanitic. Strong slightly weathered. Fine grained with rock fragments, inequigranular and hypidiomorphic. Silver coloured metallic mineral presents in specks. Sample predominantly comprised of dark greenish grey ground mass with a small number of poorly developed amphibole and feldspar phenocrysts in an aphanitic groundmass.3 carbonate veins with occasional veinlets.

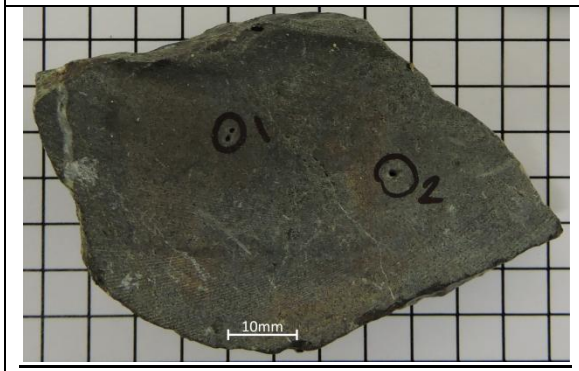

Thin section description: Black and white speckled, aphanitic (0.001-0.02 mm), massive, trachytic, **Glassy foidite**. Subtrachytic groundmass of amphibole and plagioclase. Accessory alteration minerals include serpentine, biotite, chlorite, sericite and clay. Alteration front from carbonate (calcite) fluids present and alteration pathway through the sample. Opaques associated with the alteration front with higher density of opaques in altered ground mass. Patchy iron oxide staining throughout, weathered. Slightly finer than LGC1.

Modal mineralogy	**%**	**Diagnostic properties**	**Textures**
glass	55	PPL-Colourless to brownish grey, no relief. CPL- Isotropic	Some weathering and iron oxide staining.
brown amphibole	24	PPL-green to greenish brown, moderately pleochroic, moderate to high relief, anhedral. CPL-2 perfect cleavages at 120°, extinction 10-30° from cleavage, 0.014 - 0.034 δ	Elongate acicular phenocrysts. Trachytic texture. Serpentinisation and alteration to clays and biotite, chlorite prevalent.
plagioclase	2	PPL-Colourless, low relief, inclined extinction, elongate, euhedral to subhedral CPL-Carlsbad and polysynthetic twinning, 0.007 – 0.013 δ.	Completely altered to sericite. Plagioclase laths are elongate and acicular. Undulose extinction.
opaques- magnetite and ilmenite	10	PPL and CPL black. Anhedral.	Interstitial. Stubby. Higher density of opaques within the alteration front.
clinopyroxene- aegirine	3	PPL-Pale green to olive green, pleochroic, high relief, stubby to elongate, inclined extinction, subhedral-euhedral. CPL- 0.037-.0.61δ.	Clusters of aegirine adjacent to calcite veinlets and phenocrysts.
calcite	6	PPL-Colourless to pale pink, low pleochroism, low relief, subhedral, lamellar twinning, perfect rhombohedral cleavage at 74° 55'. CPL- 0.179-0.202 δ.	Veinlets cross cutting the groundmass with the occasional subhedral phenocryst or glomerophyric cluster of phenocrysts.

Sample number: LGC6
Rock Name: Calcite Carbonatite veins in glass Lamprophyre chilled margin.

Hand Sample Description: Medium greenish grey. Crystallised, phaneritic, strong, unweathered. Fine grained with coarse calcite crystals, inequigranular, and hypidiomorphic. Carbonate-Blocky, euhedral and subhedral. White Translucent and fizzes to HCl acid-50%. Quartz-glassy and transparent, appearing grey in hand specimen.-5%. 4 dominant carbonate veins cross cutting sample with numerous veinlets off shooting veins. Chaotic, directional brecciation and spider veinlets. Metallic mineral, magnetite?

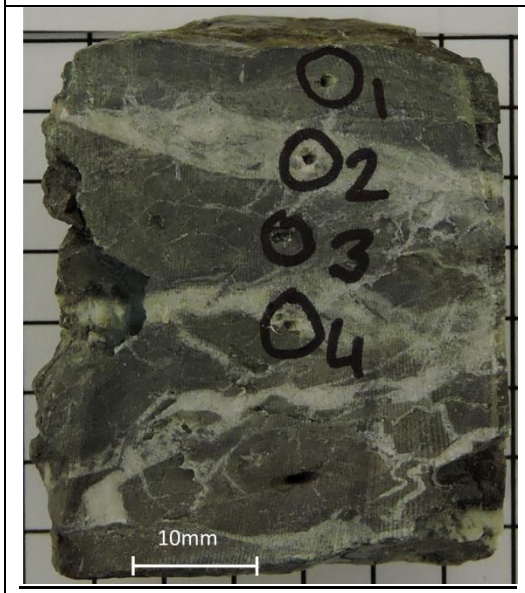

Thin section description: Moderate greenish grey and white, fine to medium grained (0.5-1 mm), massive, hypidiomorphic to idiomorphic, bimodal, CALCITE CABONATITE VEINS in a GLASS LAMPROHPYRE. Carbonate veins and veinlets crosscutting clay/glass host that is pervasively altered and displays no optical properties. Accessory quartz lenses within the calcite veins. Large veins and fingering of carbonate. Quartz is bimodal, fine medium and fine grained phenocrysts. Rare epidote veinlets and clusters within the calcite veinlets. Pervasively pseudomorphed host to clay or glass. XRD results indicate high percentages of clinopyroxene and feldspars but these are no evident in the glass/clay host.

Modal mineralogy	%	Diagnostic properties	Textures
calcite	30	PPL-Colourless to pale pink, low pleochroism, low relief, subhedral, lamellar twinning, perfect rhombohedral cleavage at 74° 55'. CPL- 0.179-0.202 δ.	Veins displaying comb textures cross cut host rock. Carbonate veins cross cut one another. Traces of dolomite. Accessory aegirine and epidote in trace levels clustered adjacent and within veinlets. Mixture of limpid rhombohedral calcite and indistinct, contaminated turbid calcite and clay carbonate.
glass	48	Yellowish brown to grey in both plane PPL and CPL. No optical properties. Glass	Cross cut by calcite veins. No optical properties. Occasional stubby opaque and calcite phenocrysts.
quartz	15	PPL- Colourless, very low relief, subhedral to anhedral. CPL-0.009 δ.	Clusters of quartz, sutured with varying extinctions. Intermingled quartz lenses in calcite veinlets. Strained extinction. Flow aligned and comb textures present
opaques	2	PPL and CPL black. Anhedral to subhedral. Stubby.	Higher density of opaques in host glass. Predominantly magnetite with some ilmenite.
epidote	5	PPL- Pale green to colourless, weakly pleochroic, high relief, subhedral. CPL- Parallel extinction and 0.004 – 0.049 δ.	Small occasional clusters and veinlets of epidote in the calcite veins.

Sample number: LGC7
Rock Name: CAMPTONITE-LAMPROPHYRE

Hand Sample Description: Medium greenish grey. Dyke, porphyritic, strong, slightly weathered. Fine to coarse grained, inequigranular, panidiomorphic. Pyroxene-Euhedral and subhedral. Dark mineral that has 90deg cleavage-60%. Plagioclase-Elongate, euhedral and subhedral. Cleavage at 90, two directions. White translucent-20%. Coarse grained altered amphibole and pyroxene phenocrysts in a feldspar-pyroxene ground mass with carbonate veins and veinlets throughout the sample. Quartz phenocryst with some chalky calcite encompassing it. Rhombohedral calcite.

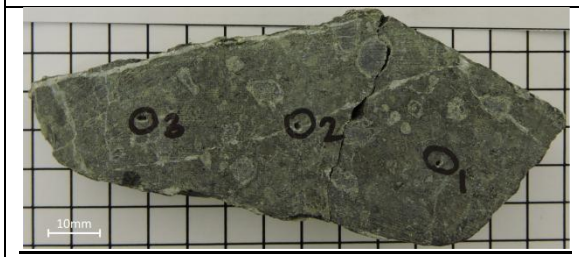

Thin section description: Dark greenish grey, fine to medium grained with coarse macrocrysts (0.2-3 mm) massive, bimodal distribution, porphyritic, fenitized CAMPTONITE-LAMPROPHYRE. Secondary minerals include chlorite, amphibole, sericite, analcime and cancrinite, calcite, clay epidote and aegirine. Feldspars poorly formed with and display pervasive sericitisation, mainly labradorite (65%). Nepheline macrocrysts commonly contains opaque inclusions, embayed, network replacement to analcime, clay, calcite and internal alteration to cancrinite. Clinopyroxene macrocrysts are concentrically zoned and display undulose extinction. Groundmass is fine to medium grained and is composed of primary pyroxenes, feldspars, nepheline and amphiboles that display alteration features. Crosscutting calcite veins throughout.

Phenocrysts	**%**	**Diagnostic properties**	**Textures & Alteration**
amphibole-riebeckite	24	PPL-green to greenish brown, moderately pleochroic, moderate to high relief, anhedral. CPL-2 perfect cleavages at 120°, extinction 10-30° from cleavage, 0.014 -0.034 δ	Undulose extinction. Displays deep red brown (z) to brown (x) pleochroism typical of kaersutite. Kaersutite phenocrysts occur in glomerophyric clusters. Pervasive to complete alteration to clay, chlorite, serpentine and partial alteration to biotite. Trains of opaques within clay. Biotite further degraded to chlorite. Network, rim and total serpentinisation.
nepheline	1	PPL-Colourless, very low relief, uniaxial -ve, euhedral, blocky. CPL-0.004 δ.	Large phenocrysts that display high δ cancrinite alteration. Concentric zoning common. Network and rim alteration to calcite and clays.
clinopyroxene-augite	2	PPL-Pale green to brownish, 2 cleavages at approximately 90°, inclined 40 to 50° extinction, moderate relief and subhedral. CPL- 0.018 – 0.034 δ.	Oscillatory zoning common. Clinopyroxene phenocrysts occur in glomerophyric clusters. Partial uralitisation to amphiboles not uncommon. Pervasive to complete to clay, chlorite, serpentine and partial alteration to biotite. Trains of opaques within carbonate clay. Biotite further degraded to chlorite. Network, rim and total serpentinisation. Calcite replacement common.
olivine	3	PPL- Colourless, moderate to high relief, rounded equant, sub to anhedral. CPL- 0.035 – 0.052 δ.	Commonly speckled with opaques. Fractured throughout with acicular chloritisation. Alteration to iddingsite common as well. Pervasive to complete to clay, chlorite, serpentine and partial alteration to biotite. Trains of opaques within carbonate clay. Biotite further degraded to chlorite. Network, rim and total serpentinisation. Calcite replacement common.
Groundmass			
calcite	7	PPL-Colourless to pale pink, low pleochroism, low relief, subhedral, lamellar twinning, perfect rhombohedral	Veins displaying comb textures cross cut host rock. Carbonate veins cross cut one another. Traces of dolomite. Accessory aegirine and

			cleavage at 74° 55'. CPL- 0.179-0.202 δ.	epidote in trace levels clustered adjacent and within veinlets. Mixture of limpid rhombohedral calcite and indistinct, contaminated turbid calcite and clay carbonate.
	clay	10	Yellowish brown to grey in both plane PPL and CPL. No optical properties. Glass?	Cross cut by calcite veins. No optical properties. Occasional stubby opaque and calcite phenocrysts.
	green amphibole	15	PPL-green to greenish brown, moderately pleochroic, moderate to high relief, anhedral. CPL-2 perfect cleavages at 120°, extinction 10-30° from cleavage, 0.014 -0.034 δ	Occasional primary amphibole. Groundmass is heavily composed of green amphibole.
	nepheline	5	PPL-Colourless, very low relief, uniaxial -ve, euhedral, blocky. CPL-0.004 δ.	Blocky nepheline typically adjacent to feldspars. Partial alteration to analcime not uncommon.
	clinopyroxene	10	PPL-Pale green to brownish, 2 cleavages at approximately 90°, inclined 40 to 50° extinction, moderate relief and subhedral. CPL- 0.018 – 0.034 δ, biaxial 2V 58-63.	Acicular phenocrysts of titanian augite (biaxial +ve 2V 40-52). Partial uralitisation common with secondary amphiboles degrading to chlorite.
	opaque Magnetite-100% 0.01-2mm	3	Opaque. Anhedral.	Throughout sample. Large phenocrysts
	plagioclase labradorite 65% ML-29° andesine-35% ML-14°	20	PPL-Colourless, low relief, inclined extinction, elongate, subhedral. CPL-Carlsbad, polysynthetic and some pericline twinning, 0.007 – 0.013 δ.	Phenocrysts are turbid and display undulose extinction. Heavily alteration to sericite is common. Part of the ground mass. Alteration to partially isotropic analcime prevalent

Sample number: LGC8
Rock Name: CAMPTONITE-LAMPROPHYRE

Hand Sample Description: Medium greenish grey. Dyke, porphyritic, strong, slightly weathered. Fine to coarse grained, inequigranular and panidiomorphic. Pyroxene-Euhedral and subhedral. Dark mineral that has 90°cleavage-60%. Plagioclase- Elongate, euhedral and subhedral. Cleavage at 90, two directions. White translucent-20%. Coarse grained altered amphibole and pyroxene phenocrysts in a feldspar-pyroxene ground mass with carbonate veins and veinlets throughout the sample. Quartz phenocryst with some chalky calcite encompassing it. Rhombohedral calcite.

Thin section description: Dark greenish grey, fine to medium grained with coarse macrocrysts (0.05-3 mm) massive, bimodal distribution, porphyritic, fenitized CAMPTONITE-LAMPROPHYRE. Secondary minerals include chlorite, amphibole, sericite, analcime and cancrinite, calcite, clay epidote and aegirine. Feldspars poorly formed with and display pervasive sericitisation, mainly labradorite (65%). Nepheline macrocrysts commonly contains opaque inclusions, embayed, network replacement to analcime, clay, calcite and internal alteration to cancrinite. Clinopyroxene macrocrysts are concentrically zoned and display undulose extinction. Groundmass is fine to medium grained and is composed of primary pyroxenes, feldspars, nepheline and amphiboles that display alteration features. Crosscutting calcite veins throughout.

Phenocrysts	%	Diagnostic properties	Textures & Alteration
amphibole-riebeckite	20	PPL-green to greenish brown, moderately pleochroic, moderate to high relief, anhedral. CPL-2 perfect cleavages at 120°, extinction 10-30° from cleavage, 0.014 -0.034 δ	Undulose extinction. Displays deep red brown (z) to brown (x) pleochroism typical of kaersutite. Kaersutite phenocrysts occur in glomerophyric clusters. Pervasive to complete alteration to clay, chlorite, serpentine and partial alteration to biotite. Trains of opaques within clay. Biotite further degraded to chlorite. Network, rim and total serpentinisation.
nepheline	10	PPL-Colourless, very low relief, uniaxial -ve, euhedral, blocky. CPL- 0.004 δ.	Large phenocrysts that display high δ cancrinite alteration. Concentric zoning common. Network and rim alteration to calcite and clays. Phenocrysts are turbid and display undulose extinction. Heavily alteration to cancrinite is common. Part of the ground mass. Alteration to partially isotropic analcime prevalent
clinopyroxene- augite	4	PPL-Pale green to brownish, 2 cleavages at approximately 90°, inclined 40 to 50° extinction, moderate relief and subhedral. CPL-0.018 – 0.034 δ.	Oscillatory zoning common. Clinopyroxene phenocrysts occur in glomerophyric clusters. Partial uralitisation to amphiboles not uncommon. Pervasive to complete to clay, chlorite, serpentine and partial alteration to biotite. Trains of opaques within carbonate clay. Biotite further degraded to chlorite. Network, rim and total serpentinisation. Calcite replacement common.
olivine	1	PPL- Colourless, moderate to high relief, rounded equant, sub to anhedral. CPL- 0.035 – 0.052 δ.	Commonly speckled with opaques. Fractured throughout with acicular chloritisation. Alteration to iddingsite common as well. Pervasive to complete to clay, chlorite, serpentine and partial alteration to biotite. Trains of opaques within carbonate clay. Biotite further

					degraded to chlorite. Network, rim and total serpentinisation. Calcite replacement common.
	Groundmass				
	calcite		8	PPL-Colourless to pale pink, low pleochroism, low relief, subhedral, lamellar twinning, perfect rhombohedral cleavage at 74° 55'. CPL- 0.179-0.202 δ.	Veins displaying comb textures cross cut host rock. Carbonate veins cross cut one another. Traces of dolomite. Accessory aegirine and epidote in trace levels clustered adjacent and within veinlets. Mixture of limpid rhombohedral calcite and indistinct, contaminated turbid calcite and clay carbonate.
	clay		15	Yellowish brown to grey in both plane PPL and CPL. No optical properties. Glass?	Cross cut by calcite veins. No optical properties. Occasional stubby opaque and calcite phenocrysts.
	green amphibole		15	PPL-green to greenish brown, moderately pleochroic, moderate to high relief, anhedral. CPL-2 perfect cleavages at 120°, extinction 10-30° from cleavage, 0.014 -0.034 δ	Occasional primary amphibole. Groundmass is heavily composed of green amphibole. Alteration to biotite and chlorite prevalent.
	nepheline		2	PPL-Colourless, very low relief, uniaxial -ve, euhedral, blocky. CPL- 0.004 δ.	Blocky nepheline typically adjacent to feldspars. Partial alteration to analcime not uncommon.
	opaque	magnetite-100% 0.01-2mm	2	Opaque. Anhedral.	Throughout sample. Large phenocrysts
	plagioclase	labradorite 65% ML-29°	23	PPL-Colourless, low relief, inclined extinction, elongate, subhedral. CPL-Carlsbad, polysynthetic and some pericline twinning, 0.007 – 0.013 δ.	Phenocrysts are turbid and display undulose extinction. Heavily alteration to sericite is common. Part of the ground mass. Alteration to partially isotropic analcime prevalent
		andesine-35% ML-14°			

Sample number: LGC9
Rock Name: Calcite Carbonatite

Hand Sample Description: Light creamy orange white. Crystallised, phaneritic, strong, unweathered. Fine grained with coarse crystals, inequigranular, and hypidiomorphic. Carbonate-Blocky, euhedral and subhedral. White Translucent and fizzes to HCl acid-80%. Quartz-glassy and transparent, appearing grey in hand specimen. White Translucent-5%.6 large coarse grained carbonate veins throughout the sample. Heavy epidote weathering emanating from epidote rich areas. Some metallic mineral, magnetite?

Thin section description: Moderate greenish grey and white, fine to medium grained (0.5-5 mm), massive, hypidiomorphic to idiomorphic, bimodal, porphyritic, CALCITE CABONATITE. Carbonate minerals throughout, sutured. Accessory quartz and plagioclase. Large veins and fingering of carbonate. Quartz is bimodal, medium and fine grained phenocrysts. Rare epidote and aegirine in clusters within the calcite veinlets. Pervasively pseudomorphed lamprophyre host to clay exhibiting ghosts of previous textures and minerals.

Modal mineralogy	**%**	**Diagnostic properties**	**Textures**
calcite	70	PPL-Colourless to pale pink, low pleochroism, low relief, subhedral, lamellar twinning, perfect rhombohedral cleavage at 74° 55'. CPL- 0.179-0.202 δ.	Veins displaying comb, crustiform textures cross cut host rock. Calcite geode present. Carbonate veins cross cut one another. Traces of dolomite. Accessory aegirine and epidote in trace levels clustered adjacent and within veinlets. Mixture of limpid rhombohedral calcite and indistinct, contaminated turbid calcite and clay carbonate.
clay	5	Yellowish brown to grey in both plane PPL and CPL. No optical properties	Fenitized groundmass. Carbonate clay.
quartz	10	PPL- Colourless, very low relief, subhedral to anhedral. CPL-0.009 δ	Clusters of quartz, sutured with varying extinctions. Intermingled quartz lenses in calcite veinlets.
Phenocrysts	**%**	**Diagnostic properties**	**Textures & Alteration**
amphibole- kaersutite	2	PPL-green to greenish brown, moderately pleochroic, moderate to high relief, anhedral. CPL-2 perfect cleavages at 120°, extinction 10-30° from cleavage, 0.014 -0.034 δ.	Undulose extinction. Displays deep red brown (z) to brown (x) pleochroism typical of kaersutite. Kaersutite phenocrysts occur in glomerophyric clusters. Pervasive to complete alteration to clay, chlorite, serpentine and partial alteration to biotite. Trains of opaques within clay. Biotite further degraded to chlorite. Network, rim and total serpentinisation.
clinopyroxene- augite and riebeckite	1	PPL-Pale green to brownish, 2 cleavages at approximately 90°, inclined 40 to 50° extinction, moderate relief and subhedral. CPL- 0.018 – 0.034 δ.	Oscillatory zoning common. Clinopyroxene phenocrysts occur in glomerophyric clusters. Partial uralitisation to amphiboles not uncommon. Pervasive to complete to clay, chlorite, serpentine and partial alteration to biotite. Trains of opaques within carbonate clay. Biotite further degraded to chlorite.

					Network, rim and total serpentinisation. Calcite replacement common.
	Groundmass				
	green amphibole		5	PPL-green to greenish brown, moderately pleochroic, moderate to high relief, anhedral. CPL-2 perfect cleavages at 120°, extinction 10-30° from cleavage, 0.014 -0.034 δ.	Occasional primary amphibole. Groundmass is heavily composed of green amphibole. Alteration to biotite and chlorite prevalent.
	nepheline		1	PPL-Colourless, very low relief, uniaxial -ve, euhedral, blocky. CPL- 0.004 δ.	Blocky nepheline typically adjacent to feldspars. Partial alteration to analcime not uncommon.
	opaque		2	Opaque. Anhedral.	Throughout sample. Large phenocrysts
	plagioclase	labradorite 65% ML-29°	4	PPL-Colourless, low relief, inclined extinction, elongate, subhedral. CPL-Carlsbad, polysynthetic and some pericline twinning, 0.007 – 0.013 δ.	Phenocrysts are turbid and display undulose extinction. Heavily alteration to sericite is common. Part of the ground mass. Alteration to partially isotropic analcime prevalent
		andesine-35% ML-14°			

Sample number: LGC10
Rock Name: Calcite Carbonatite

Hand Sample Description: Light creamy white. Crystallised, phaneritic, strong, unweathered. Fine grained with coarse crystals, inequigranular, and hypidiomorphic. Carbonate-Blocky, euhedral and subhedral. White Translucent and fizzes to HCl acid-70%. Quartz-glassy and transparent, appearing grey in hand specimen-5%. 5 large coarse carbonate veins throughout the sample. Heavy epidote weathering emanating from epidote rich areas. Limpid and turbid calcite laminates Some metallic mineral, magnetite?

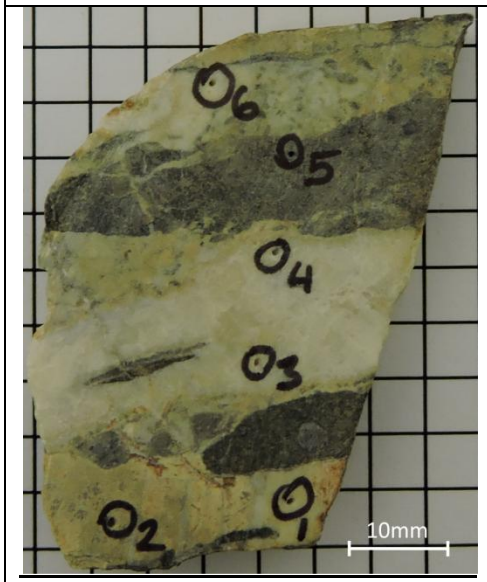

Thin section description: Moderate greenish grey and white, fine to medium grained (0.5-5 mm), massive, hypidiomorphic to idiomorphic, bimodal, porphyritic, CALCITE CABONATITE. Carbonate minerals throughout, sutured. Accessory quartz and plagioclase. Large veins and fingering of carbonate. Quartz is bimodal, medium and fine grained phenocrysts. Rare epidote and aegirine in clusters within the calcite veinlets. Pervasively pseudomorphed lamprophyre host to clay exhibiting ghosts of previous textures and minerals.

Modal mineralogy	**%**	**Diagnostic properties**	**Textures**
calcite	60	PPL-Colourless to pale pink, low pleochroism, low relief, subhedral, lamellar twinning, perfect rhombohedral cleavage at 74° 55'. CPL- 0.179-0.202 δ.	Vein structures that cross cut host rock. Carbonate veins cross cut one another. Limpid and turbid calcite laminates with chaotic spider veinlets. Traces of dolomite. Accessory aegirine and epidote in trace levels clustered adjacent and within veinlets. Mixture of limpid rhombohedral calcite and indistinct, contaminated turbid calcite and clay carbonate.
clay	10	Yellowish brown to grey in both plane PPL and CPL. No optical properties.	Fenitized groundmass. Carbonate clay.
quartz	10	PPL- Colourless, very low relief, subhedral to anhedral. CPL-0.009 δ.	Clusters of quartz, sutured with varying extinctions. Intermingled quartz lenses in calcite veinlets.
Phenocrysts	**%**	**Diagnostic properties**	**Textures & Alteration**
amphibole- kaersutite	5	PPL-green to greenish brown, moderately pleochroic, moderate to high relief, anhedral. CPL-2 perfect cleavages at 120°, extinction 10-30° from cleavage, 0.014 -0.034 δ.	Undulose extinction. Displays deep red brown (z) to brown (x) pleochroism typical of kaersutite. Kaersutite phenocrysts occur in glomerophyric clusters. Pervasive to complete alteration to clay, chlorite, serpentine and partial alteration to biotite. Trains of opaques within clay. Biotite further degraded to chlorite. Network, rim and total serpentinisation.
clinopyroxene- augite and riebeckite	2	PPL-Pale green to brownish, 2 cleavages at approximately 90°, inclined 40 to 50° extinction, moderate relief and subhedral. CPL- 0.018 – 0.034 δ.	Oscillatory zoning common. Clinopyroxene phenocrysts occur in glomerophyric clusters. Partial uralitisation to amphiboles not uncommon. Pervasive to complete to clay, chlorite, serpentine and partial alteration to biotite. Trains of opaques within carbonate clay. Biotite further degraded to chlorite.

				Network, rim and total serpentinisation. Calcite replacement common.
	Groundmass			
	green amphibole	5	PPL-green to greenish brown, moderately pleochroic, moderate to high relief, anhedral. CPL-2 perfect cleavages at 120°, extinction 10-30° from cleavage, 0.014 -0.034 δ.	Occasional primary amphibole. Groundmass is heavily composed of green amphibole. Alteration to biotite and chlorite prevalent.
	opaque magnetite and ilmenite	2	Opaque. Anhedral.	Throughout sample. Large phenocrysts
	plagioclase	10	PPL-Colourless, low relief, inclined extinction, elongate, subhedral. CPL-Carlsbad, polysynthetic and some pericline twinning, 0.007 – 0.013 δ.	Phenocrysts are turbid and display undulose extinction. Complete to pervasive alteration to sericite and clay is common. Alteration to partially isotropic analcime prevalent.

Sample number: LGC11
Rock Name: Calcite carbonatite veins in lamprophyre

Hand Sample Description: Light creamy white veins with medium grey matrix. Crystallised, phaneritic, strong, unweathered. Fine grained with coarse crystals, inequigranular, and hypidiomorphic. Carbonate-Blocky, euhedral and subhedral. White Translucent and fizzes to HCl acid-50%. Quartz-glassy and transparent, appearing grey in hand specimen. White Translucent-5%.7 carbonate veins and veinlets throughout the sample. Limpid and turbid calcite laminates Some metallic mineral, magnetite?

Thin section description: Moderate greenish grey and white, fine to medium grained (0.5-5 mm), massive, hypidiomorphic to idiomorphic, bimodal, porphyritic, CALCITE CABONATITE VEINS in a LAMPROPHYRE. Carbonate minerals throughout, sutured. Accessory quartz and plagioclase. Large veins and fingering of carbonate with fenitized host either end of sample. Quartz is bimodal, medium and fine grained phenocrysts. Rare epidote and aegirine in clusters within the calcite veinlets. Pervasively pseudomorphed lamprophyre host to clay exhibiting ghosts of previous textures and minerals.

Modal mineralogy	**%**	**Diagnostic properties**	**Textures**
calcite	30	PPL-Colourless to pale pink, low pleochroism, low relief, subhedral, lamellar twinning, perfect rhombohedral cleavage at 74° 55'. CPL- 0.179-0.202 δ.	Vein structures that cross cut host rock. Carbonate veins cross cut one another. Traces of dolomite. Accessory aegirine and epidote in trace levels clustered adjacent and within veinlets. Mixture of limpid rhombohedral calcite and indistinct, contaminated with clay carbonate.
clay	15	Yellowish brown to grey in both plane PPL and CPL. No optical properties.	Fenitized groundmass. Carbonate clay.
quartz	15	PPL- Colourless, very low relief, subhedral to anhedral. CPL-0.009 δ.	Clusters of quartz, sutured with varying extinctions. Intermingled quartz lenses in calcite veinlets.
Phenocrysts	**%**	**Diagnostic properties**	**Textures & Alteration**
amphibole- kaersutite	8	PPL-green to greenish brown, moderately pleochroic, moderate to high relief, anhedral. CPL-2 perfect cleavages at 120°, extinction 10-30° from cleavage, 0.014 -0.034 δ.	Undulose extinction. Kaersutite phenocrysts occur in glomerophyric clusters. Pervasive to complete alteration to clay, chlorite, serpentine and partial alteration to biotite. Trains of opaques within clay. Biotite further degraded to chlorite. Network, rim and total serpentinisation.
clinopyroxene- augite and riebeckite	7	PPL-Pale green to brownish, 2 cleavages at approximately 90°, inclined 40 to 50° extinction, moderate relief and subhedral. CPL-0.018 – 0.034 δ.	Oscillatory zoning common. Clinopyroxene phenocrysts occur in glomerophyric clusters. Partial uralitisation to amphiboles not uncommon. Pervasive to complete to clay, chlorite, serpentine and partial alteration to biotite. Trains of opaques within carbonate clay. Biotite further degraded to chlorite. Network, rim and total serpentinisation. Calcite replacement common.

	Groundmass			
	green amphibole	9	PPL-green to greenish brown, moderately pleochroic, moderate to high relief, anhedral. CPL-2 perfect cleavages at 120°, extinction 10-30° from cleavage, 0.014 -0.034 δ.	Occasional primary amphibole. Groundmass is heavily composed of green amphibole. Alteration to biotite and chlorite prevalent.
	opaque magnetite and ilmenite	2	Opaque. Anhedral.	Throughout sample. Typically fine grained.
	plagioclase	14	PPL-Colourless, low relief, inclined extinction, elongate, subhedral. CPL-Carlsbad, polysynthetic and some pericline twinning, 0.007 – 0.013 δ.	Phenocrysts are turbid and display undulose extinction. Complete to pervasive alteration to sericite and clay is common. Alteration to partially isotropic analcime prevalent.

Sample number: LGC12
Rock Name: OLIVINE GABBRO

Hand Sample Description: Dark greenish grey. Crystallised, porphyritic, strong. Unweathered. Fine to medium grained, equigranular and panidiomorphic. Pyroxene-Blocky, euhedral and subhedral. Dark mineral that has 90deg cleavage-60%. Plagioclase-Elongate euhedral and subhedral. Cleavage at 90, two directions. White Translucent-30%. Carbonate veins throughout the sample.

Thin section description:. Black and white speckled, fine to medium grained (0.1-5 mm), massive, phaneritic, OLIVINE GABBRO. Accessory minerals include biotite, calcite, chlorite and opaques. Plagioclase phenocrysts exhibit well developed and are interlocked with other feldspars and are mainly oligoclase (70%). Clinopyroxene contains opaque inclusions and display micrographic textures of sericite. Iron oxide staining prevalent throughout. Calcite veins throughout. Alteration front present. Fenitization of primary mineral to clay prevalent.

Major minerals		**%**	**Diagnostic properties**	**Textures & Alteration**
plagioclase	oligoclase -70% ML-8° bytownite -30% ML-44°	20	PPL-Colourless, low relief, inclined extinction, elongate, euhedral to subhedral. CPL-Carlsbad, polysynthetic and some pericline twinning, 0.007 – 0.013 δ.	Fractures throughout. Concentric zoning with albite rich rim and anorthite rich core and sericite alteration rind with occasional sericite lamellae. Bent plagioclase phenocrysts common indicating mechanical deformation. Both large phenocrysts and fine grained
orthoclase		4	PPL-Colourless, very low relief, no extinction, Carlsbad twinning, anhedral, perthitic textures. CPL- 0.005 – 0.007 δ.	Perthitic textures common, undulose extinction and indistinct twinning. Carlsbad twinning.
clinopyroxene augite and riebeckite		25	PPL-Pale green to brownish, 2 cleavages at approximately 90°, inclined 40 to 50° extinction, moderate relief and subhedral. CPL- 0.018 – 0.034 δ.	Opaques speckled throughout some clinopyroxene. Uralitisation network replacement to actinolite common. Sieve textures common. Occasional titanian augite, predominantly augite. Degradation sequence as follows clinopyroxene to amphibole to chlorite. Frequent secondary amphibole alteration to chlorite.
orthopyroxene		5	PPL-Colourless to pale cream with pink to green pleochroism, moderate to high relief, cleavage at 88-93°, euhedral and parallel extinction.	Concentric zoning and typically defined cleavages.
olivine		10	PPL- Colourless, moderate to high relief, rounded equant, sub to anhedral. CPL- 0.035 – 0.052 δ.	Fractured throughout with acicular chloritisation. Partial serpentinisation a common occurrence with occasional total serpentinisation. Alteration to iddingsite common as well.
Accessory minerals				
amphibole- kaersutite		10	PPL-green to greenish brown, moderately pleochroic, moderate to high relief, anhedral. CPL-2 perfect cleavages at 120°, extinction 10-30° from cleavage, 0.014 -0.034 δ	Intercumulus amphibole displays concentric zoning with opaque inclusions. Defined cleavages, interstitial. Typically titanium rich

					kaersutite. Secondary amphibole typically actinolite. This secondary actinolite is a degradation product of clinopyroxene.
	calcite		5	PPL-Colourless to pale pink, low pleochroism, low relief, subhedral, lamellar twinning, perfect rhombohedral cleavage at 74° 55'. CPL- 0.179-0.202 δ.	Vein structures that cross cut host rock. Carbonate veins cross cut one another. Traces of dolomite. Accessory aegirine and epidote in trace levels clustered adjacent and within veinlets. Mixture of limpid rhombohedral calcite and indistinct, contaminated with clay carbonate.
	clay		10	Yellowish brown to grey in both plane PPL and CPL. No optical properties.	Fenitized groundmass. Carbonate clay.
	opaque	Magentite -85% 0.2-0.4mm	10	Opaque. Anhedral.	Overgrowths in some plagioclase and clinopyroxene. Typically around phenocryst edges. Interstitial and inclusions in phenocrysts. Interstitial opaques typically larger. Common to find an encompassing rim of opaques around olivine's that at are altering to iddingsite.
		Ilmenite-15% 0.05-0.1mm			
	apatite		1	PPL-Colourless, low relief, parallel extinction, stubby hexagonal, euhedral and no cleavage. CPL-0.007 δ.	Found within feldspars as inclusions. Rare singular phenocrysts.

APPENDIX C: PHOTOMICROGRAPHS

B 1. Photomicrographs of LGC1, glassy foidite. A, B, C and D, Trachytic kaersutite with partial to completely isotropic glass with an alteration front introducing opqaues and altering minerals to clays. Groundmass composed of plagioclase, kaersutite and pervasively pseudomorphed clinopyroxene. B, Large euhedral magnetite. D, Skeletal acicular kaersutite phenocrysts. Plag-plagioclase, mag-magnetite, cpx-clinopyroxene, pseudo.-pseudomorphed, iso.-isotropic.

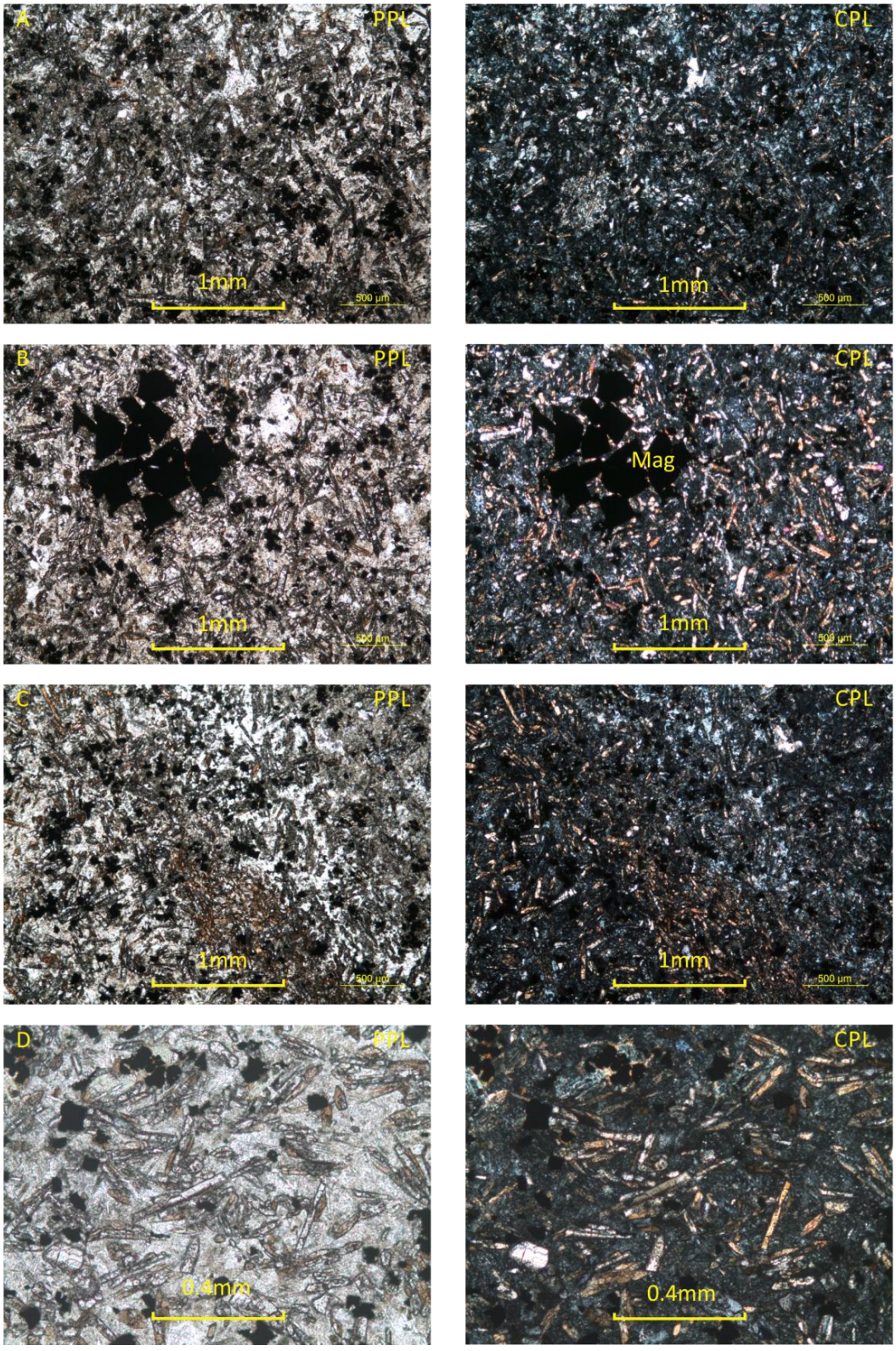

B2. Photomicrographs of LGC2, calcite carbonatite. A-Pseudomorphed host lamprophyre by carbonate fluids, strained nepheline. Calcite and quartz ocelli. B- Rim alteration of completely pseudomorphed mineral to turbid calcite and clay. C-Limpid calcite veinlet and carbonate clay with occasional quartz ocelli. Opq- opaques, qtz-quartz, neph-nepheline, L.-limpid, T.-turbid, pseudo.-pseudomorphed.

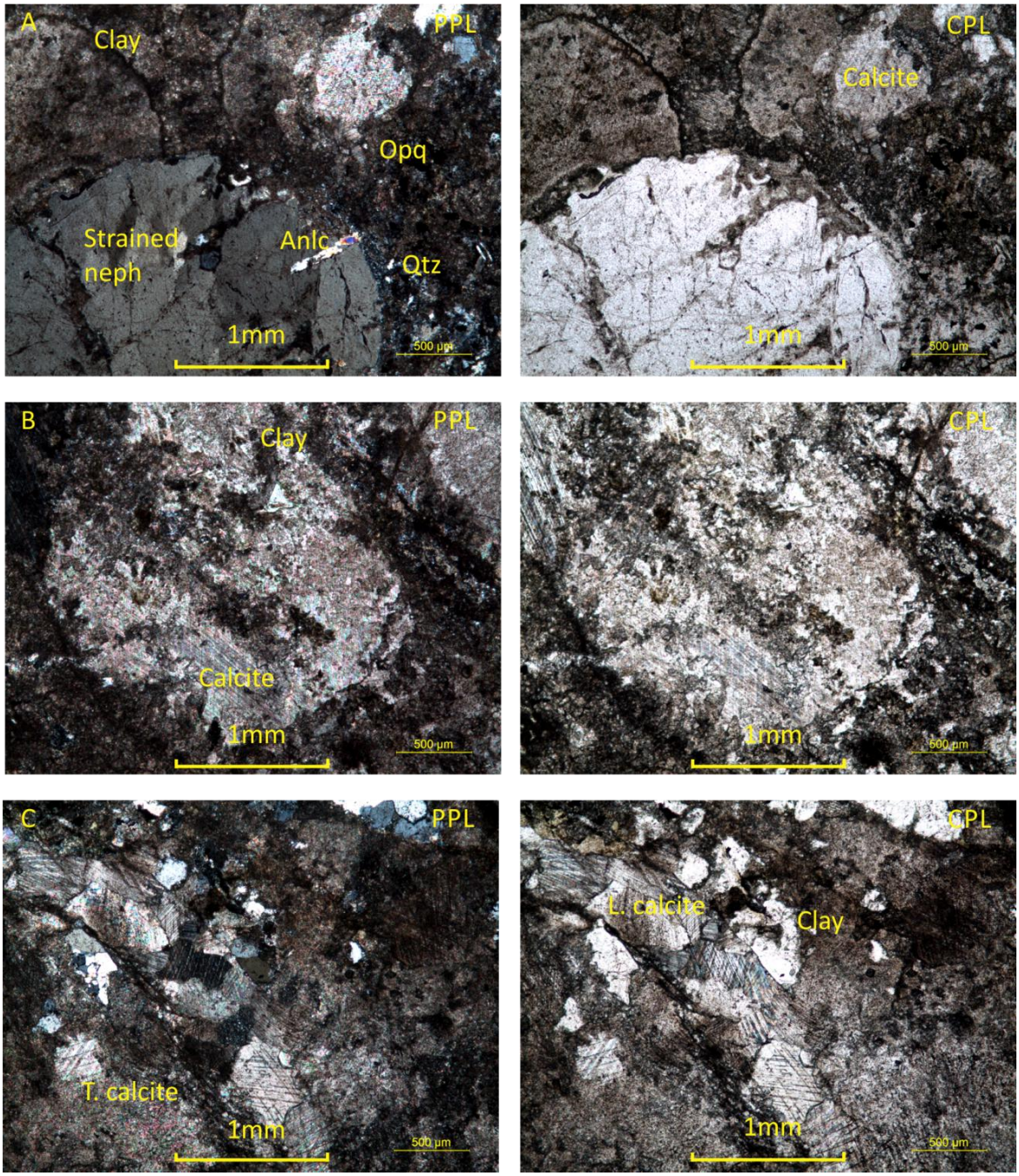

B3. Photomicrographs of LGC3. A-Metasomatised host to carbonate clay with micro quartz. B- Polycrystalline texture mainly displayed by limpid calcite with turbid calcite/pseudomorphed carbonate clay. C- Pseudomorphed clay with turbid calcite. Occasional limpid calcite ocelli. D- Pseudomorphed clay with turbid calcite and micro quartz. Occasional limpid calcite ocelli. E- Calcite veinlet between carbonate clay and turbid calcite. Qtz-quartz, L.-limpid, T.-turbid, pseudo.-pseudomorphed.

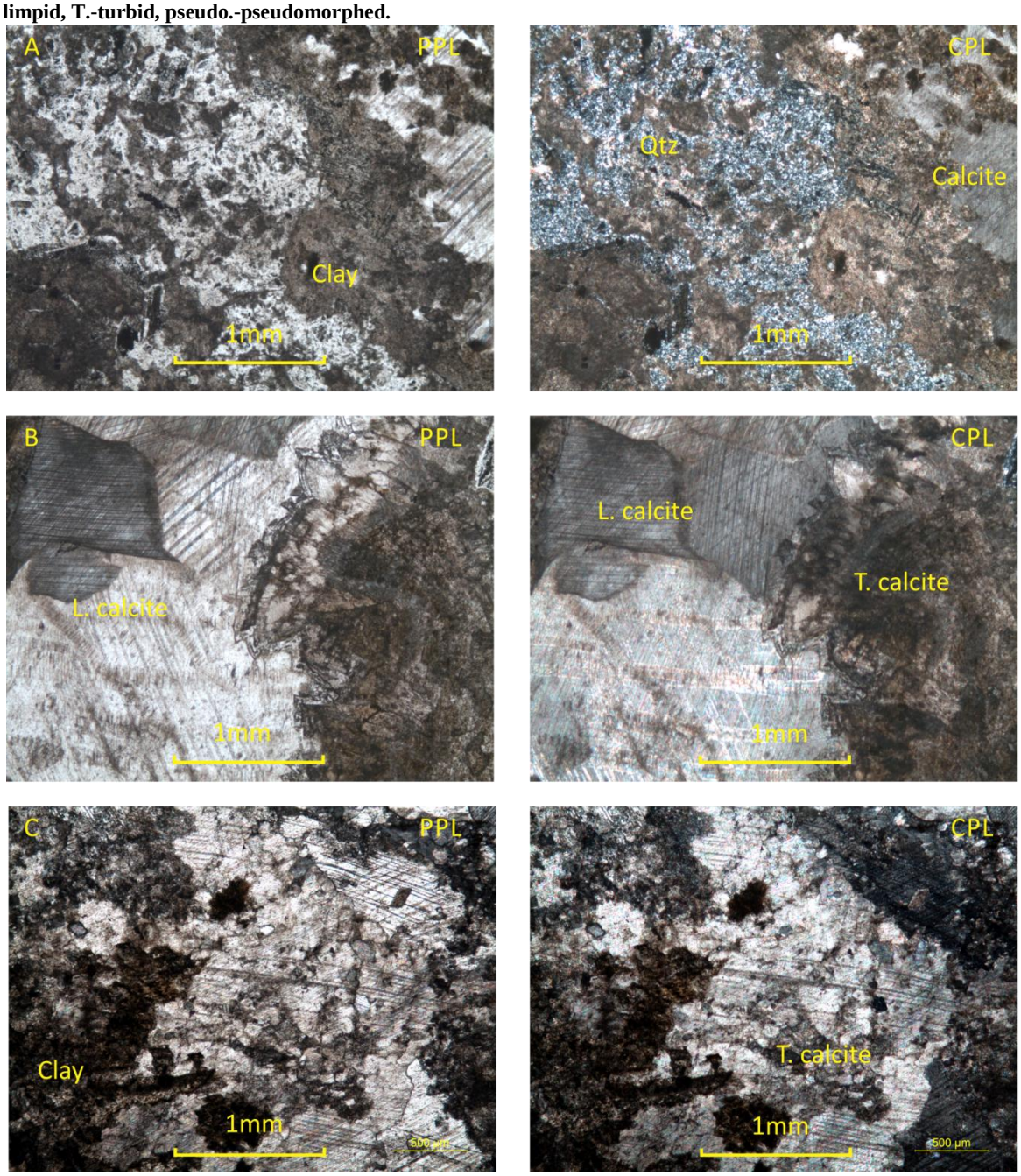

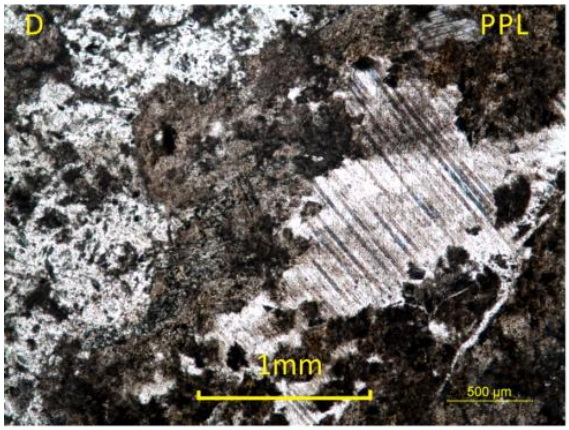
D
PPL
1mm
500 µm

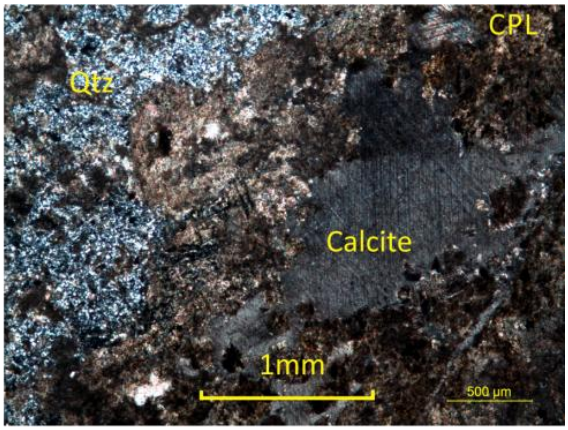
CPL
Qtz
Calcite
1mm
500 µm

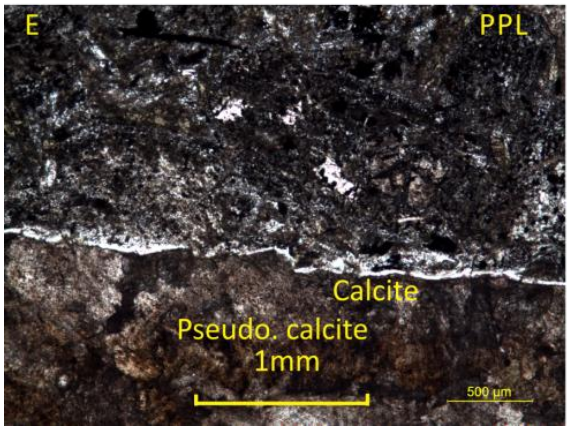
E
PPL
Calcite
Pseudo. calcite
1mm
500 µm

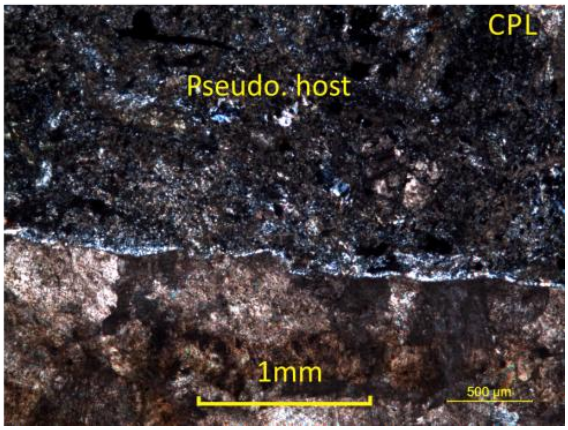
CPL
Pseudo. host
1mm
500 µm

B3.5. Photomicrographs of LGC 3.5, calcite carbonatite. A- Polycrystalline texture mainly displayed by limpid calcite with turbid calcite/pseudomorphed carbonate clay. Opaques throughout. B- Pseudomorphed clay with turbid calcite. C- Pseudomorphed clay boundary with turbid calcite. Occasional limpid calcite ocelli. D-Limpid and Turbid calcite with micro quartz comb textures. Opq-opaques, pseudo.-pseudomorphed.

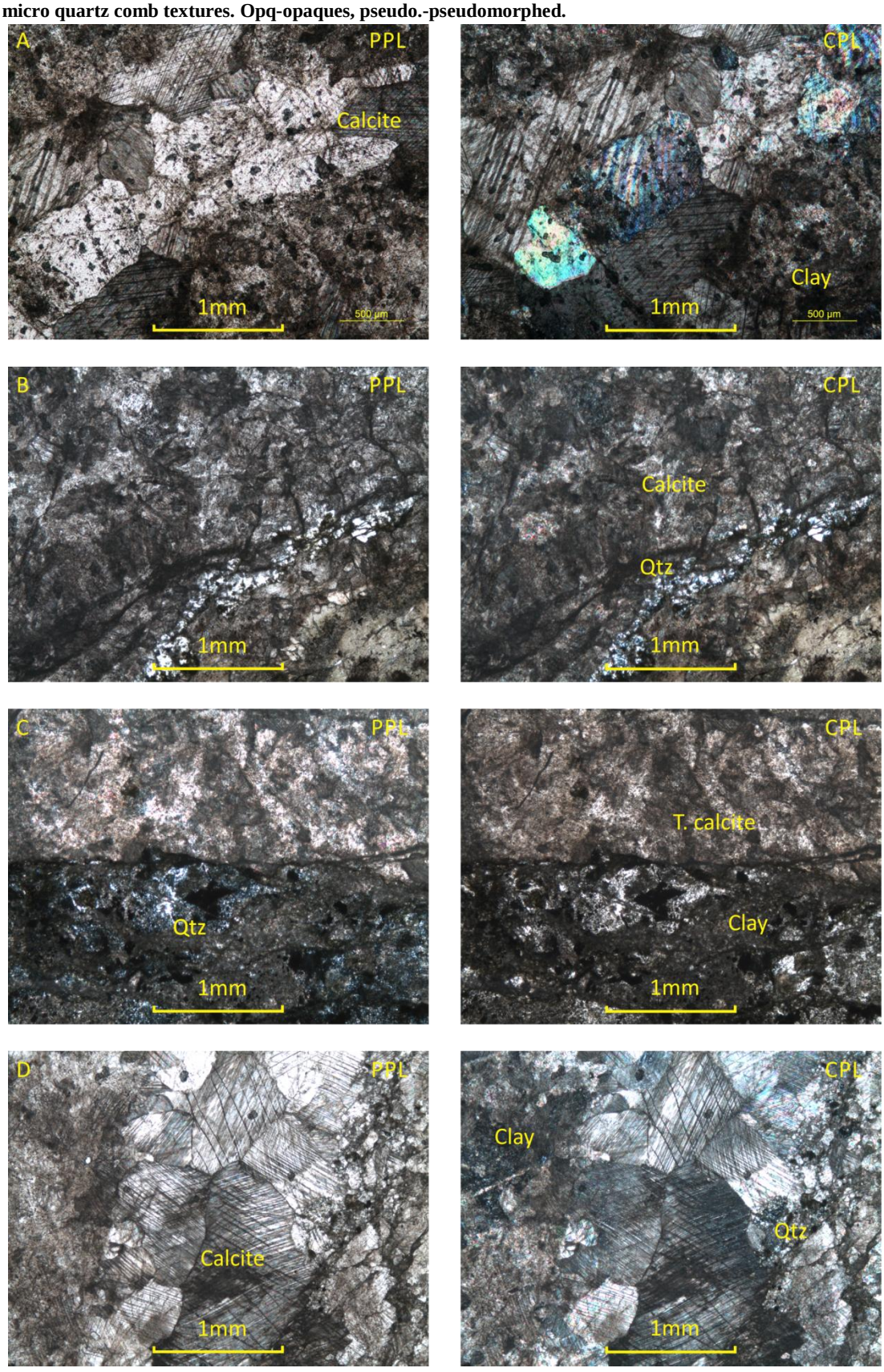

B4. Photomicrographs of LGC 4. A- Polycrystalline texture quartz and lipid calcite ocelli in carbonate clay and metasomatised host lamprophyre groundmass. B- Polycrystalline texture quartz and lipid calcite veins in carbonate clay and metasomatised host lamprophyre groundmass. Quartz display comb textures. C-Limpid calcite veinlet in carbonate clay and metasomatised host lamprophyre groundmass. Qtz-quartz

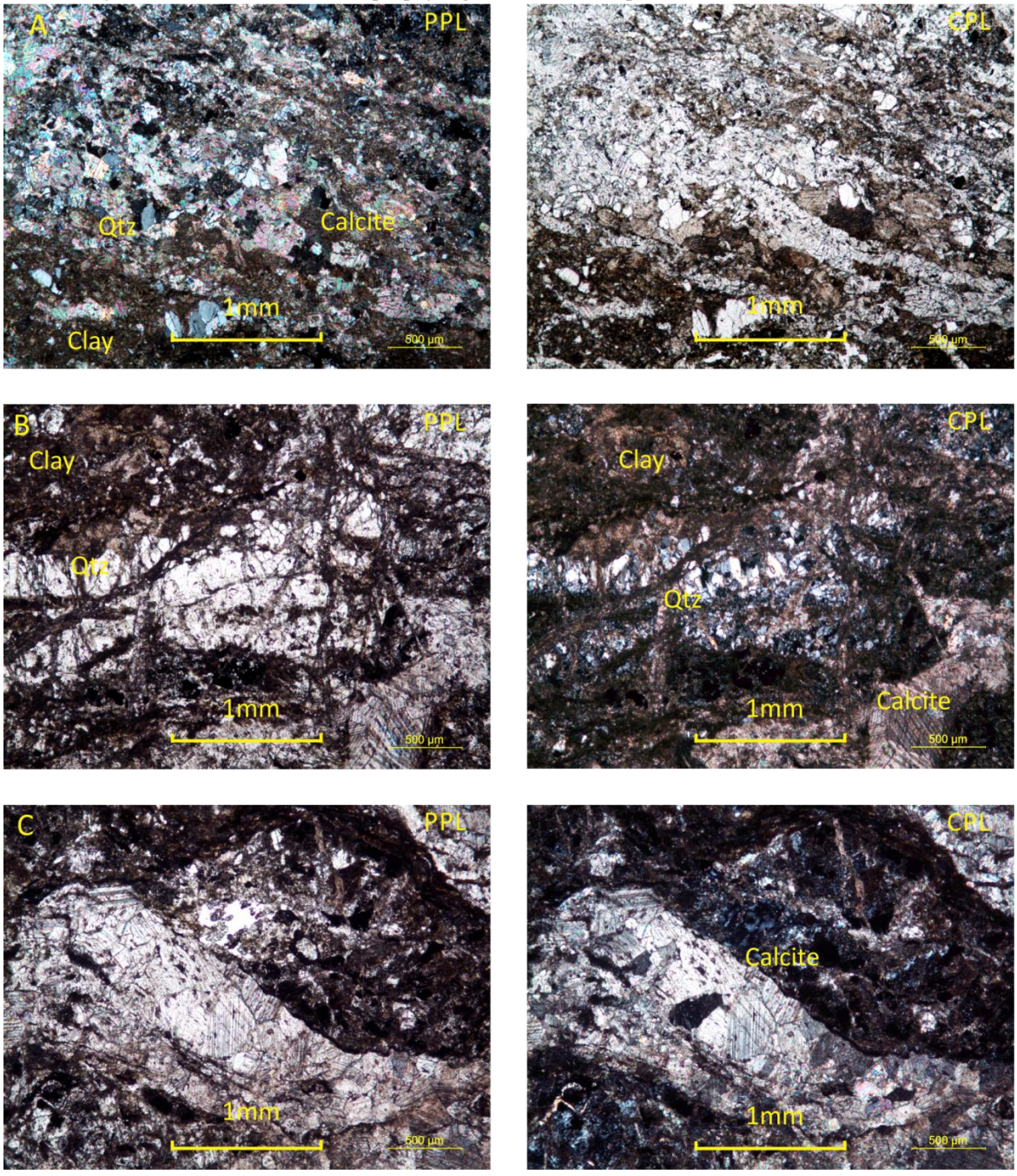

B5. Photomicrographs of LGC5, glassy foidite. A, B, C and D. Trachytic kaersutite with partial to completely isotropic glass with an alteration front introducing opaques and altering minerals to clays. Groundmass composed of plagioclase, kaersutite and pervasively pseudomorphed clinopyroxene. Plag-plagioclase, opq-opaque, cpx-clinopyroxene, pseudo.-pseudomorphed, iso.-isotropic, alt.-alteration.

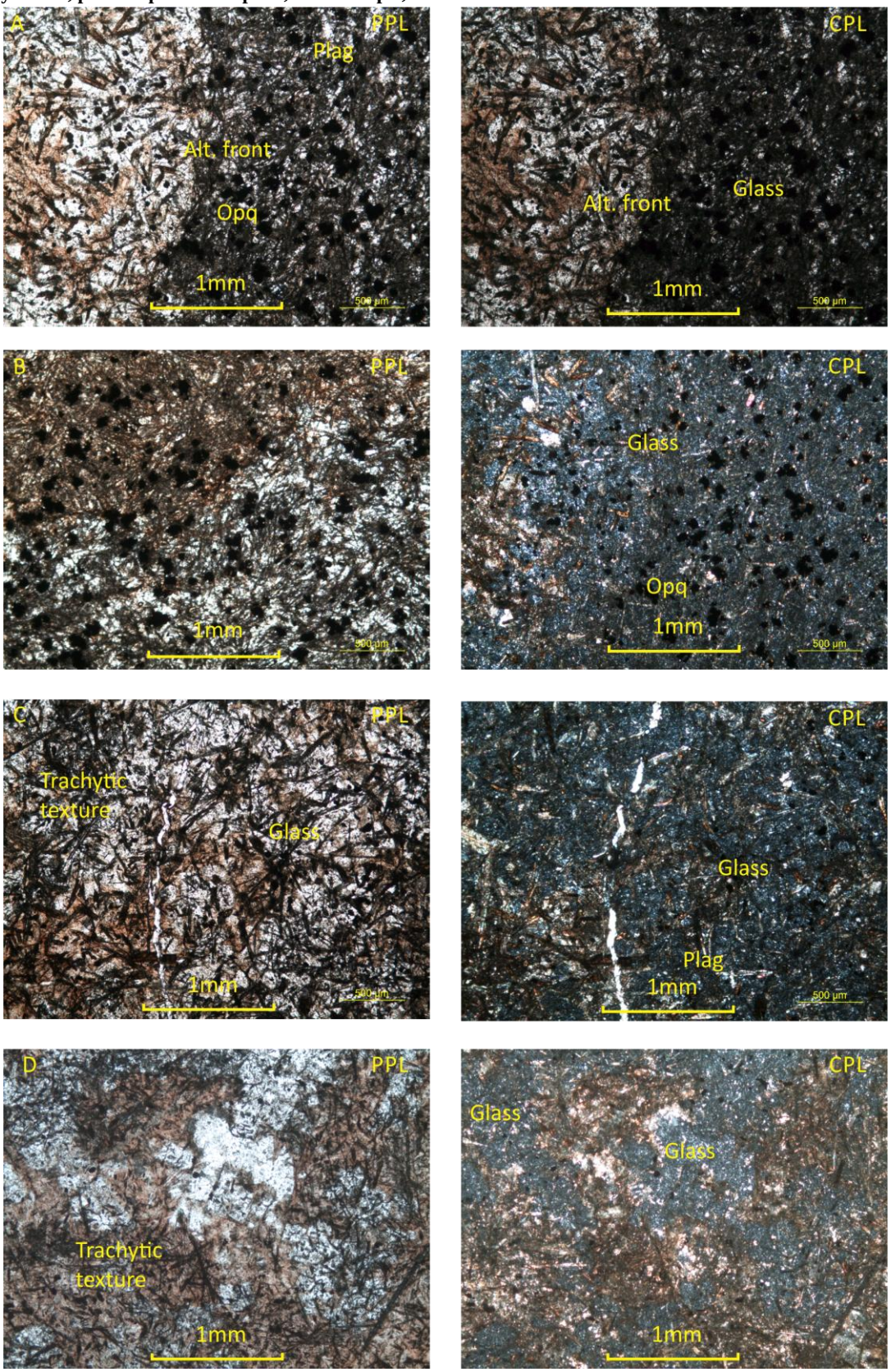

B6. Photomicrographs of LGC6, calcite carbonatite. A and B-Directional spider veins in mafic glass. Turbid and limpid calcite in veins. Quartz comb texture. Polycrystalline texture mainly displayed by limpid calcite. Qtz-quartz, T.-turbid, L.-limpid.

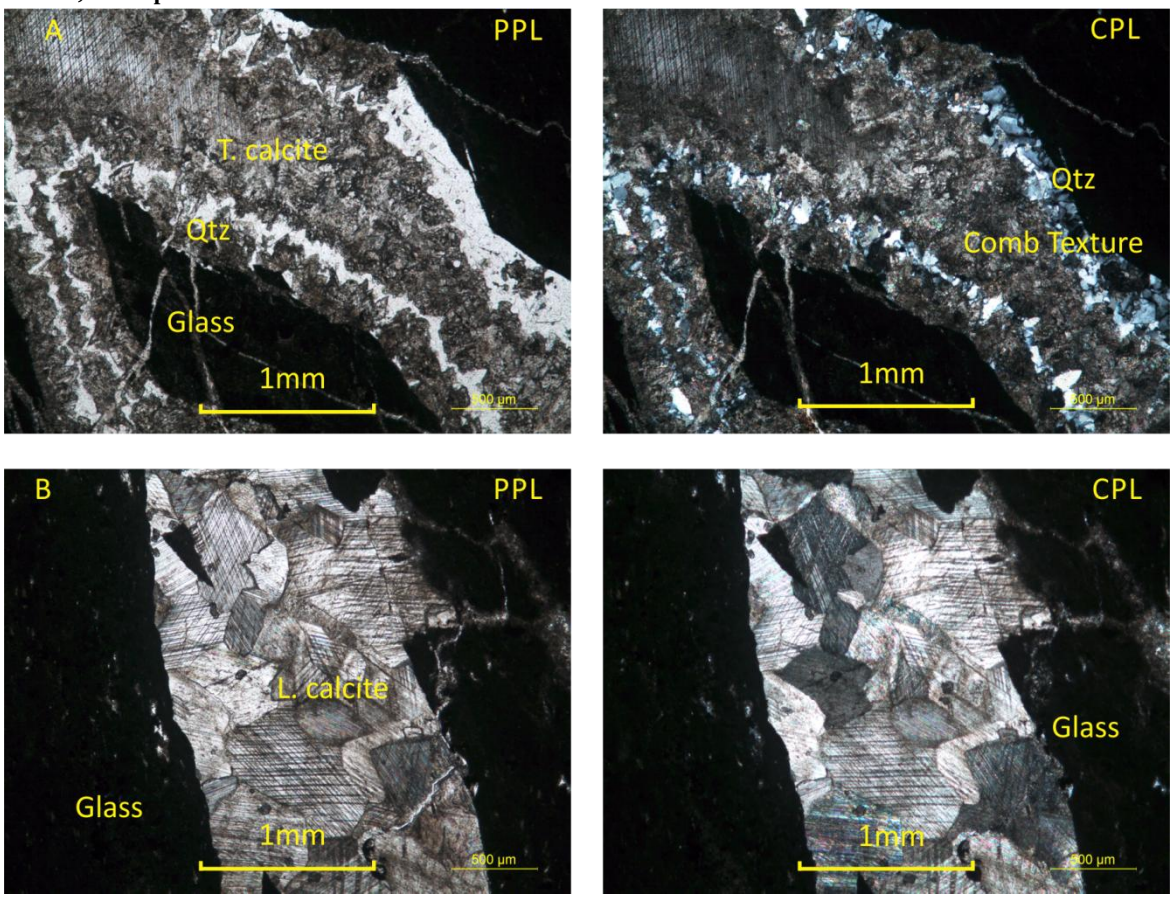

B7. Photomicrographs of LGC7. A-Pseudomorphed olivine, amphibole and plagioclase groundmass with polycrystalline texture displayed by limpid calcite. B-Completely pseudomorphed olivine phenocryst to carbonate clay with calcite ocelli. Serpentine rim alteration. C-Serpentinisation of olivine phenocryst in a carbonate clay and turbid calcite groundmass. D-Exsolution of clinopyroxene to carbonate clay, amphibole with opaques along rim alteration. Pseudomorphed olivine, amphibole and plagioclase groundmass with polycrystalline texture displayed by limpid calcite. E- Pseudomorphed olivine, amphibole and plagioclase groundmass with polycrystalline texture displayed by limpid calcite and serpentinisation of olivine phenocryst. Plag-plagioclase, neph-nepheline, amphi-amphibole, ol-olivine, pseudo-pseudomorphed, gm-groundmass, L. limpid and T. Turbid.

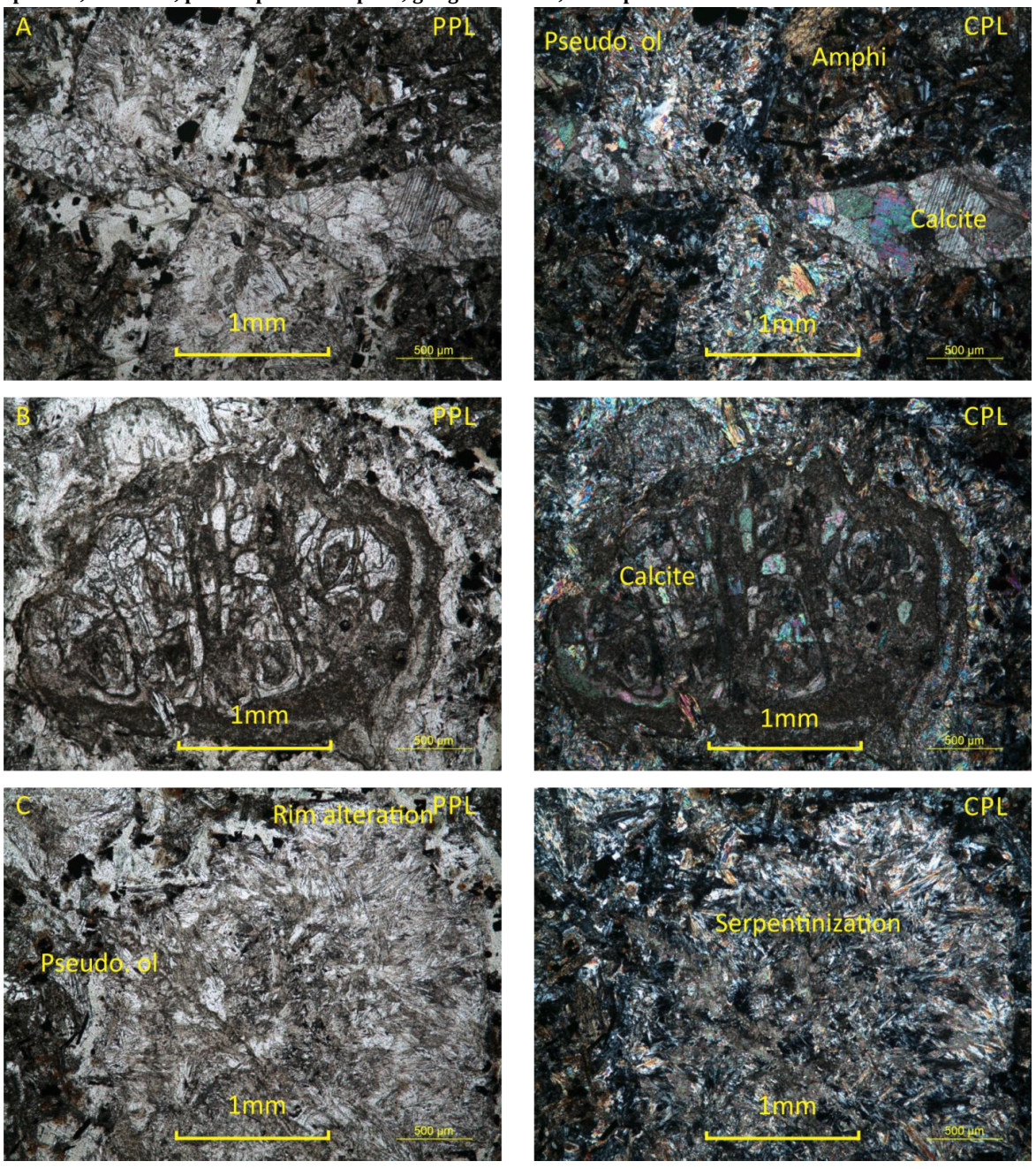

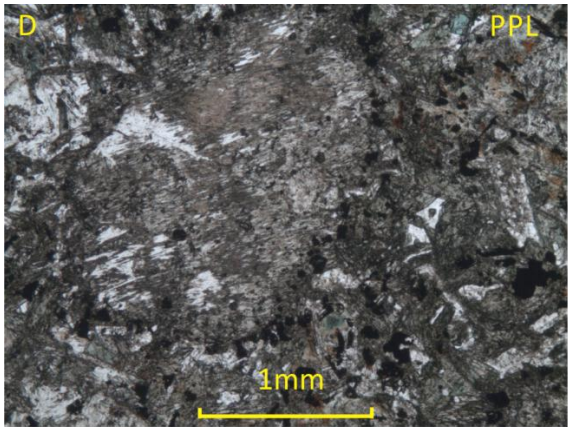
D
PPL
1mm

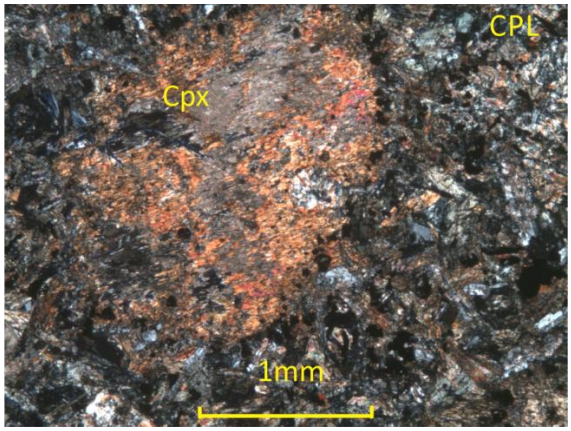
CPL
Cpx
1mm

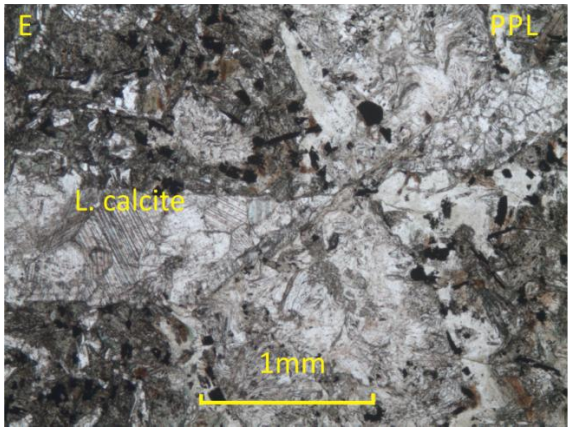
E
PPL
L. calcite
1mm

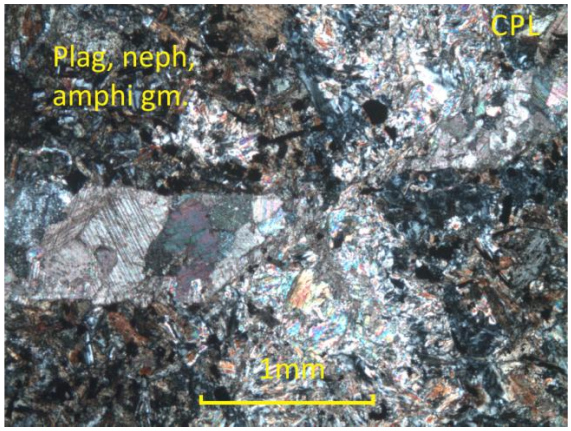
CPL
Plag, neph,
amphi gm.
1mm

B8. Photomicrograph of LGC8. A-Limpid calcite veinlet in plagioclase, ampibole and clay groundmass. Radial cracks in plagioclase interpreted as resulting from the apparent volume increase associated with serpentinisation of olivine. Coronitic textures are moderately well developed in plagioclase. B- Limpid calcite veinlet in nephenline, ampibole and clay groundmass. C- Serpentinisation of olivine phenocryst in a carbonate clay and turbid calcite groundmass. D-Exsolution of clinopyroxene to carbonate clay, amphibole with opaques along rim alteration. Pseudomorphed olivine, amphibole and plagioclase groundmass with polycrystalline texture displayed by limpid calcite. E- Radial cracks and exsolution of nepheline to carbonate clay. Plag-plagioclase, neph-nepheline, amphi-amphibole, ol-olivine, pseudo-pseudomorphed and cpx-clinopyroxene.

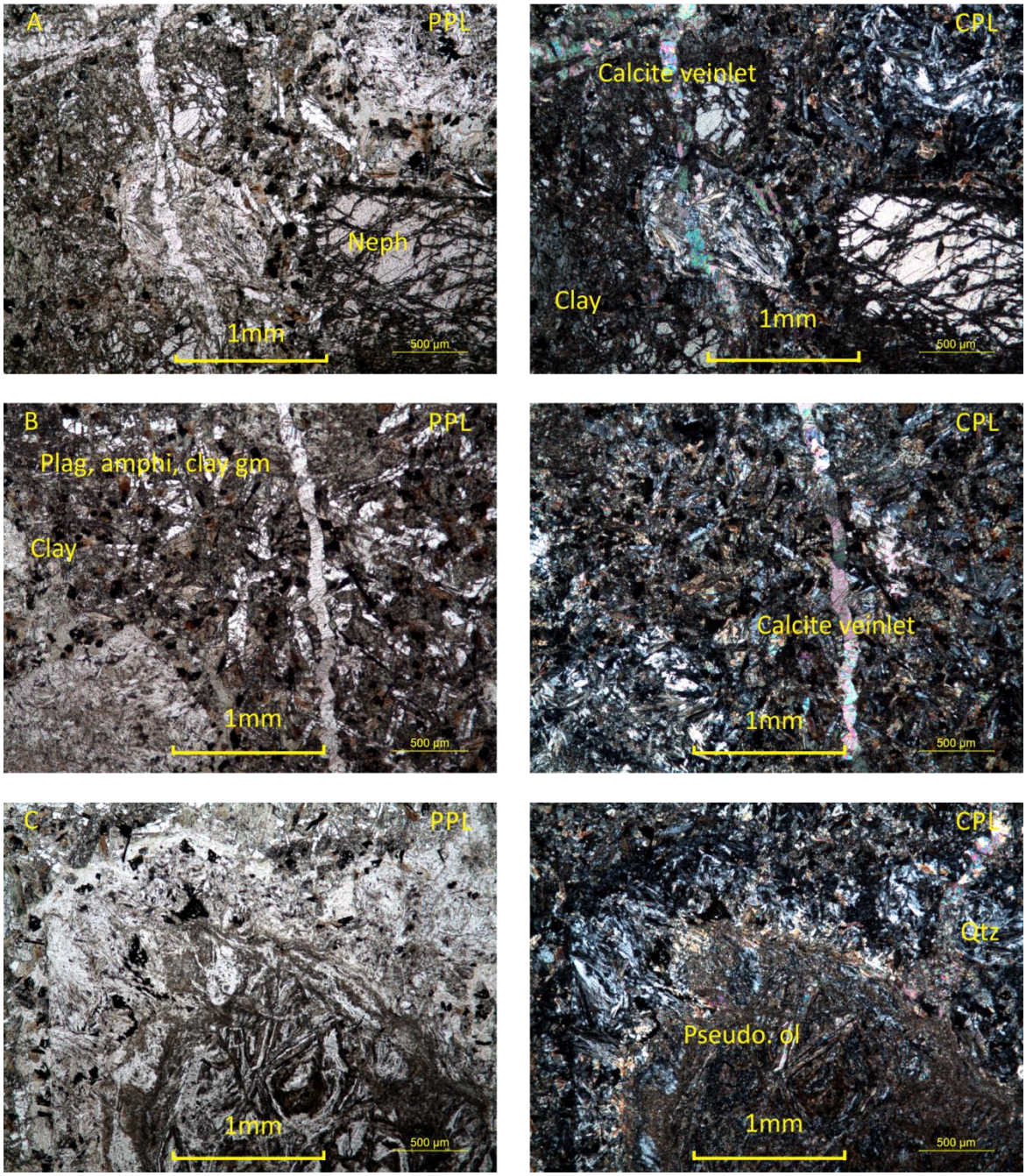

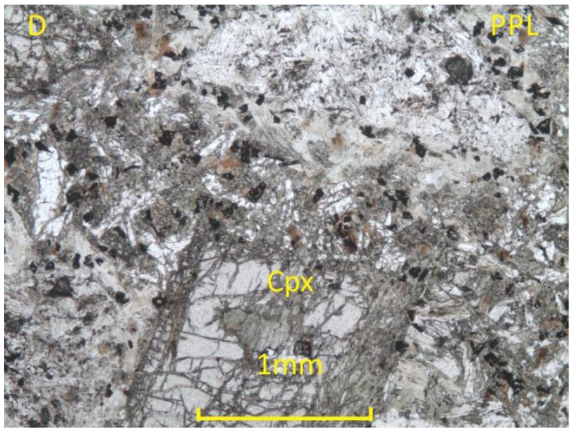
D
PPL
Cpx
1mm

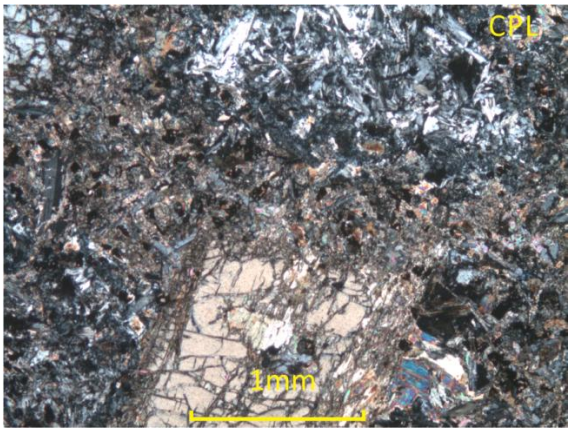
CPL
1mm

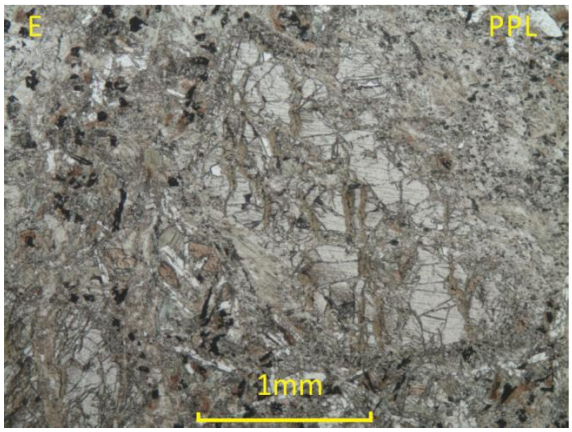
E
PPL
1mm

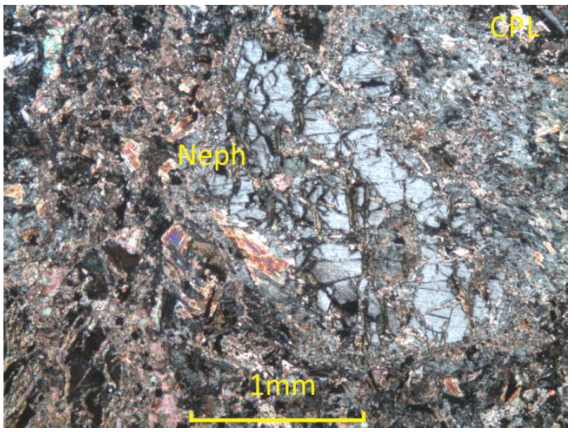
CPL
Neph
1mm

B9. Photomicrographs of LGC9. A-Turbid calcite with oscillatory extinction. B- Limpid calcite with comb texture quartz. C-Carbonate clay, micro quartz and limpid calcite veinlet. D-Turbid calcite with quartz lenses and ocelli. E-Turbid calcite with quartz lenses and ocelli. Qtz-quartz, L. limpid and T. Turbid.

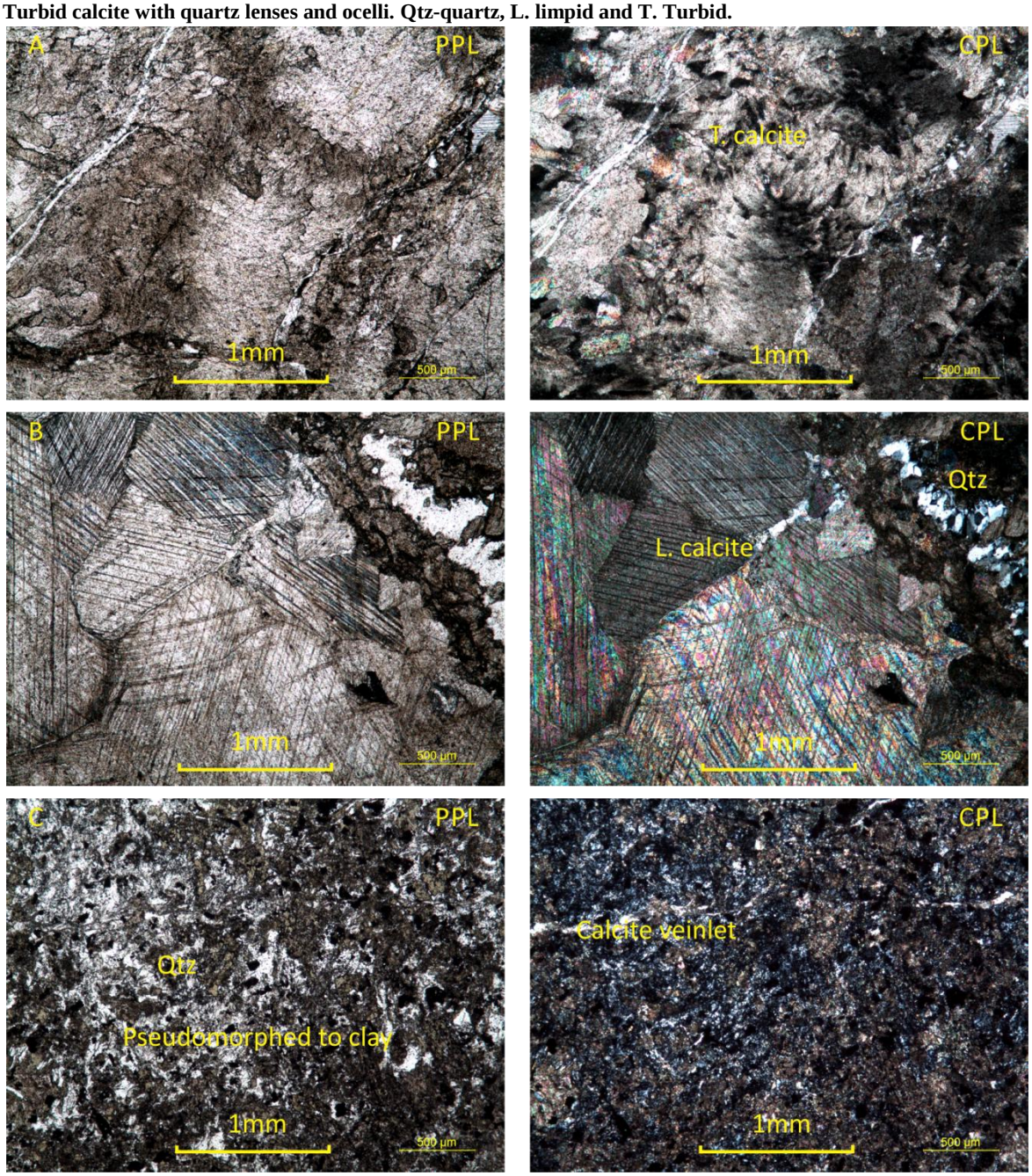

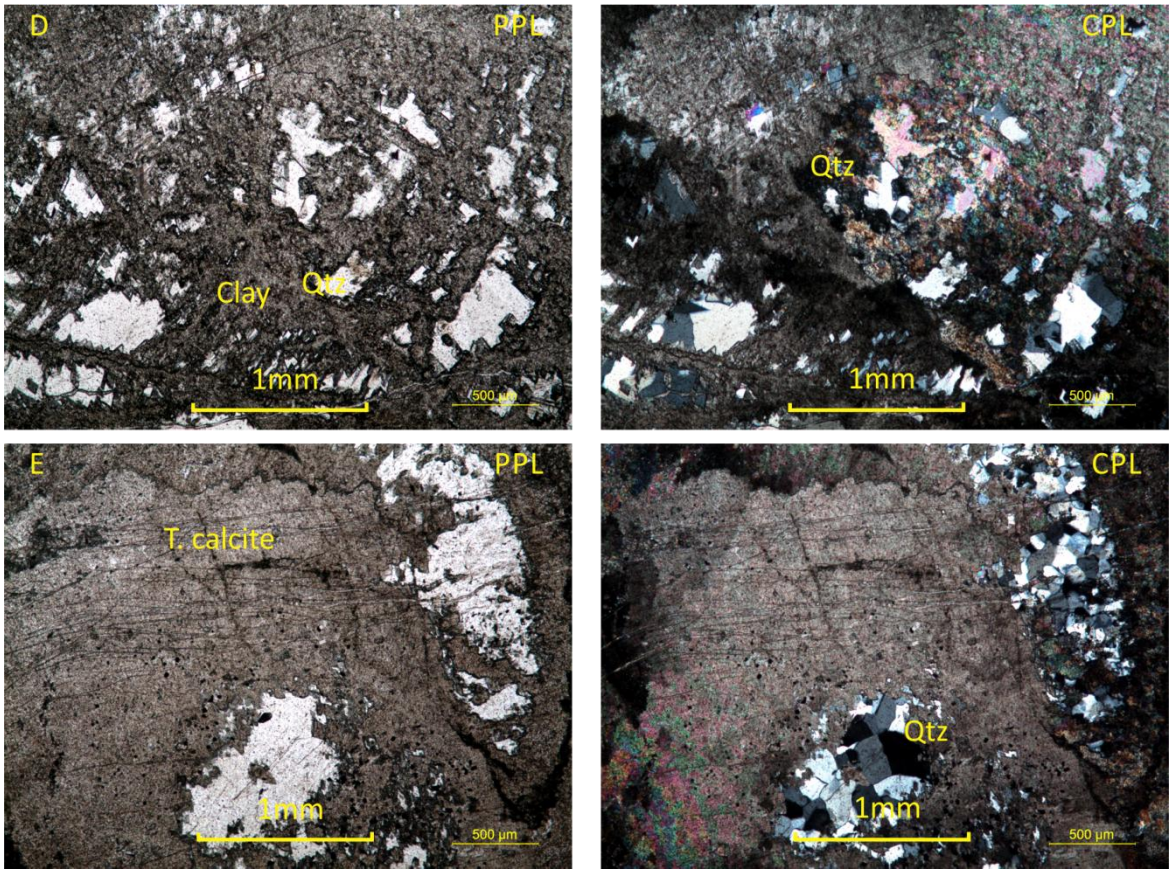
D
PPL
Clay
Qtz
1mm
500 µm
CPL
Qtz
1mm
500 µm
E
PPL
T. calcite
1mm
500 µm
CPL
Qtz
1mm
500 µm

B10. Photomicrographs of LGC9. A-Metasomatised groundmass with replacement of phenocryst by microquartz. B-Turbid calcite with oscillatory extinction. C- Limpid calcite with comb texture quartz at vein boundary with carbonate clay, micro quartz and turbid calcite vein. D-Limpid calcite with quartz lenses and ocelli. E- Turbid calcite with quartz lenses, comb textures and ocelli. Opq-opaques, plag-plagioclase, amphi-amphibole, qtz-quartz, L. limpid and T. Turbid.

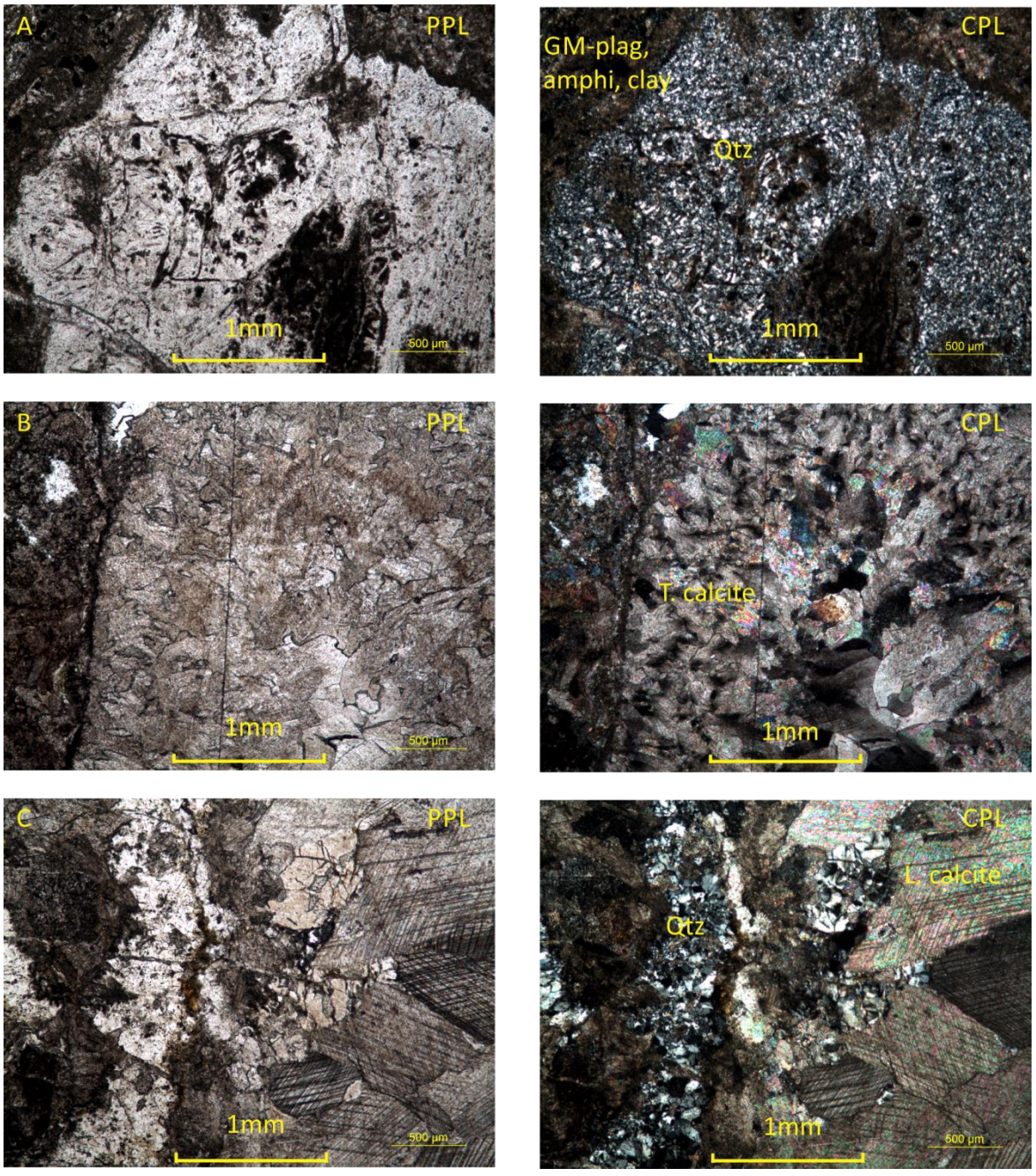

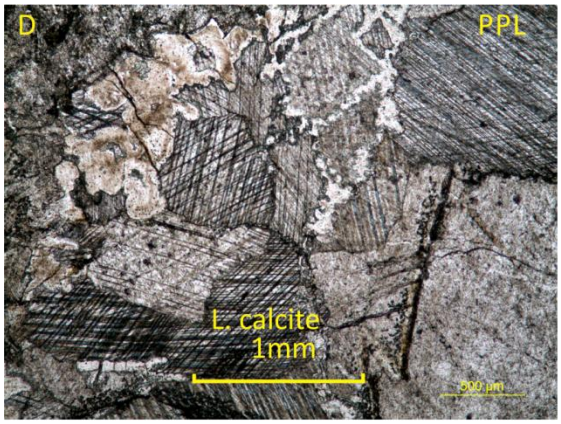
D
PPL
L. calcite
1mm
500 µm

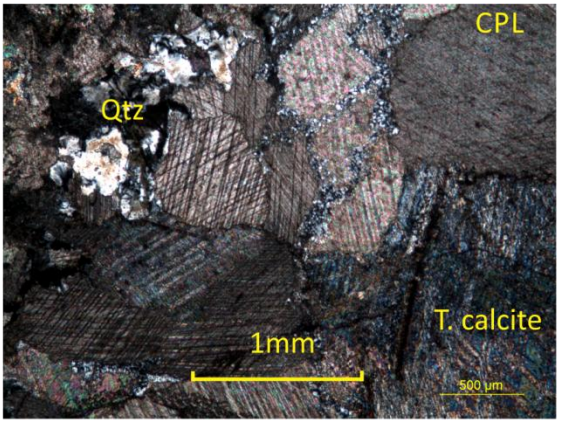
CPL
Qtz
1mm
T. calcite
500 µm

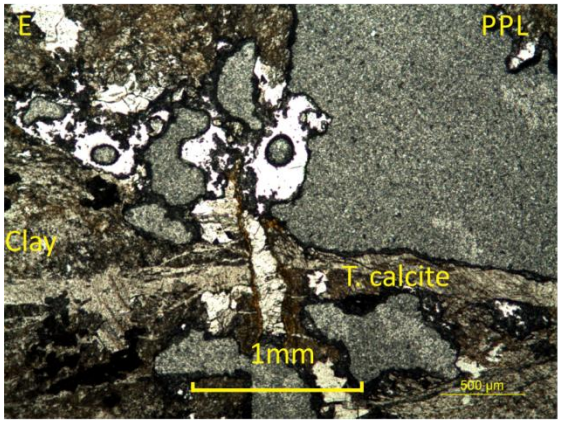
E
PPL
Clay
T. calcite
1mm
500 µm

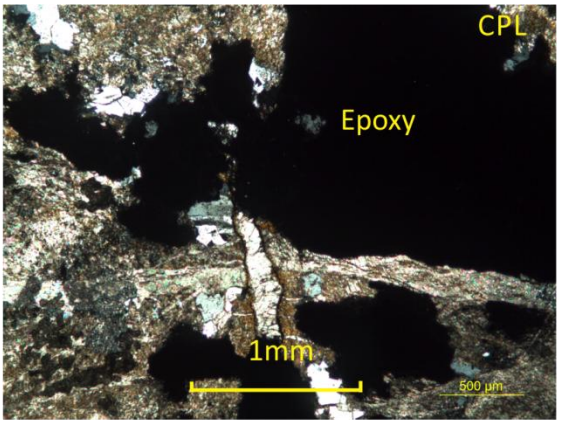
CPL
Epoxy
1mm
500 µm

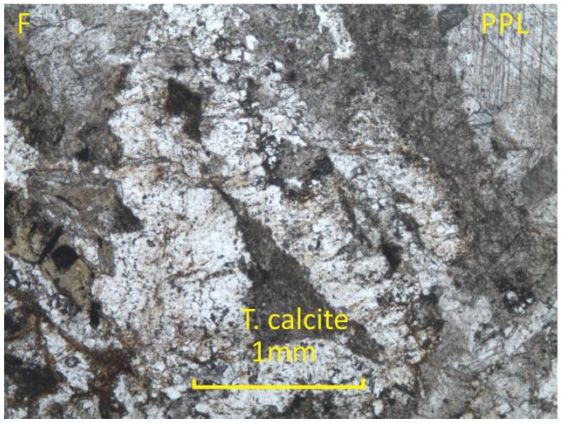
F
PPL
T. calcite
1mm

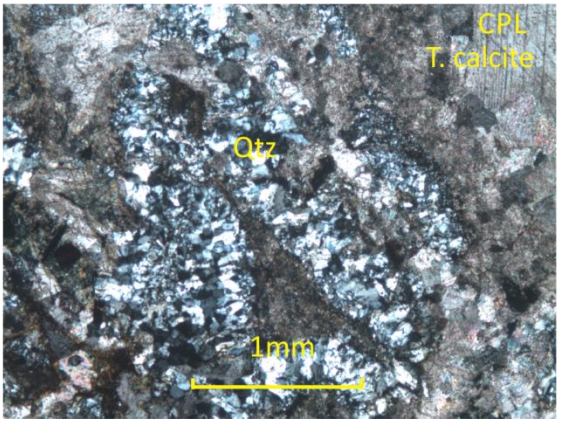
CPL
T. calcite
Qtz
1mm

B11. Photomicrographs of LGC11. Plagioclase, olivine and replacement quartz in carbonate clay. B, Replacement quartz and calcite ocelli in carbonate clay. C-Plagioclase in groundmass that has pseudomorphed to carbonate clay. Pseudo.-pseudomorphed, plag-plagioclase, ol-olivine and qtz-quartz

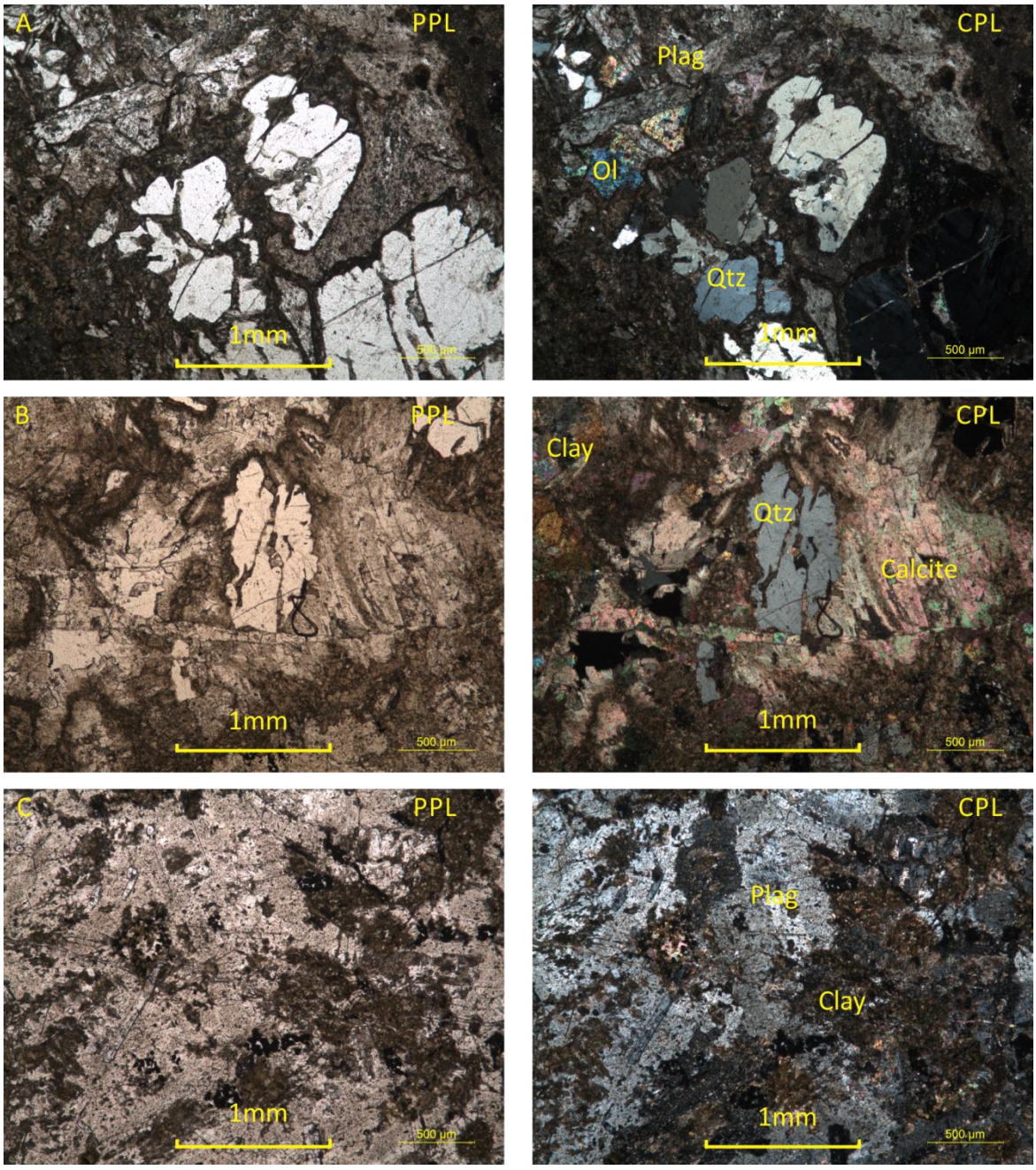

B12. Photomicrographs of LGC12. A-Fine grained plagioclase, kaersutite, opaques and clay. B-Plagioclase phenocryst in a fine grained plagioclase, kaersutite, opaques and clay groundmass. C- Plagioclase phenocryst in a fine grained plagioclase, kaersutite, opaques and clay groundmass. D-Coarse plagioclase displaying oscillatory extinction and bent crystal features. Opq-opaques, plag-plagioclase, amphi-amphibole, mag-magnetite and il-ilmenite.

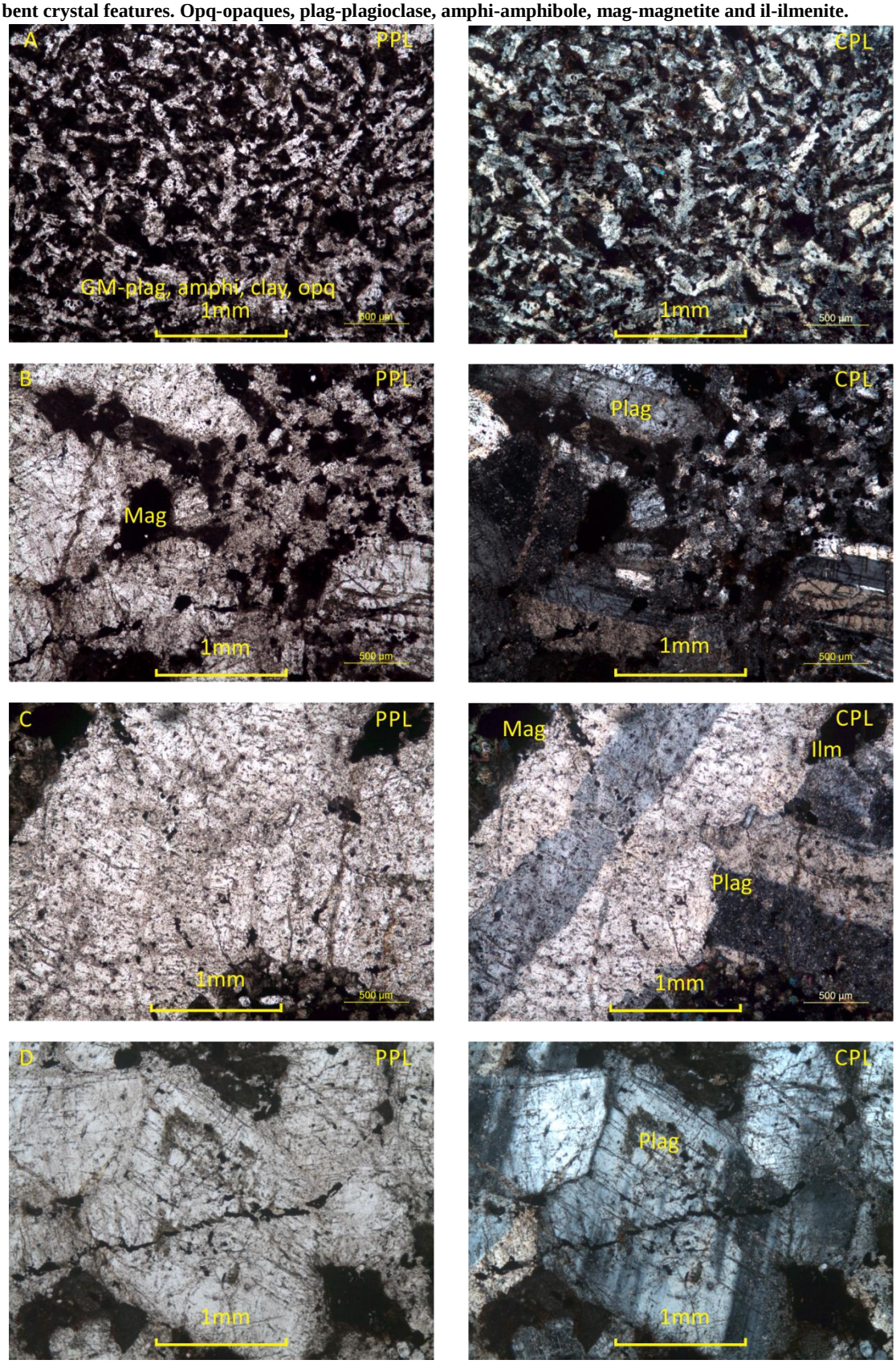

APPENDIX D: PORTABLE XRF ANALYSES

Table D1. Trace element concentrations for the LGC outcrop samples measured by pXRF.

	LGC1	LGC2	LGC3	LGC3.5	LGC4	LGC5	LGC6	LGC7	LGC8	LGC9	LGC10	LGC11	LGC12
Ti	32678	7193	12017	9238	23533	25757	15383	21041	13243	957	3902	1026	25046
Ti +/-	551	230	281	278	430	473	369	410	357	138	197	137	431
V	267	84	176	-	-	136	185	-	-	-	-	-	171
V +/-	48	25	30	90	115	42	37	117	106	61	70	62	39
Cr	-	108	2132	460	1307	-	-	999	596	-	-	107	-
Cr +/-	147	33	68	47	62	139	124	61	55	87	98	33	123
Mn	2064	1175	866	1546	750	2251	808	1241	1642	1057	1008	2310	1089
Mn +/-	71	45	45	57	48	69	49	59	64	45	45	62	51
Fe	117951	25652	57164	52615	64937	86275	60181	117204	61162	7215	19632	19375	90007
Fe +/-	1086	256	485	506	594	804	597	1023	632	113	225	215	770
Co	43	7	17	-	11	37	31	45	11	-	-	7	44
Co +/-	4	2	3	9	3	4	3	4	3	4	6	2	4
Ni	-	-	752	209	433	-	-	952	273	-	-	-	-
Ni +/-	100	56	33	27	32	84	78	45	33	48	56	51	83
Cu	30	-	62	35	47	-	-	105	71	-	-	-	50
Cu +/-	9	20	8	8	8	23	26	10	10	22	21	21	8
Zn	117	28	120	73	92	91	55	117	68	-	-	-	58
Zn +/-	7	4	6	6	6	6	6	7	6	10	11	11	5
As	27	16	9	14	50	28	828	47	11	-	29	-	13
As +/-	3	2	2	3	3	3	12	3	3	7	3	7	3
Zr	563	101	124	49	101	771	431	195	123	-	28	9	242
Zr +/-	7	3	3	3	3	9	6	4	4	8	3	3	4
Mo	-	11	-	-	-	-	12	-	9	-	-	12	-
Mo +/-	8	2	6	7	7	8	3	7	3	7	7	2	7
Ag	-	-	-	-	-	-	-	-	-	-	-	-	-

Ag +/-	19	18	17	19	18	19	20	18	21	20	19	19	18
Cd	-	-	-	-	-	-	-	-	-	-	-	-	-
Cd +/-	67	62	59	66	63	66	69	63	71	70	67	65	60
Sn	-	-	-	-	-	-	-	-	-	-	-	-	-
Sn +/-	76	71	67	74	72	75	78	72	80	79	76	74	68
Sb	-	-	-	-	-	-	60	-	-	-	-	-	-
Sb +/-	41	38	36	40	38	40	14	39	43	43	41	40	36
W	-	-	37	-	114	-	126	-	-	-	-	-	-
W +/-	31	21	9	22	12	28	13	25	25	22	21	20	24
Pb	-	-	-	-	-	-	-	-	-	-	-	-	-
Pb +/-	10	8	8	8	8	10	11	9	9	9	8	8	9
Bi	-	-	-	-	-	-	-	-	-	-	-	-	-
Bi +/-	78	60	55	60	58	78	79	60	69	64	62	59	65
Ca +/-	-	-	-	-	-	-	-	-	-	-	-	-	-
Se	4	-	-	-	-	4	5	-	-	-	-	-	4
Se +/-	1	2	3	3	3	1	1	3	3	3	3	3	1
Rb	73	29	84	12	67	73	132	24	21	-	12	-	30
Rb +/-	3	2	3	2	2	3	4	2	2	5	2	5	3
Sr	1298	729	217	397	135	557	1202	221	552	406	440	499	1134
Sr +/-	14	8	3	6	3	7	13	4	8	6	6	6	11
Hg	-	-	-	-	-	-	-	-	-	-	-	-	10
Hg +/-	10	7	8	8	10	9	13	8	8	8	8	7	3
Th	39	13	15	-	12	70	48	17	16	-	-	-	16
Th +/-	5	4	4	12	4	5	5	4	5	13	13	12	4
U	-	-	-	-	-	-	-	-	-	-	-	-	-
U +/-	26	19	13	16	13	19	25	14	20	17	17	17	23

Table D2. Trace element concentrations of the cut hand samples measured by pXRF.

	LGC1	LGC2	LGC3	LGC3.5	LGC4	LGC5	LGC6	LGC7	LGC8	LGC9	LGC10	LGC11	LGC12
Ti	36112	1875	12931	720	8705	21806	19054	21223	25749	1273	18453	117	8780
Ti +/-	838	246	436	218	405	587	610	609	703	208	541	216	390
V	-	-	-	-	-	-	-	-	-	-	-	-	-
V +/-	-	-	-	-	-	-	-	-	-	-	-	-	-
Cr	46	26	1871	100	3258	-3	79	1919	1461	89	146	51	37
Cr +/-	66	38	83	41	110	51	61	98	96	37	54	44	48
Mn	828	1317	761	2355	557	1292	848	1018	860	770	558	1495	441
Mn +/-	55	45	40	61	41	53	51	56	57	35	41	51	37
Fe	92540	12550	23147	7818	31741	60223	72537	88161	99397	5249	57931	34420	56171
Fe +/-	919	150	236	111	320	575	719	834	977	82	546	342	506
Co	942	21	246	74	202	481	517	714	636	44	448	244	645
Co +/-	97	33	44	28	52	73	84	90	99	22	71	54	67
Ni	-77	11	266	15	79	-67	-46	339	62	-2	-40	-22	-75
Ni +/-	17	10	15	10	13	13	15	21	19	9	13	11	12
Cu	39	-7	35	5	5	-14	-11	70	32	-14	75	-18	66
Cu +/-	9	7	8	7	7	7	8	10	9	6	9	6	8
Zn	107	10	67	19	39	66	54	83	74	7	81	7	49
Zn +/-	7	3	5	4	5	5	6	6	6	3	6	3	5
As	6	4	10	2	27	3	630	14	12	4	22	21	1
As +/-	2	2	2	2	2	2	11	2	2	2	2	2	2
Zr	536	20	140	16	71	728	330	135	179	7	226	11	202
Zr +/-	7	2	3	2	2	8	5	3	4	2	4	2	4
Mo	3	8	9	13	4	0	10	6	6	7	10	13	8
Mo +/-	4	3	3	3	3	4	4	3	3	3	3	3	3
Ag	14	-16	47	5	-4	-11	8	11	12	12	2	12	-4
Ag +/-	14	13	13	14	13	13	14	14	14	13	13	13	13
Cd	-17	-13	-31	29	-22	10	5	-47	-1	-63	0	-7	-69
Cd +/-	25	23	23	24	23	23	25	24	25	23	23	23	22

Sn	7	-5	4	-22	-10	-24	2	-41	-15	-2	-32	-58	1
Sn +/-	25	22	22	23	23	23	24	23	24	23	22	22	21
Sb	-76	-38	-4	21	-54	-2	36	-100	11	-32	-51	20	-24
Sb +/-	27	25	24	26	25	25	26	25	27	25	25	25	24
W	6	17	29	11	73	16	87	7	21	11	13	8	12
W +/-	9	7	8	7	9	8	11	8	9	6	8	6	7
Pb	1	1	0	1	-1	8	3	-5	-9	1	-3	1	5
Pb +/-	3	2	2	2	2	3	3	3	3	2	3	2	3
Se	0	0	2	1	2	0	0	-1	1	2	0	0	2
Se +/-	1	1	1	1	1	1	1	1	1	1	1	1	1
Rb	102	17	92	16	63	68	111	22	36	10	49	10	40
Rb +/-	5	2	3	3	3	3	4	2	3	2	3	3	3
Sr	1524	482	256	627	193	493	1092	207	498	351	527	555	1196
Sr +/-	17	6	4	8	3	6	12	4	7	5	7	7	12
Hg	13	10	9	6	-1	0	13	2	9	11	10	-6	-3
Hg +/-	9	7	7	7	8	7	11	7	9	6	7	6	6
Th	-	-	-	-	-	-	-	-	-	-	-	-	-
Th +/-	-	-	-	-	-	-	-	-	-	-	-	-	-
U	-97	-39	-8	-37	-2	-13	-70	-9	-34	-21	-27	-30	-60
U +/-	10	6	5	7	5	7	9	5	7	5	6	6	8

APPENDIX E: STABLE ISOTOPE HANDSAMPLE ISOSCAPE

E1. Carbon and oxygen stable isotope composition and drill number.

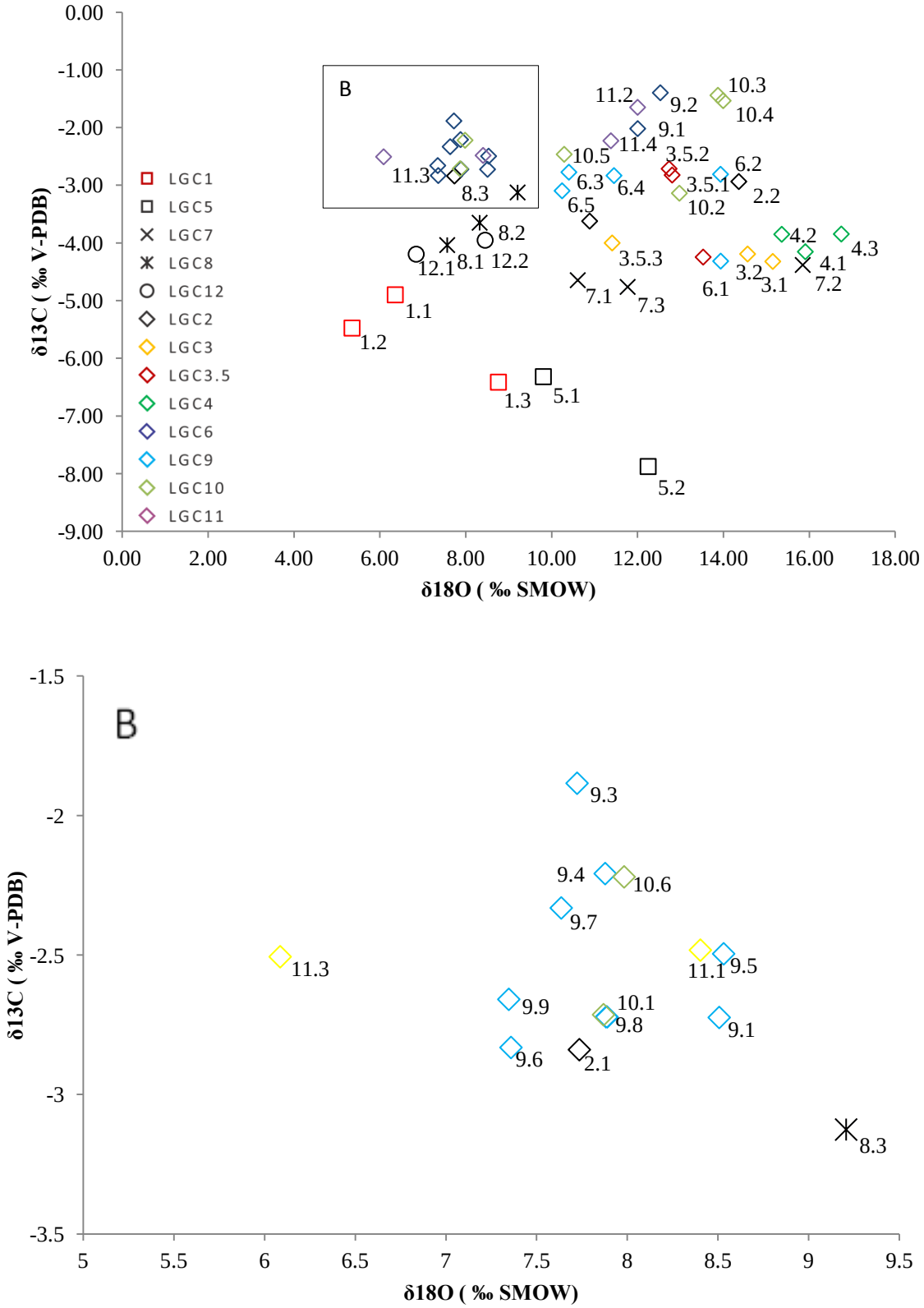

E2. Stable Isotope hand sample composition and drill locations

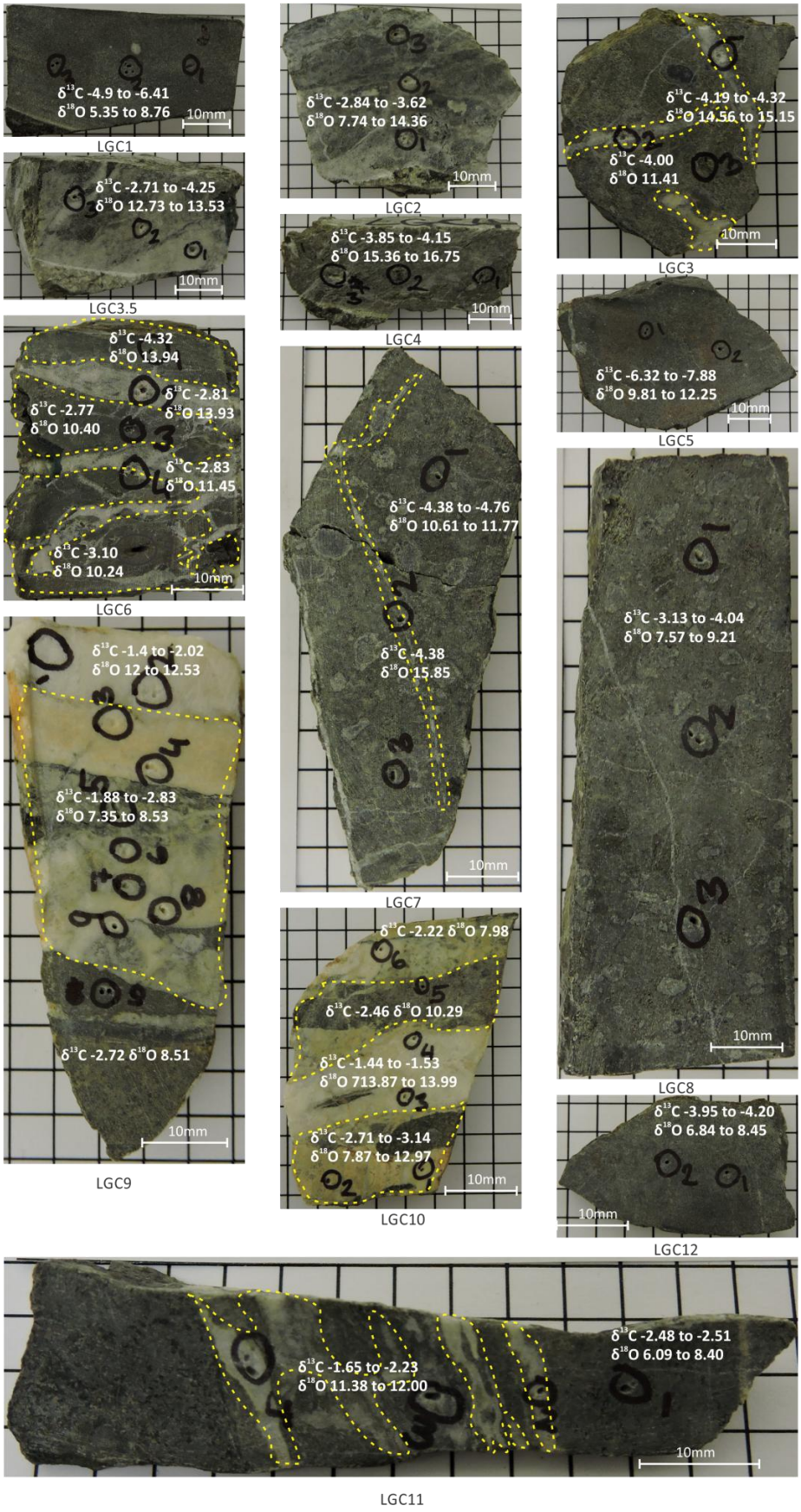

APPENDIX F: XRD PLATES

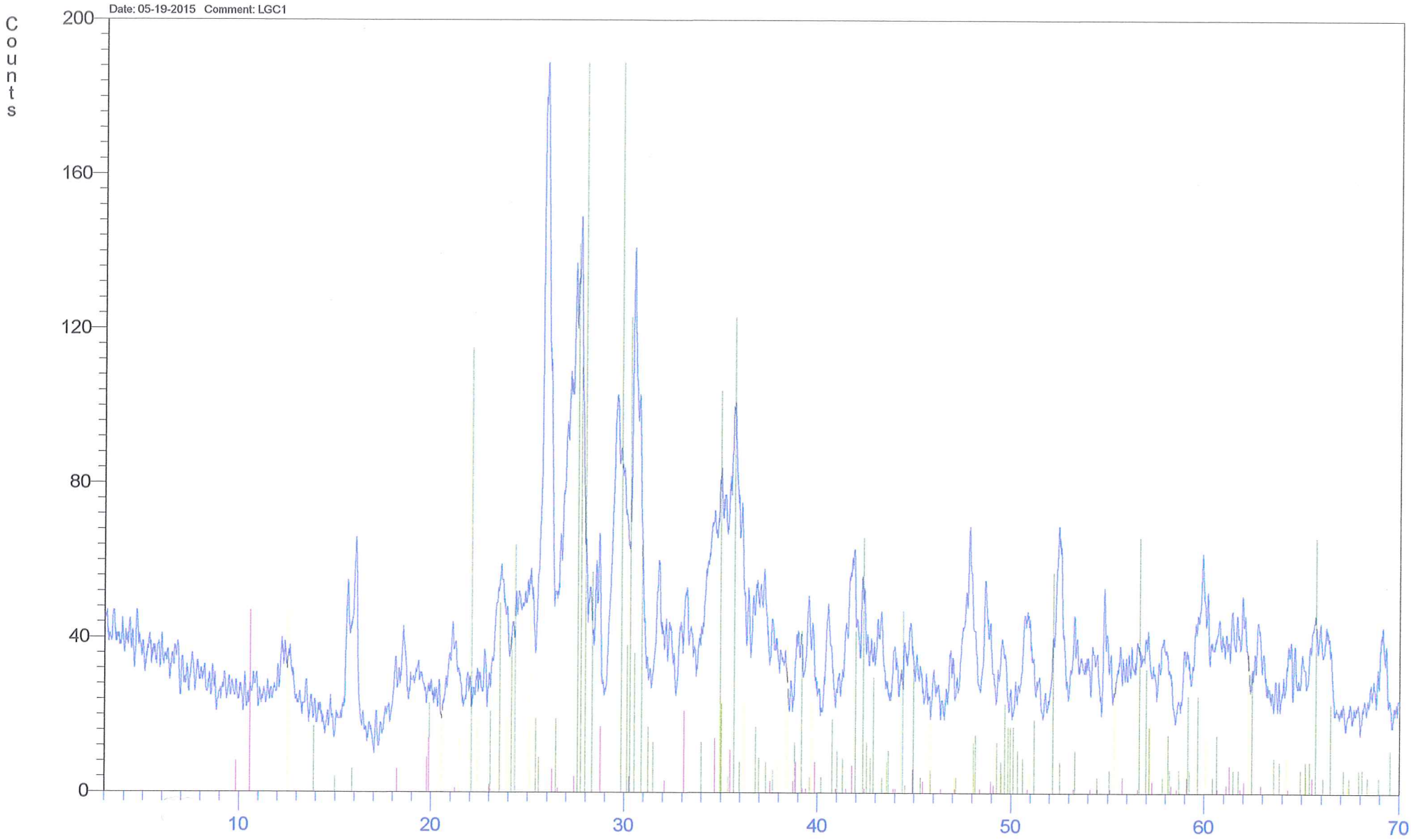

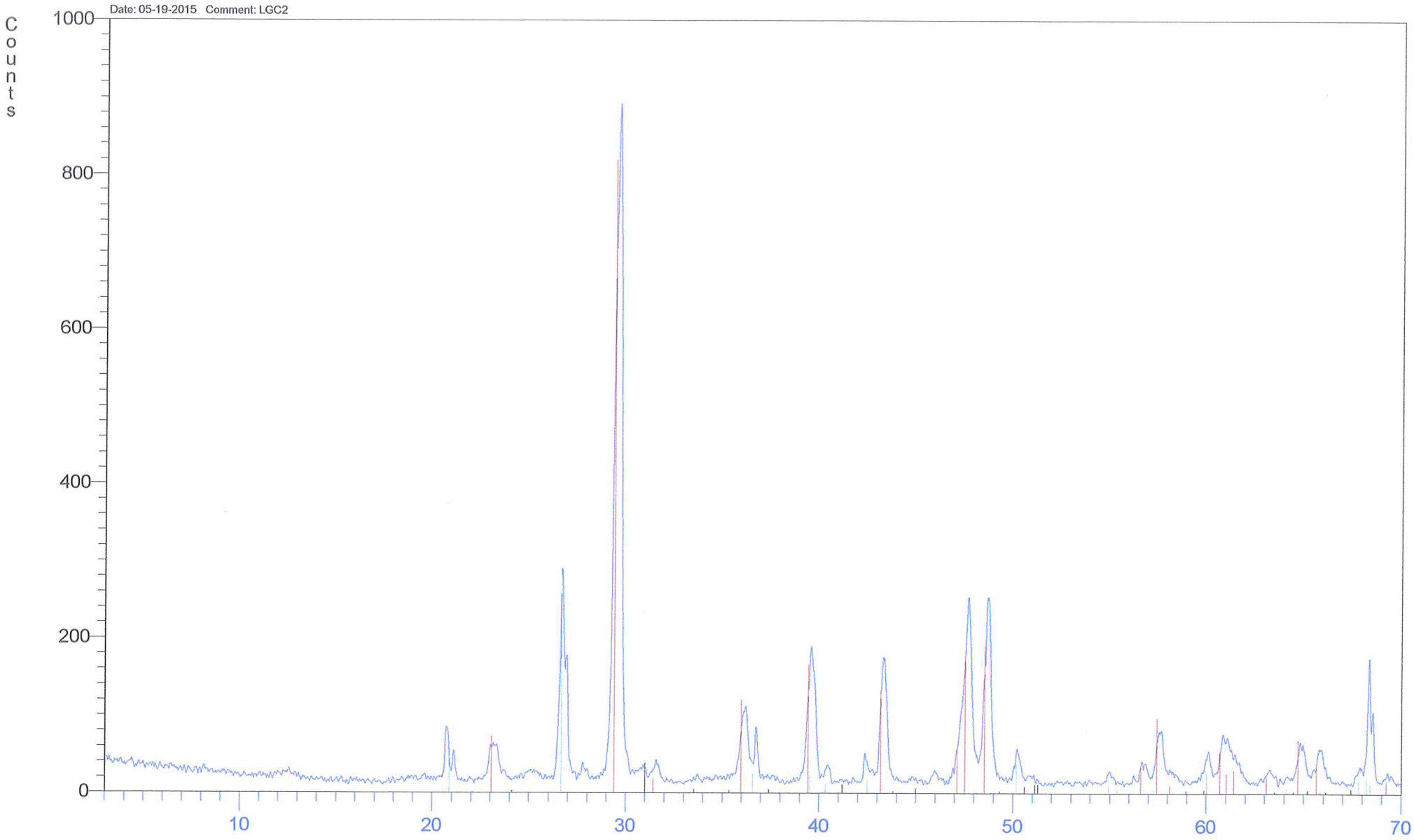
Date: 05-19-2015 Comment: LGC2
Counts
1000
800
600
400
200
0
10
20
30
40
50
60
70
Degrees 2-Theta

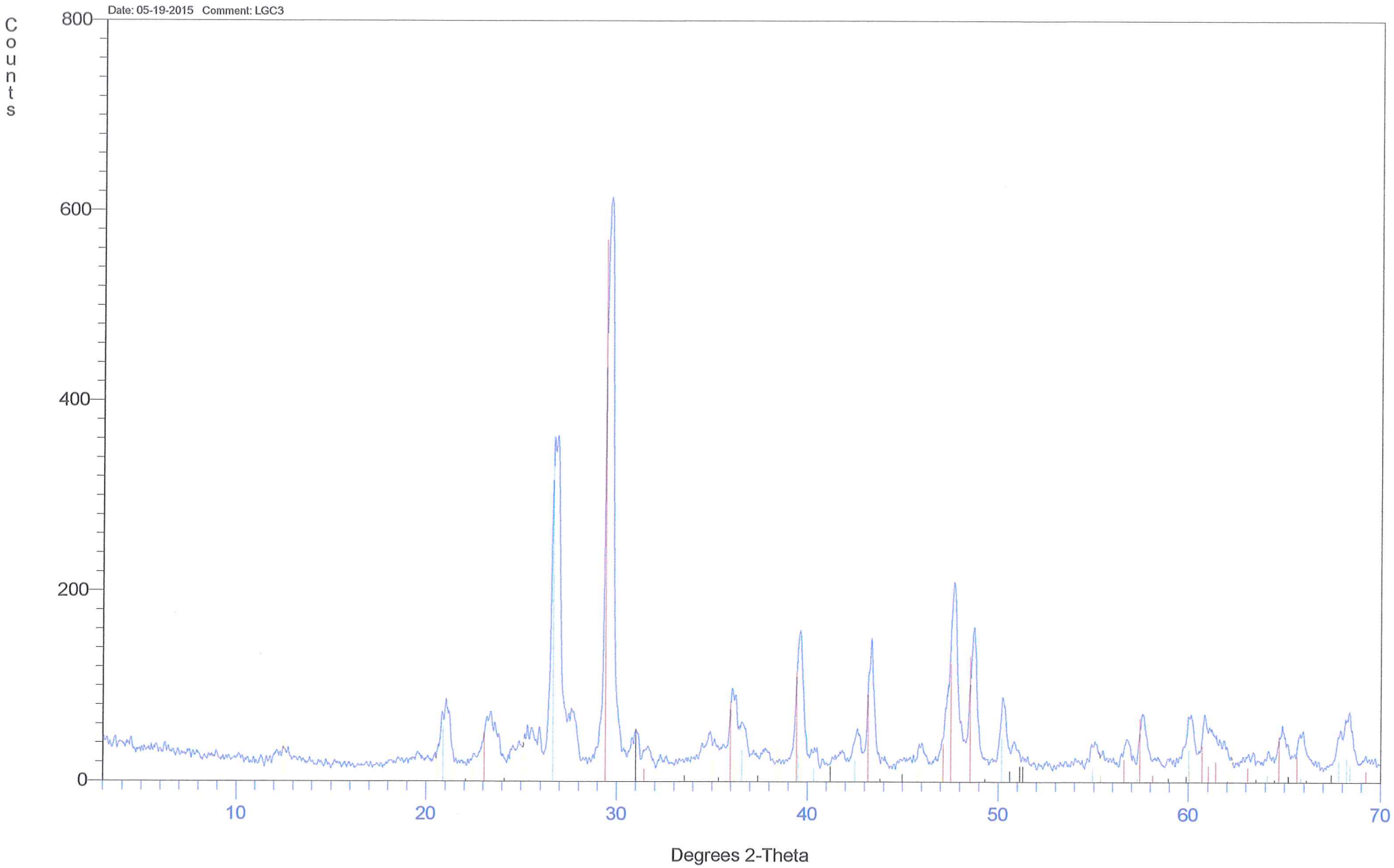
Date: 05-19-2015 Comment: LGC3
Counts
800
600
400
200
0
10
20
30
40
50
60
70
Degrees 2-Theta

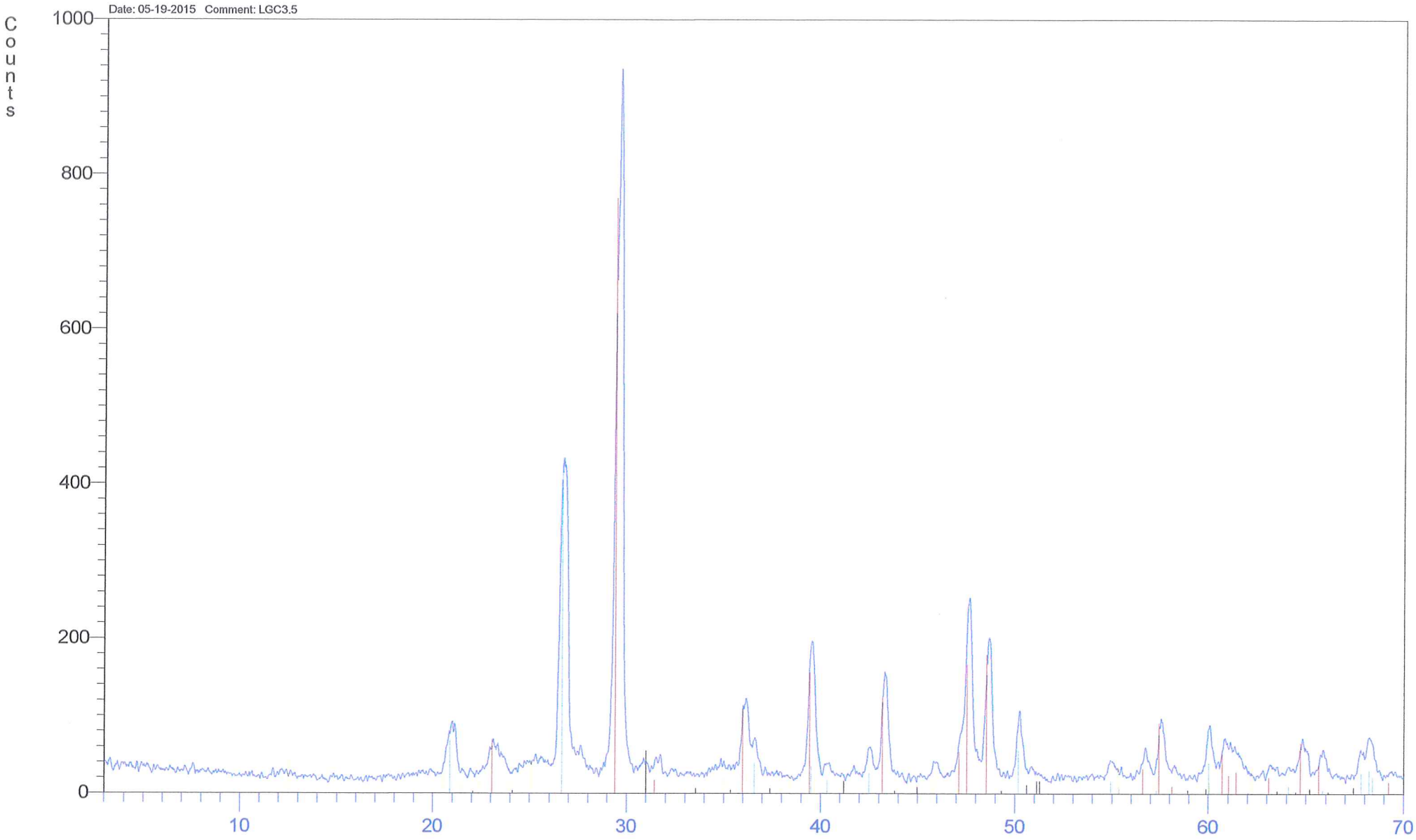
Date: 05-19-2015 Comment: LGC3.5
Counts
1000
800
600
400
200
0
10
20
30
40
50
60
70
Degrees 2-Theta

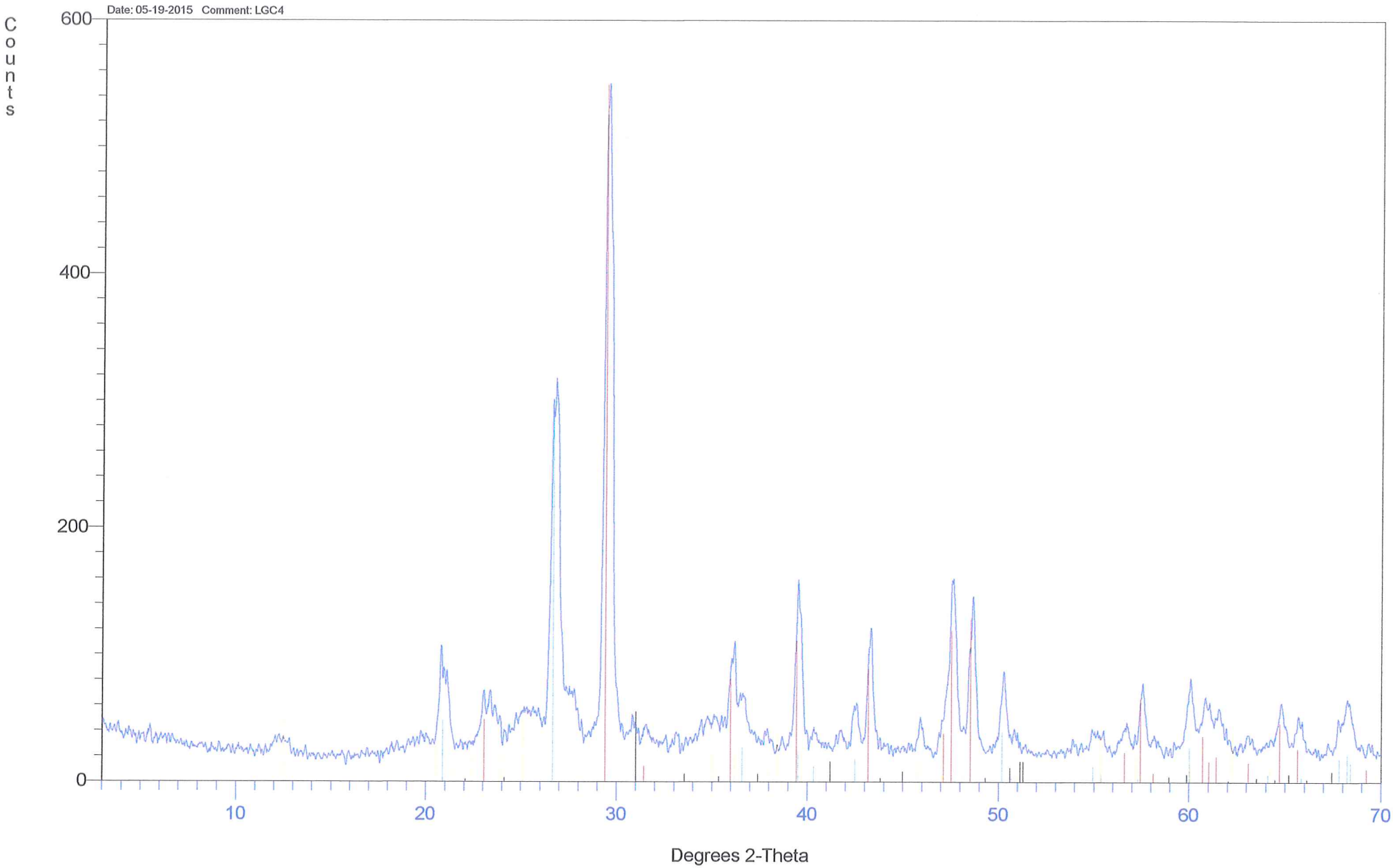
Date: 05-19-2015 Comment: LGC4
Counts
600
400
200
0
10
20
30
40
50
60
70
Degrees 2-Theta

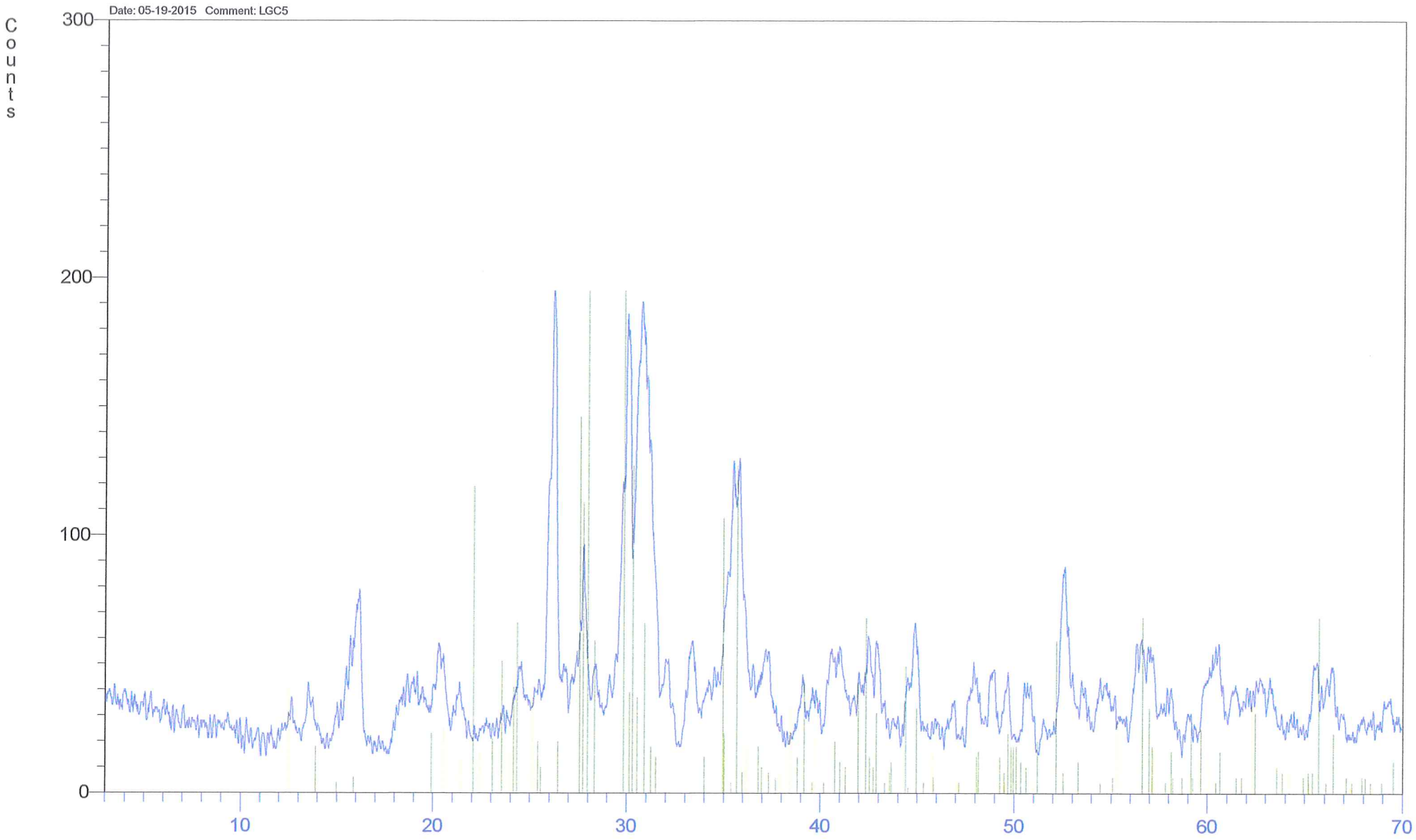
Date: 05-19-2015 Comment: LGC5
Counts
300
200
100
0
10
20
30
40
50
60
70
Degrees 2-Theta

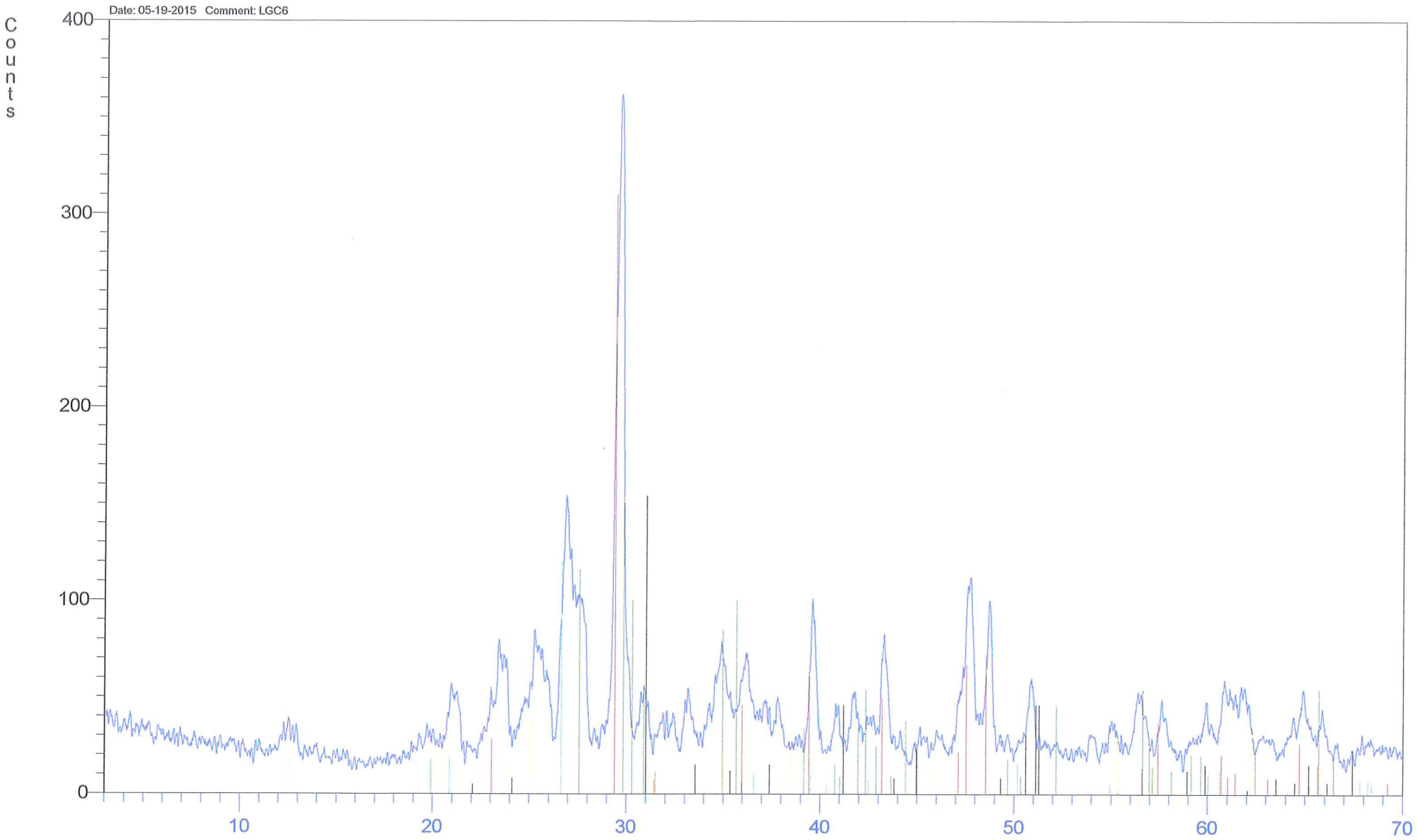
Date: 05-19-2015 Comment: LGC6
Counts
400
300
200
100
0
10
20
30
40
50
60
70
Degrees 2-Theta

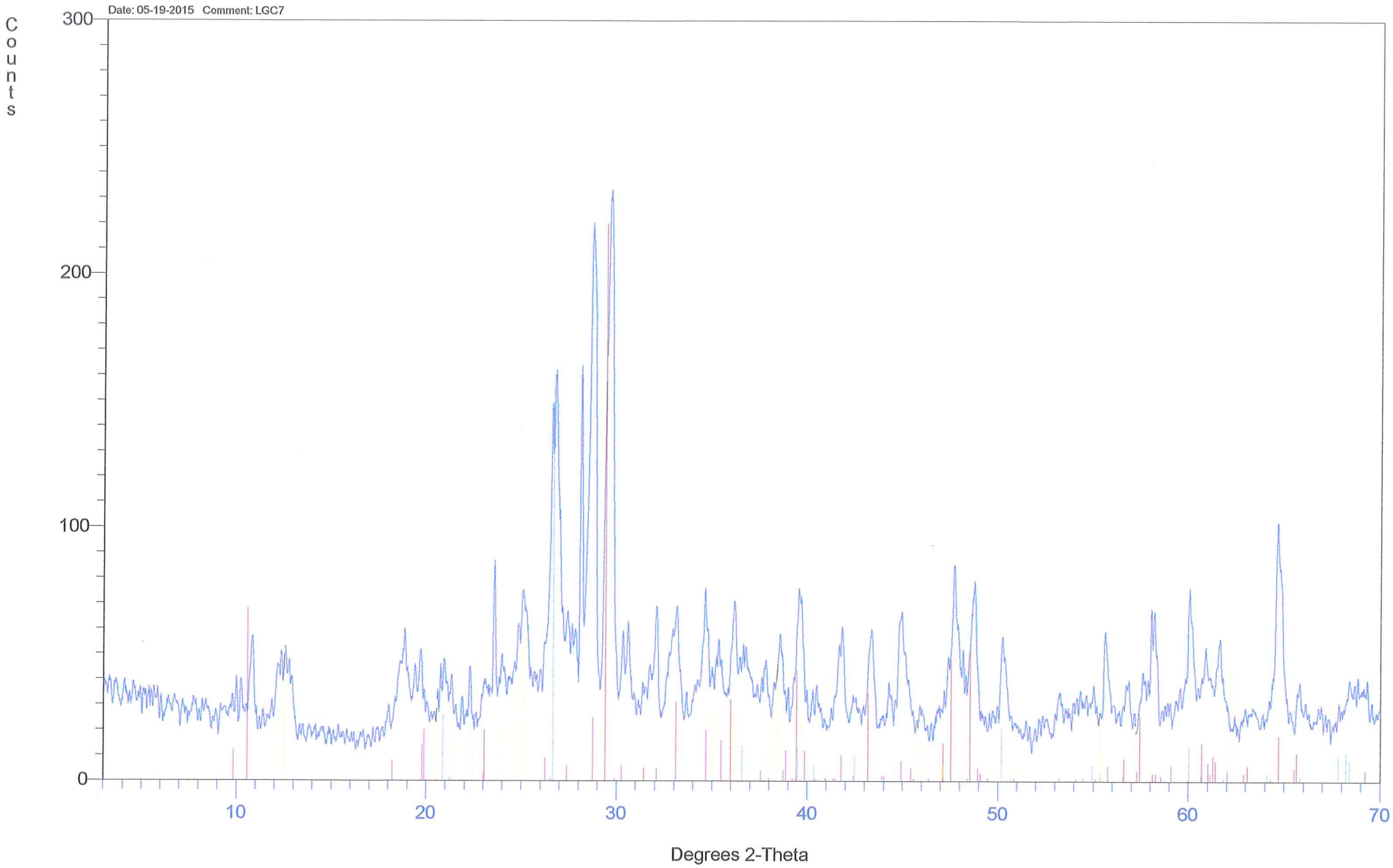
Date: 05-19-2015 Comment: LGC7
Counts
300
200
100
0
10
20
30
40
50
60
70
Degrees 2-Theta

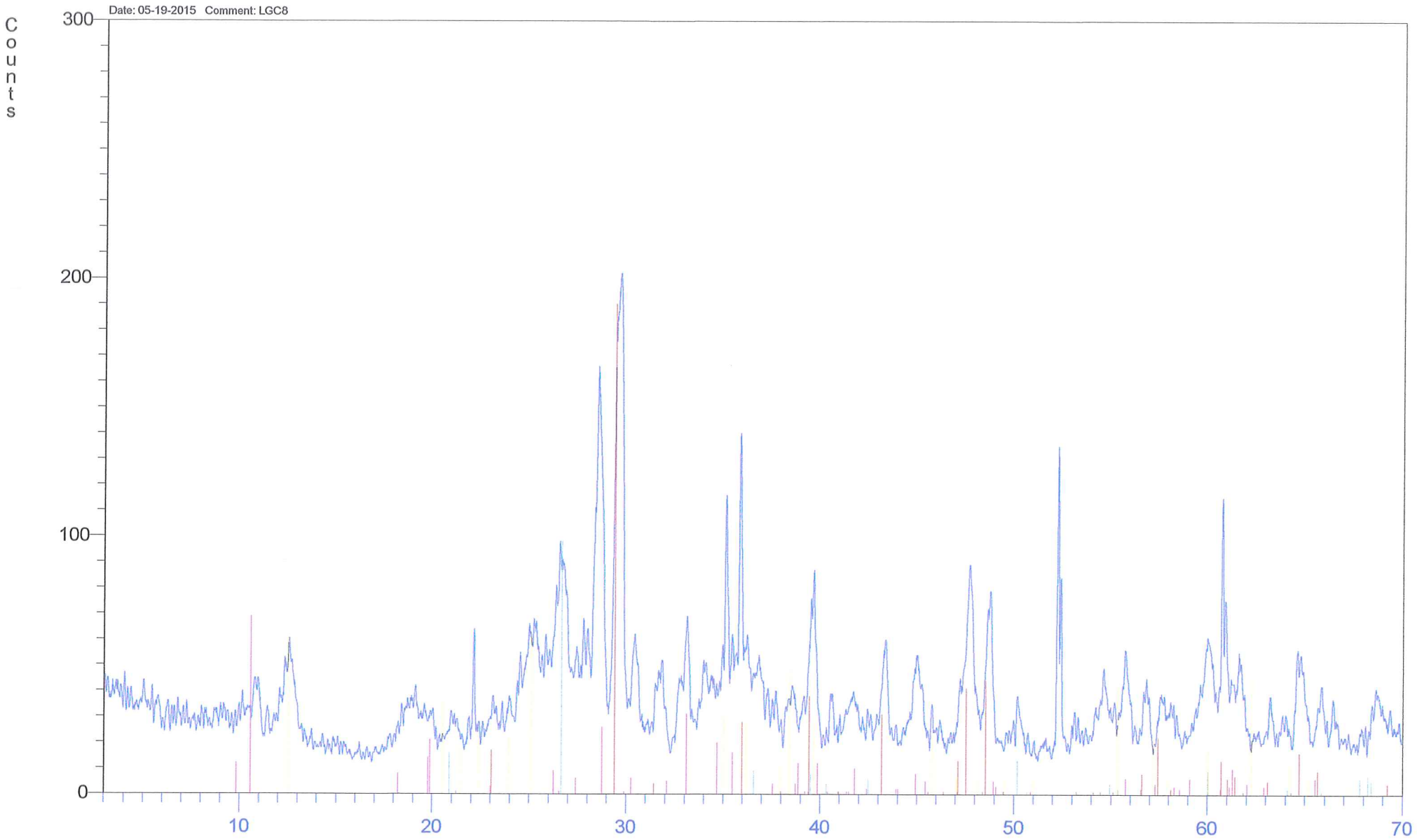
Date: 05-19-2015 Comment: LGC8
Counts
300
200
100
0
10
20
30
40
50
60
70
Degrees 2-Theta

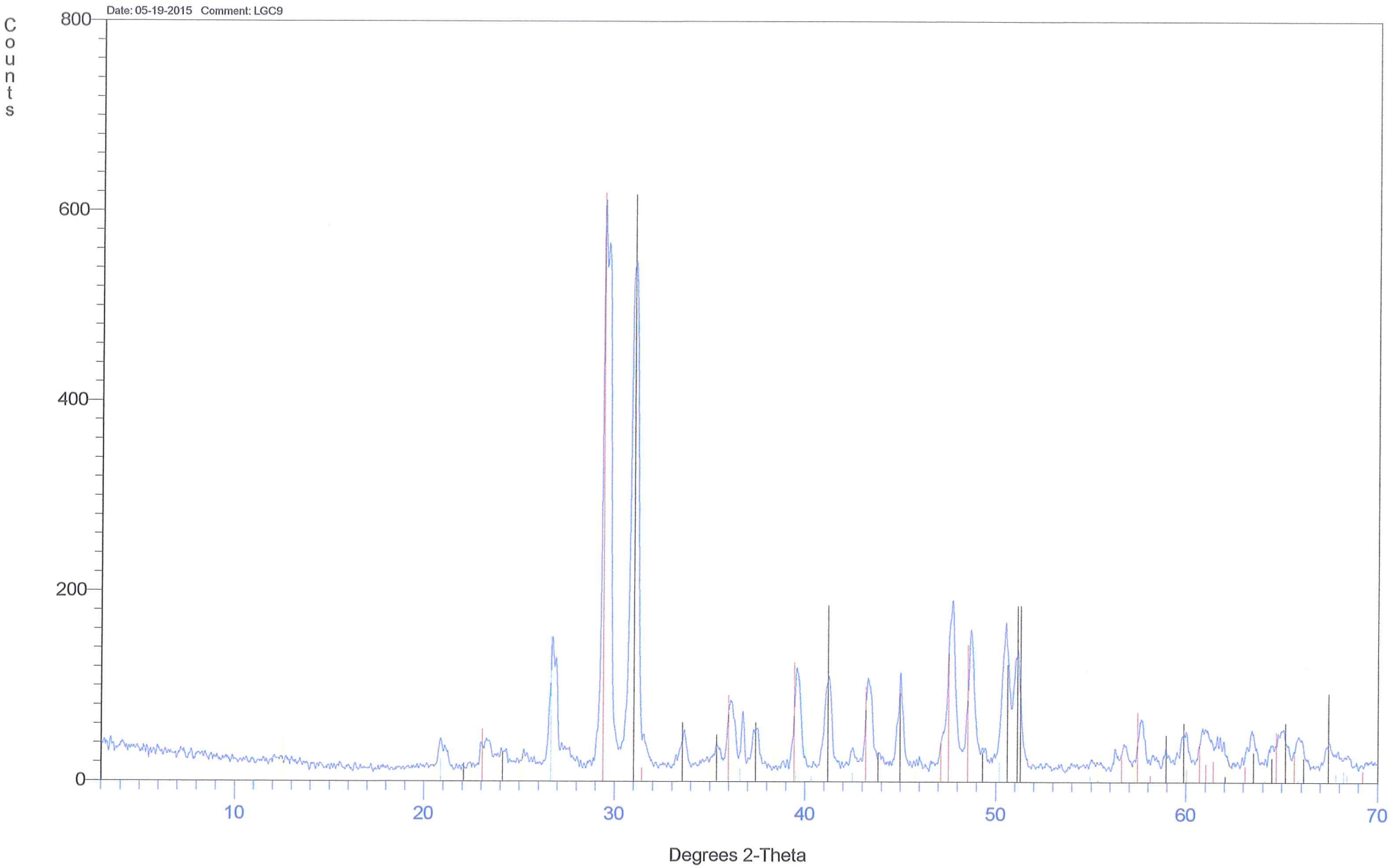
Date: 05-19-2015 Comment: LGC9
Counts
800
600
400
200
0
10
20
30
40
50
60
70
Degrees 2-Theta

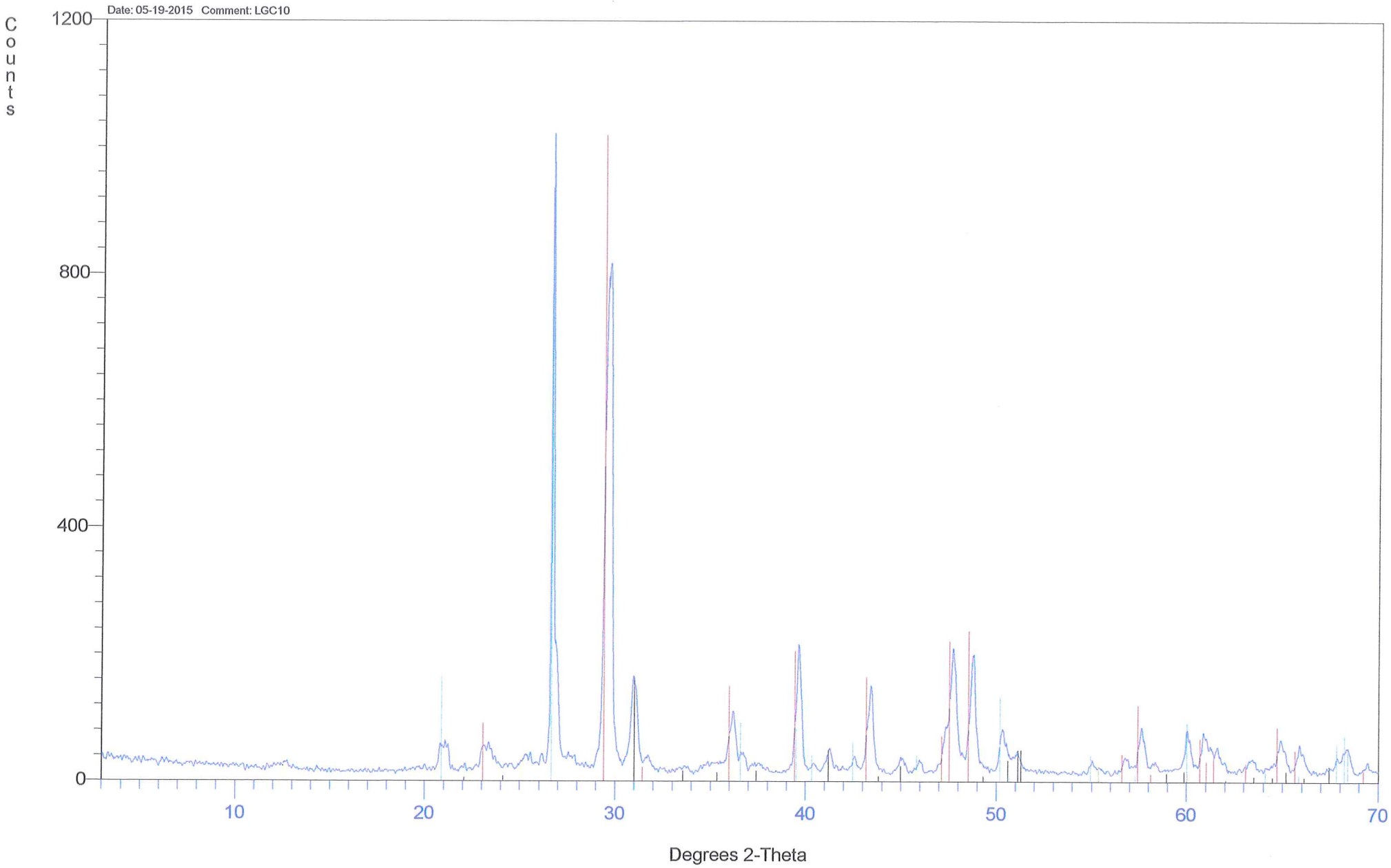
Date: 05-19-2015 Comment: LGC10
Counts
1200
800
400
0
10
20
30
40
50
60
70
Degrees 2-Theta

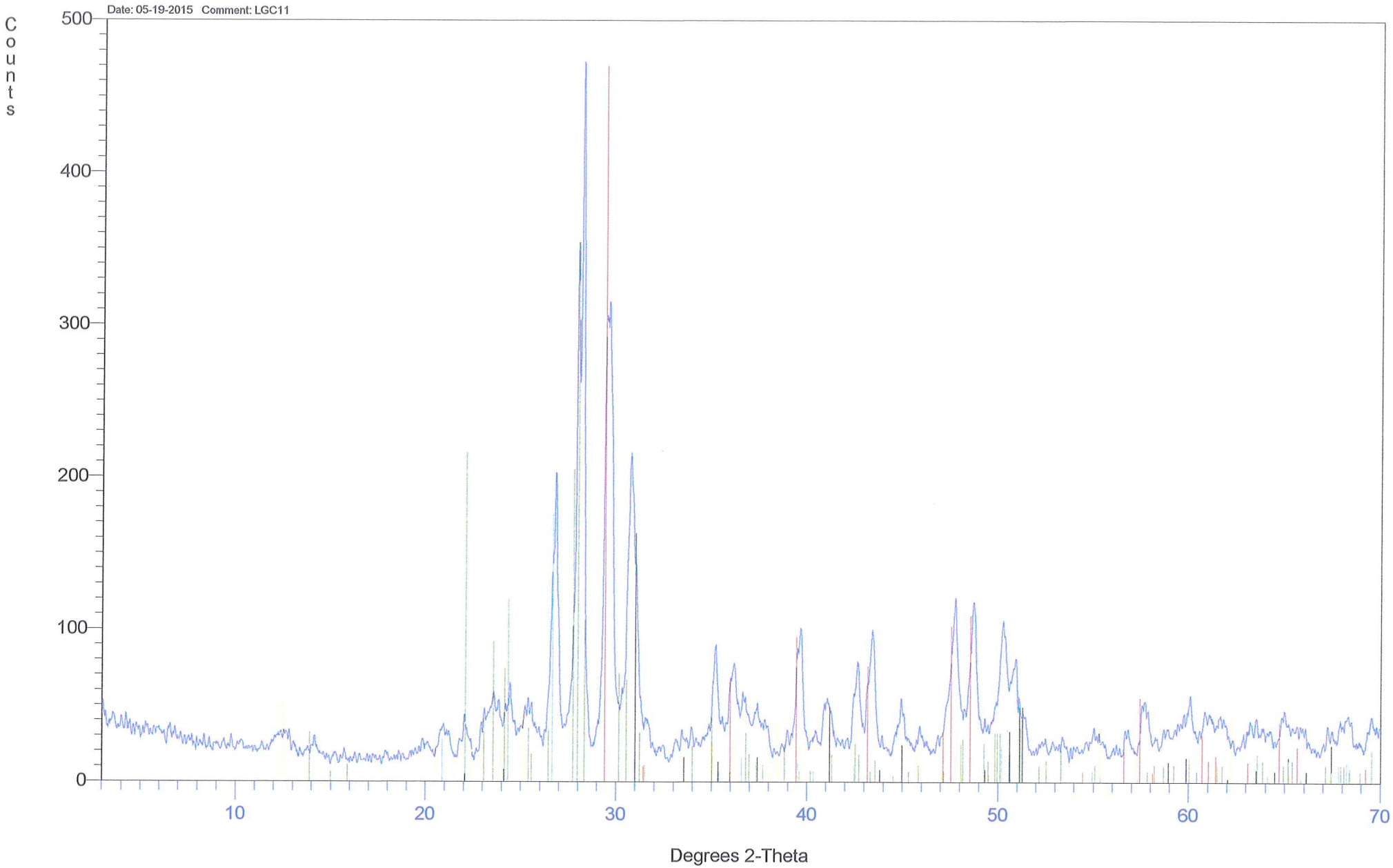
Date: 05-19-2015 Comment: LGC11
Counts
500
400
300
200
100
0
10
20
30
40
50
60
70
Degrees 2-Theta

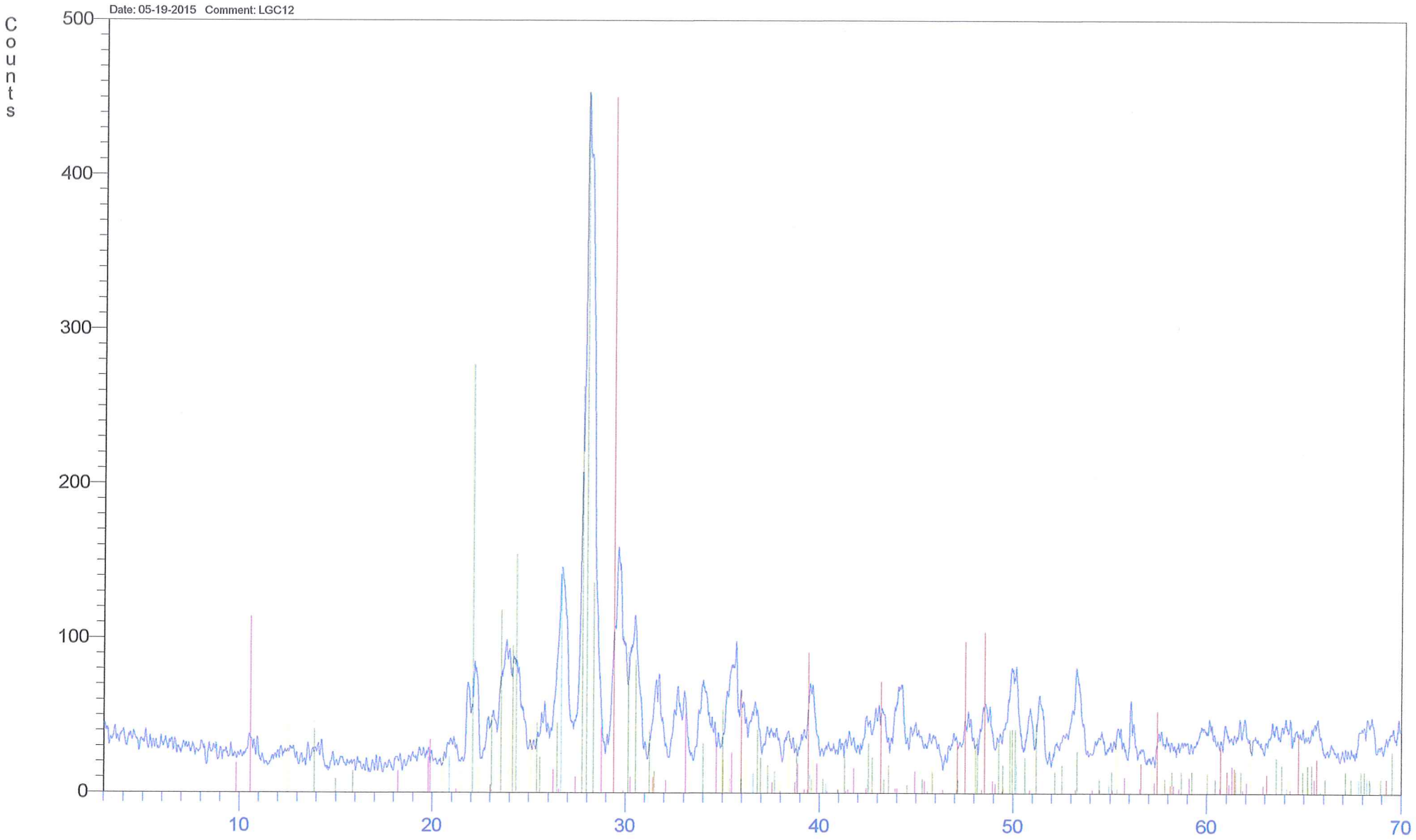
Date: 05-19-2015 Comment: LGC12
Counts
500
400
300
200
100
0
10
20
30
40
50
60
70
Degrees 2-Theta